Study on the Detection Performance of MIMO radar systems

Jingxu Han

A dissertation submitted to the Department of Electrical Engineering,
University of Cape Town, in fulfilment of the requirements
for the degree of Master of Science in Engineering.

Cape Town, October 2010

Declaration

I declare that this dissertation is my own, unaided work. It is being submitted for the degree of Master of Science in Engineering in the University of Cape Town. It has not been submitted before for any degree or examination in any other university.

Signature of Author .....

Cape Town

October 2010

Abstract

Inspired by the recent advantages of Multiple-Input Multiple-Output (MIMO) technologies in wireless communications, the MIMO concept was adopted in the radar context. By exploiting the potentials of MIMO techniques in respect of combating the fading of a channel, a MIMO radar system was created to handle a similar problem by exploiting widely separated antennas, namely, the variations in the returned signal power from different aspects of a target of interest. Compared with conventional radar systems, such a multiple-antenna radar system may result in a better understanding or estimation of a target's radar cross section by angular or spatial diversity, which consequently delivers a better performance.

This dissertation studied the detection performance of MIMO radar systems: the study can be divided into two parts, viz. detection of stationary targets and detection of moving targets.

With respect to the detection of stationary targets, firstly, the detection performance of MIMO radar systems in white Gaussian noise was examined. A comparison between MIMO and phased array radar systems was then presented to illustrate their respective properties. Secondly, the robustness of MIMO radar systems to clutter was investigated. It was found that MIMO radar systems are better able to remove the effects of clutter than that of phased array radar systems. Thirdly, a more practical distributed MIMO radar system in respect of bandwidth limitations was proposed. Three classical distributed algorithms, namely, OR, AND, and Majority Logic (MAJ), were applied to existing MIMO radar systems. Lastly, a MIMO passive radar system based on FM waveform was introduced. By using the Neyman-Pearson hypothesis, an optimal receiver for the MIMO passive radar was developed.

Taking Doppler shift into account, detection performance of moving targets was investigated. The effects of instantaneous Doppler shift on the detection performance were first examined. Afterwards, the detection of moving targets including range considerations was discussed.

Additionally, the pertinent Matlab source codes used throughout the dissertation are attached. These will assist both newcomers and current radar researchers who study the detection performance of MIMO radar systems.

To my mother

Guiqin Jia

Acknowledgements

I would first like to express profound and sincere gratitude to Prof. M. R. Inggs for offering me this study position and his indispensable supervision, guidance and patience for completing this dissertation. No words can ever describe how much I am indebted to you.

I would like to thank Dr. Yoann Paichard for his guidance during the development of this dissertation when he was in University of Cape Town. Regine Lord, thank you for helping me to edit this dissertation. I would also like to thank Simon Winberg for offering me a tutor job, not only for the relating financial support but also for the experience I gained from that.

I must also thank all the members of the Radar Remote Sensing Group. So many unforgotten events we have been through together, such as pain ball shooting, soccer, drinking, etc.

Jinjing Li, thank you for all the support and help that you have offered. I am forever in your debt.

Finally, I would like to thank my family, their support and encouragement made this dissertation possible.

Contents

Declaration **i**

Abstract **ii**

Acknowledgements **iv**

List of Symbols **x**

Nomenclature **xii**

1 Introduction **1**

1.1 Overview 1

1.2 Motivation 3

1.3 Objectives of the Work 4

1.4 Dissertation Outline 4

2 Background **6**

2.1 Doppler Shift 6

2.2 Matched Filters 11

2.2.1 The Matched Filter Detector 11

2.2.2 Analysis of the Matched Filter 14

2.2.3 Performance of the Matched Filter Detector 20

2.3 Ambiguity Function 22

2.4 Literature Review 29

2.5 Summary 33

3 Detection Performance in respect of Stationary Targets **34**

3.1 Detection Performance of MIMO Radar Systems 35

3.1.1 MIMO radar probability of detection calculations 35

3.1.2 Comparison between MIMO and phased array radar systems . . . 40

3.1.3 Robustness of the MIMO radar systems to clutter 45

3.2 Distributed Detection of MIMO Radars 49
3.2.1 OR Rule 49
3.2.2 AND Rule 50
3.2.3 MAJ Rule 50
3.2.4 Detection Performance of Distributed MIMO Radar Systems . . . 50
3.3 MIMO Passive Radar Detection based on the FM signals 53
3.3.1 Derivation of the Probability Density Function of Null Hypothesis 54
3.3.2 Probability Density in the Presence of a Target 57
3.3.3 Detection Performance of MIMO passive radar systems based on FM waveform 59
3.4 Summary 62

4 Detection of Moving Targets **63**
4.1 Doppler Frequency Calculation for a MIMO Radar System 63
4.2 Detection of Moving Targets 65
4.2.1 The Probability of False Alarm 66
4.2.2 Detection Performance of Moving Targets 70
4.2.3 Monte Carlo Simulations 73
4.3 Summary 80

5 Conclusions **81**

A Matlab Source Codes **84**

Bibliography **86**

List of Figures

2.1 Doppler geometrical relationship. 7
2.2 Normalized Doppler shift versus target velocity aspect angle. 9
2.3 Absolute value of Doppler frequency for different velocities. 10
2.4 Doppler frequency versus uniformly varying velocities. 10
2.5 The matched filter detector. 11
2.6 PDF relationship between probability of detection and probability of false alarm. 18
2.7 Detection performance of matched filter detector. 20
2.8 Mis-detection performance of the matched filter receiver. 21
2.9 Probability of detection versus SNR in relation to different numbers of processing samples. 21
2.10 The AF surface of white Gaussian r.v. 24
2.11 The AF output of white Gaussian r.v on dB scale. 25
2.12 The frequency modulation signal. 27
2.13 The ambiguity function of FM signals. 28
2.14 The ambiguity function output of FM signals on dB scale. 28

3.1 Detection performance of MIMO radar systems. 38
3.2 Probability of mis-detection of MIMO radar systems. 39
3.3 ROC performance on various SNR. 39
3.4 Comparative detection performance of MIMO, MISO, and phased array radar systems. 42
3.5 Miss detection performance of MIMO, MISO, and phased array radars. . 43
3.6 The impact of different number of receive antennas on the detection performance. 44
3.7 Detection performance versus SCR. 47
3.8 Probability of detection versus SNR in the presence of clutter. 48
3.9 The process flow of the distributed MIMO radar systems. 50
3.10 Distributed detection performance. 51

3.11 Detection performance versus signal to clutter ratio. 52
3.12 The impact on the different number of antennas with same order of diversity. 52
3.13 The impact on the different number of antennas in the presence of clutter. 53
3.14 The accuracy of derivations. 56
3.15 Detection performance against different reflected power. 60
3.16 Impact of the integration time length on the detection performance. 61
3.17 ROC of MIMO passive radar systems. 61

4.1 The moving target scheme of a MIMO radar system. 64
4.2 The Doppler shift relationship for a two by one MIMO radar system. . . . 65
4.3 The probability of false alarm vs threshold. 69
4.4 The impact of different number of antennas on threshold. 69
4.5 Detection performance of MIMO, MISO, and phased array radar systems. 74
4.6 Impact of different number of antennas on the detection performance. . . 75
4.7 Comparison between static and moving targets for MIMO radar system. . 75
4.8 Detection performance on various total phase. 76
4.9 ROC of MIMO and phased array radar systems. 77
4.10 SNR calculation by range. 79
4.11 Detection performance versus range. 79
4.12 Cumulative detection with various numbers of antennas. 80

List of Tables

4.1 Definitions. 72
4.2 Simulation parameters. 73
4.3 Simulation parameters. 78

List of Symbols

$A_m(t)$	—	The amplitude of the signal
B_n	—	Receiver noise bandwidth
c	—	Speed of light
D	—	The size of target
E	—	Transmit power
$Ex(\cdot)$	—	The expected value operation
f_c	—	The carrier frequency
f_d	—	Doppler Frequency
f_s	—	The sample frequency
F_r	—	Pulse repetition frequency
F_R	—	Propagation parameter for receiver-target path
F_T	—	Propagation parameter for transmitter-target path
$F^{-1}_{\chi^2_n}$	—	The inverse CDF of a chi-square distribution
$f_\triangle$	—	The frequency deviation
G_R	—	Receive power gain
G_T	—	Transmit power gain
H_0	—	Null hypothesis
H_1	—	Alternative hypothesis
I_{MN}	—	The identity matrix with size MN by MN
j	—	The imaginary unit
k	—	Boltzmann's constant
L_R	—	Receive system loss
L_T	—	Transmit system loss
M	—	The number of transmit antennas
N	—	The number of receive antennas
N_f	—	The number of Fourier frequencies
N_s	—	The number of processing samples
$N(\mu, \sigma^2)$	—	The Gaussian distribution with mean μ and variance σ^2
P	—	The transmitting power
P_d	—	The probability of detection
P_{fa}	—	The probability of false alarm

P_{miss}	—	The probability of miss detection
R_R	—	Path Length between Target and Receivers
R_T	—	Path Length between Target and Transmitters
s	—	Signals
s_d	—	Direct transmitting signal
t	—	Pulse repetition interval
T	—	The integration time
T_s	—	Receiver noise temperature
V	—	Velocity
$V_{ar}(\cdot)$	—	The variance operation
w	—	AWGN
α	—	The amplitude of Swerling targets
α_c	—	The amplitude of clutter
γ	—	Threshold
δ	—	Aspect angle of velocity
ε	—	Energy
λ	—	Wavelength
κ	—	Range product
θ	—	The initial phase
σ^2	—	Variance
σ_B	—	Radar cross section
τ	—	Time delay
φ	—	The phased caused by the unknown Doppler frequency
ψ, φ	—	Position coefficients
χ^2_n	—	The chi-square distribution with n degrees of freedom
$\chi(\tau,\ f_d)$	—	The ambiguity function
$\Phi(x)$	—	The normal CDF
$\lvert\cdot\rvert$	—	The absolute value
$(\cdot)^H$	—	Hermitian (conjugate) transpose
$(\cdot)^T$	—	Transpose operation

Nomenclature

AF—Ambiguity Function.

AWGN—Additive White Gaussian Noise.

CAF—Cross Ambiguity Function.

CDF—Cumulative Distribution Function.

CFAR—Constant False Alarm Rate.

CLT—Central Limit Theorem.

DAB—Digital Audio Broadcasting.

DF—Direction finding.

DFT—Discrete Fourier Transform.

Doppler frequency—A shift in the radio frequency of the return from a target or other object as a result of the object's radial motion relative to the radar.

DVB—Digital Video Broadcasting.

FM—Frequency Modulation.

GLRT—Generalized Likelihood Ratio Test.

LOS—Line of Sight.

MAJ—Majority Logic.

MIMO—Multiple Input Multiple Output.

MISO—Multiple Input Single Output.

N-P Hypothesis—Neyman-Pearson hypothesis.

OFDM—Orthogonal Frequency Division Multiplexing.

PDF—Probability Density Function.

PM—Phased Modulation.

PRF—Pulse repetition frequency.

RCS—Radar Cross Section.

RDR—Reflected to Direct signal power Ratio.

ROC—Receive Operating Characteristic.

SCR—Signal to Clutter Ratio.

SIRV—Spherically Invariant Random Vector.

SNR—Signal to Noise Ratio.

WCDMA—Wideband Code Division Multiple Access.

Chapter 1

Introduction

Radar, an acronym for RAdio Detection And Ranging, has long been a powerful tool for detecting and locating electrically conductive objects. The term radar was coined by the U.S. Navy in the 1940s. By emitting electromagnetic waves and receiving the scattered energy, a radar system can identify the range, altitude, speed, and other relevant information from objects of interest. Originally, radar systems were mainly developed for military purposes and specifically to monitor movement of enemy aircraft, ships and ground-based vehicles. Currently, in addition to being used by the military, radar systems are involved in various civilian fields, such as air-traffic control, weather forecasting, earth crust mapping and so on.

In respect of radar systems, multiple-antenna technique is not a new technique. In the 80's, a multistatic radar concept was invented by ONERA-the French Aerospace Lab, namely, Synthetic Impulse Antenna Radar (SIAR). However, at that moment, this new system did not show its overwhelming advantages compared with conventional radar systems, which thus was deemed impractical. Recently, inspired by the advantages of MIMO in wireless communication domain, a novel multiple antenna radar system was introduced by Fishler, et al (2004), which was referred to as MIMO radar [28]. By exploiting the potentials of MIMO techniques in respect of overcoming fading of a channel, such a radar system delivers a better detection performance than monostatic radar system or conventional multistatic radar. Owing to the novelty of MIMO radar, thus so far only sporadic research has been done on the detection performance of MIMO radar systems.

In this dissertation, the background and detection theory of radar systems is introduced. Both stationary and moving target detection of MIMO radar systems are then examined and conducted. The relevant Matlab source codes are attached.

1.1 Overview

MIMO has been the subject of considerable research in the field of wireless communications during the past four decades. By exploiting the spatial diversity of multiple antennas

as either transmitter or receiver, a communication system not only increases its channel capacity but also decreases the fading effect in a wireless channel [71, 72]. Unlike the conventional single antenna communication system, all the information streams emitted by multiple transmit antennas utilise experiencing multiple transmit paths in order to overcome the effect of channel fading over a single communication path.

Radar scanners suffer the variations of the returned signal power from different aspects of a target of interest. This is referred to as Radar Cross Section (RCS) [64]. In terms of MIMO, it is important to note that the fluctuations of RCS and the fading of a channel are mathematically similar. Both may be regarded as probability distributions of known random variables. For instance, Swerling I model and Rayleigh fading channels are both Rayleigh distribution of random variables. Consequently, this has given rise to the idea of combining MIMO and radar.

The existing MIMO radar systems may be divided into two categories. One was introduced by Lincoin Laboratory, Massachusetts Institute of Technology in the U. S [12, 14]. This MIMO radar system was based on the conventional phased array radar system, where each coherent sub array emitted orthogonal waveforms. However, in the wireless communication domain, MIMO is a technology aiming to produce spatially independent signals, hereby introducing spatial diversity, and consequently improving the performance of a wireless communication system.

Alternatively, E. Fishler, et al (2004) created another type of MIMO radar system, which in contrast to the conventional phased array radar systems utilises widely separated antennas. This kind of MIMO radar made its debut at the IEEE international radar conference [28]. Unlike the traditional phased array radar systems, this novel radar system used multiple antennas to improve the performance by increasing the distances between the antennas. The results showed that such a MIMO radar system obtains far better results than conventional radar systems in terms of target detection, parameter estimation, range resolution, etc [34]. This dissertation will concentrate on the detection study of this new MIMO radar system, which embraces stationary and moving targets detection, MIMO passive radar detection, distributed MIMO radar detection and MIMO radar detection under clutter circumstances.

Improving the detection performance has always been an important concern. As one of vital radar theories, detection theory has become highly sophisticated with the development of statistical communication theory. There are too many outstanding scholars with significant contributions in this field to be listed here. Given the scope of this dissertation, the contributions of only four innovators are reviewed herein, namely, Woodward, North, Marcum and Swerling.

Inspired by information theory development, Woodward introduced an important concept, namely, Ambiguity Function (AF). This is a useful function of measuring radar solutions and ambiguity [75]. His approach is based on radar waveform, and it will be detailed in Chapter 2.

North is well known for the contribution on the matched filter theory [57]. By maximizing the signal to noise ratio, the matched filter approach can optimally detect signals immersed in noisy backgrounds. This will be discussed in detail in Chapter 2.

A comprehensive statistical analysis of radar detection was presented in the classic works of Marcum [56] and Swerling [66]. Marcum addressed the problem of detecting nonfluctuating targets in a white Gaussian noise background. Swerling extended this model to fluctuating targets with a background of white Gaussian noise. In order to commemorate their contributions, people named nonfluctuating targets and fluctuating targets as the Marcum target model and the Swerling target model, respectively. Their results acted as a catalyst to the development of target detection, and then considerable work was done in the field of radar detection.

1.2 Motivation

There are two primary motivations to undertake this dissertation. One is the success of the MIMO concept in wireless communication systems and the other one is the lack of studies on predicting the detection performance of MIMO radar systems, in particular, with regard to the detection and location of moving targets. It is commonly agreed that radar systems experience a drop in detection performance with increased frequency shift due to Doppler effects. As a result, in this dissertation, detection performance of the MIMO radar system in respect of both stationary and moving targets will be evaluated on one hand, devise a design in such a way to meet the detection requirements on the other hand.

As mentioned previously, since radar detection theory is highly sophisticated with the development of statistical communication theory, the intention of this dissertation is not to introduce or develop any novel detection algorithm or method of signal processing, but to analyse and theorise the detection performance of MIMO radar systems based on the classical algorithms (e.g. N-P test). Necessary numerical simulation results are presented to validate analysis, which exploit the detection performance of MIMO radar systems as a function of other parameters, such as the number of either transmit or receive antennas, various detection algorithms and the different signal to interference and noise ratios.

In order to benefit both newcomers and radar researchers who carry on detection study of MIMO radar systems, the pertinent Matlab source codes used throughout the dissertation are attached. These will help to demonstrate the functioning of the MIMO radar system, thus creating a better understanding.

Therefore, main contributions in this dissertation are to analyse the detection performance of MIMO radar systems, especially with regard to moving target detection, to simulate systems under various scenarios in order to validate analysis, to design a MIMO passive radar system, and to provide relevant Matlab source codes to facilitate the work of other radar researchers.

1.3 Objectives of the Work

The principal aims of this dissertation are following:

- To conduct a theoretical analysis of the MIMO radar's operating specifications;
- To perform research on the classical radar detection algorithms in noise;
- To analyse the detection performance of MIMO radar systems both theoretically and numerically, based on classical radar detection algorithms;
- To study the detection performance of a MIMO passive radar system based on FM broadcasting signals;
- To examine the Doppler effects on target detection when using MIMO radar systems;
- To develop Matlab source codes to demonstrate and test MIMO radar systems.
- To draw conclusions in respect of the detection abilities of MIMO radar systems and to provide recommendations on how to improve or enhance such detection performance.

1.4 Dissertation Outline

The five Chapters of this dissertation, which sets out to analyse and evaluate the detection performance of MIMO Radar systems, organised as follows:

- Chapter 1 introduces the overview and motivation of the work, and it states specific aims of the work presented in this dissertation.
- Chapter 2 studies the background with reference to this work, which may be divided into three sections, namely, the Doppler effect, the use of matched filters, and the ambiguity function. A literature review on the detection of either conventional radar systems or MIMO radar systems is presented. Some brief results are described as well.
- Chapter 3 analyses and evaluates the performance of MIMO radar systems with regard to detecting stationary targets. Detection theory in respect of MIMO radar systems is analysed in depth and the simulation results under various scenarios are provided. These include detection performance results with clutter or without clutter, comparative results between MIMO Radar and conventional phased array radar, detection results of MIMO passive radar based on Frequency Modulation (FM) broadcasting signals, and detection performance results obtained by utilising different distributed detection algorithms.

- Chapter 4 moves on to address the moving targets detection problems of MIMO radar systems. A more comprehensive Doppler shift calculation for a MIMO passive radar system is investigated based on the literature review contained in Chapter 2. Numerical results are then presented under different scenarios. This is assisted to design a system capable of detecting a moving target, while taking the probability of false alarm into account .

- Chapter 5 concludes the work done by summarising and listing the findings and achievements of this work. Lastly, this dissertation is sealed with discussions and recommendations of future work.

Chapter 2

Background

An overview of the theory and concepts pertinent to the use of radar systems to detect targets is presented in this chapter. As the aim of this dissertation is to calculate the probability of various MIMO radar systems to detect targets, this chapter summarises the relevant theories and concepts relating to Doppler frequency, matched filters, and the ambiguity function. In addition, a critique is provided of the important literature relating to detection studies and to the various available configurations of MIMO radar systems.

2.1 Doppler Shift

The impact of relative motion between antennas and targets on a radar system may be characterised into 2 aspects. One is a dialation in the receive signal. Another one is frequency shift. This dialation will induce serious distortions in the reconstructed images. In order to process the received signal with a serious dialation, both wideband and narrowband compensations have been proposed, respectively, which may effectively eliminate the impact of dialation. The purpose of this dissertation is to investigate the detection performance of MIMO radar systems. Therefore, the analysis of frequency shift will be carried out.

When observing an electromagnetic wave, the amount of the frequency change of a wave due to its motion is referred to as the Doppler shift, which is usually expressed in hertz. In order to distinguish stationary objects from moving targets, this section examines the Doppler shift for a radar system made up of a single transmitter and receiver, called bistatic radar. It is well known that even a tiny motion causes a change in the Doppler frequency, which leads to a performance variance in a radar system. Therefore, it is crucial to study of the effects of Doppler effects for a radar system. For the purposes of this dissertation, the analysis how the Doppler relationship changes the radar waveform is conducted, as it is reflected from the moving target. Furthermore, the Doppler shift of moving targets, as detected with a stationary transmitter and receiver, is investigated in this dissertation.

The Doppler shift is defined as the time rate or change of the total path length of the scattered signal, normalized by the wavelength λ. It should be noted that the frequency shift may be caused by the motion of either target or one of the transmitter or receiver. Aiming to investigate the moving target detection of MIMO radar systems, it is assumed that moving targets and stationary transmitter and receiver are implemented in this dissertation. Thus, the Doppler shift may be described by the contribution of range rates from both transmitter and receiver, which may be mathematically and geometrically expressed as follows:

$$f_d = \frac{1}{\lambda}\left[\frac{d}{dt}(R_T + R_R)\right] \tag{2.1}$$

$$f_d = \frac{1}{\lambda}\left(\frac{dR_T}{dt} + \frac{dR_R}{dt}\right) \tag{2.2}$$

where the symbol of f_d represents Doppler frequency and R_T, R_R denote path length between targets to transmitters and receivers, respectively.

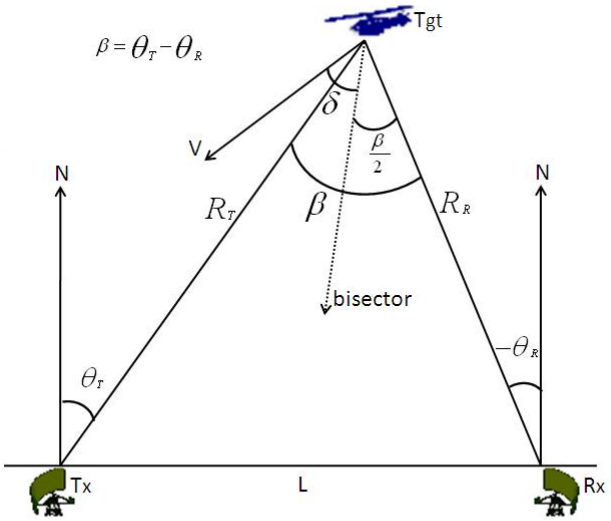

Figure 2.1: Doppler geometrical relationship.

Figure 2.1 depicts the Doppler relationship scenario of a radar system and a moving target, where symbols of V, δ, and β represent the magnitude of velocity, the aspect angle of velocity, and the angle between the transmitter and receiver with vertex at the target, respectively. It is shown from Fig. 2.1 that the term dR_R/dt is the projection of the target's velocity vector onto the receiver-to-target Line Of Sight (LOS), which is in the form of:

$$\frac{dR_R}{dt} = V\cos(\delta + \frac{\beta}{2}) \tag{2.3}$$

where $\beta = \theta_T - \theta_R$. The symbols of θ_T and θ_R signify the transmitter's look angle and

receiver's look angle, respectively. It should be noted that the look angle of antennas are measured positive clockwise from the north of the coordinate system. Therefore, the receiver's look angle is negtive in Fig. 2.1.

Similarly, the term dR_T/dt is the projection of the target's velocity vector onto the transmitter-to-target LOS, which may be given as:

$$\frac{dR_T}{dt} = V\cos(\delta - \frac{\beta}{2}) \tag{2.4}$$

Combining Eqn. 2.2, 2.3 and 2.4, it yields the Doppler frequency initiated by the moving target only, which is given as:

$$f_d = \frac{2V}{\lambda}\cos\delta\cos\left(\frac{\beta}{2}\right) \tag{2.5}$$

where V is the velocity of the target and $\beta/2$ represents the bistatic bisector. It may be observed from Eqn. 2.5 that the Doppler frequency is determined by the projected velocity component of the target along the bistatic bisector. Furthermore, it is also shown from Eqn. 2.5 that, at the baseline ($\beta/2 = 90^o$), the Doppler shift is zero for all velocities. This is a general result for all the values of the target velocity aspect angle (δ). In addition, another special case, namely, when a target of interest is moving at a tangent to a bistatic contour ($|\delta| = 90^o$) is also given zero Doppler shift.

Consider a special case, where $R = R_T = R_R$, Eqn. 2.5 will be deduced as:

$$f_d = 2\frac{V}{\lambda} = 2\frac{dR}{\lambda dt} \tag{2.6}$$

This is the well-known monostatic Doppler shift expression. The symbol of R signifies the distance between the target of interest and the antenna.

A Doppler relationship normalized by ($2V/\lambda$) is illustrated in Fig. 2.2. The target velocity aspect angle (δ) is uniformly varying from -180 degrees to $+180$ degrees, whereas, the bistatic angles (β) are 0 degrees, 90 degrees, and 180 degrees. Obviously, the system will be reduced to the monostatic radar if β equals 0^o.

In Fig. 2.2, Zero Doppler shift is found ($\beta/2 = 90^o$), as mentioned before. In addition, for all given bistatic angles (β), a positive bistatic target Doppler shift may be observed when the target velocity aspect angle lies between -90 degrees and $+90$ degrees ($-90^o < \delta < +90^o$).

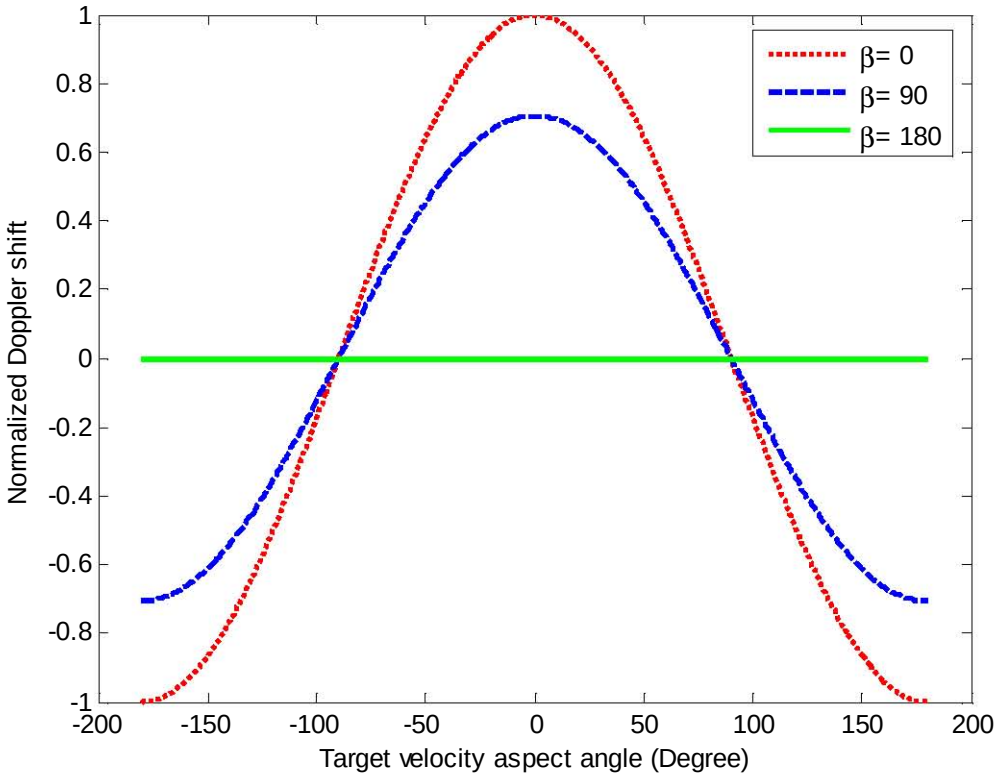

Figure 2.2: Normalized Doppler shift versus target velocity aspect angle.

The next simulation is carried out on the frequency of 94 MHz. The velocities of two moving targets are 250 m/s and 150 m/s. The absolute values of Doppler shift are presented in Fig. 2.3. It can clearly be seen that the faster moving target yields a bigger Doppler frequency.

Lastly, an analysis of Doppler relationship versus uniformly varying velocity is plotted in Fig. 2.4. The same parameters are utilised as Fig. 2.3. The carrier frequency is 94 MHz. While the velocities of the moving target are uniformly varying from -250 m/s to 250 m/s. The aspect angles of velocities are 45 degree and 60 degree, respectively.

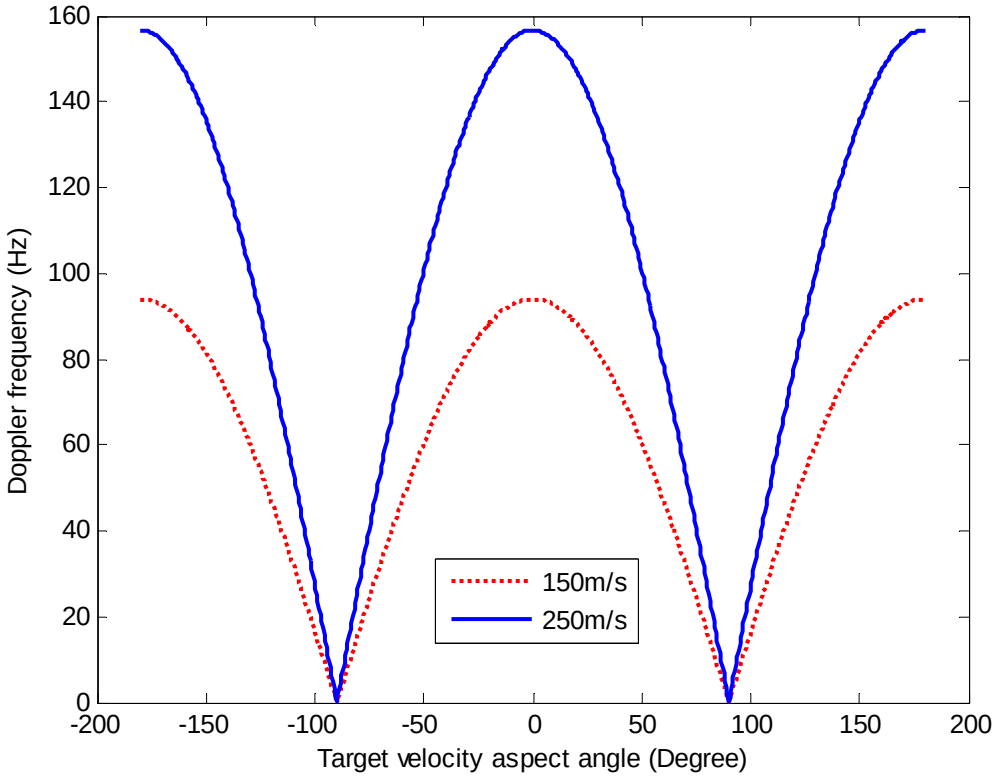

Figure 2.3: Absolute value of Doppler frequency for different velocities.

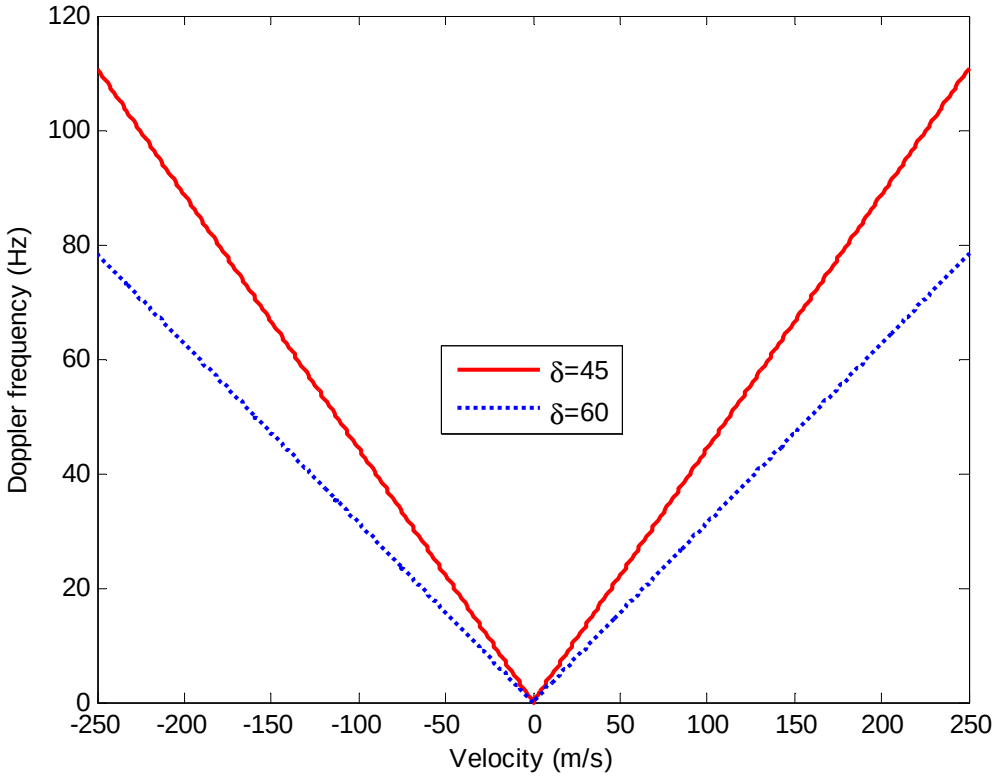

Figure 2.4: Doppler frequency versus uniformly varying velocities.

2.2 Matched Filters

This section is devoted to the design and analysis of matched filters. A matched filter is a kind of linear filter that is used to maximise Signal to Noise Ratio (SNR) in the presence of additive stochastic noise. It is well known that SNR is a vital parameter in respect of radar application. Matched filters are therefore utilised extensively in a radar system to extract useful information about a target of interest from additive white Gaussian noise. In this section, firstly, a matched filter detector for a radar system is described. Based on the Neyman-Pearson hypothesis, an optimal radar detector will be developed. It is evident, from the comparative results that the performance of a matched filter receiver is the same as that of an optimal receiver. Secondly, an analysis is provided of output SNR and of the processing gain of a matched filter detector. Lastly, the detection performance of the matched filter detector under various scenarios is presented.

2.2.1 The Matched Filter Detector

A receiver that may optimally detect emitted signals in the presence of additive white Gaussian noise by exploiting maximum SNR is referred to as a matched filter detector or a matched filter receiver. In order to detect weak target echoes in the presence of noise, a matched filter correlates each echo with a delayed replica of the original transmitted signal. As a classical cooperative signal detector, the matched filter is only optimal for a a-priori 'known' signal, which means that the information of the transmitted signals has to be known by the detector. A matched filter detector flowchart is shown in Fig. 2.5.

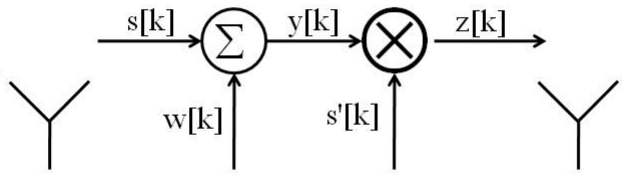

Figure 2.5: The matched filter detector.

where the symbol of $s[k]$ denotes the information signal at time k, $w[k]$ signifies the channel noise at time k, and $s'[k]$ represents the impulse response of matched filter at time k, which is the delayed replica of original signal. It should be noted that the operation between signal $y[k]$ and $s'[k]$ is a convolution and not a multiplication.

It should be noted that the signals of $s[k]$ and $w[k]$ are uniformly sampled versions of the continuous signals. Since the output of matched filter is discrete in any case, the received signals $y[k]$ are of the form after passing through the noise channels:

$$y[k] = s[k] + w[k], k = 1, 2, ..., K \tag{2.7}$$

where $s[k]$ are the transmitted signals, and $w[k]$ denote zero mean additive white Gaussian noise with variance σ^2. In the next chapter, the analysis of detection performance of MIMO radar systems will be conducted in continuous time. Another fact should also be noted that the signals of $\mathbf{S}$ and $\mathbf{W}$ are vectors of $s[k]$ and $w[k]$ for all K, which will be analysed in the next subsection.

An echo is then passed through a matched filter. The process of using a matched filter detector is equivalent to correlating an echo with a delayed replica of the transmitted signal. That is the reason why a cooperative detector needs to know the original transmitted signals. Matched filters are so called because they are matched to the original transmitted signals, namely mirrored signals. For instance, the impulse response $s'[k]$ of the matched filter is of the form [1]:

$$s'[k] = s[K-k] \text{ or } s'[K-k] = s[k], k = 1, 2, ..., K \tag{2.8}$$

By exploiting the mirrored version of the transmitted signals, the maximum attainable SNR will be yielded at the output of the matched filter. It is important to note that the highest SNR occurs only at a specific moment in time. Furthermore, a matched filter receiver is the form of the signal that is to be detected [44].

$$z[k] = \sum_{i=1}^{K} s'[k-i] y[i] \tag{2.9}$$

Substituting Eqn. 2.7 into Eqn. 2.9, the output of the matched filter is given as:

$$z[k] = \sum_{i=1}^{K} s'[K-i] (s[i] + w[i]) \tag{2.10}$$

Substitute Eqn. 2.8 into Eqn. 2.10:

$$z[k] = \sum_{i=1}^{K} s[K-(k-i)] (s[i] + w[i]) \tag{2.11}$$

It can be observed, from Eqn. 2.11, that the matched filter receiver is a correlation between the transmitted signals and the received signals. The impulse response of matched filter is the flipping and shifting version of the transmitted signal.

At a particular moment $k = K$, the above formula becomes:

$$z[K] = \sum_{i=1}^{K} s[i] y[i] = \sum_{i=1}^{K} s[i] (s[i] + w[i]) \tag{2.12}$$

The above equation is the theoretical maximum output of the matched filter, which is equivalent to the Neyman-Pearson detector. The SNR analysis of Eqn. 2.12 will be

conducted in next subsection, where it is proved that the maximum value of SNR may be achieved at moment $k = K$.

For the purpose of comparison, the output of the Neyman-Pearson detector will be derived. With respect to the Neyman-Pearson test, the two hypotheses H_0 (noise only without signals and clutter) and H_1(signal and noise) are defined as:

$$H_0 : y[k] = w[k],\ k = 0, 1, ..., K \tag{2.13}$$

$$H_1 : y[k] = s[k] + w[k],\ k = 0, 1, ..., K \tag{2.14}$$

where y is the measurement, s denotes the transmitted signals, and w is white Gaussian noise with zero mean and variance σ^2. The aim of the Neyman-Pearson hypothesis is to maximise the probability of detection, subject to a constant probability of false alarm. The probability of false alarm is defined as the probability of declaring a target present while in fact the target is absent.

Since the noise is a Gaussian distribution variable, the hypotheses H_0 and H_1 are of the form:

$$P(y \mid H_0) = \frac{1}{(2\pi\sigma^2)^{K/2}} exp\left[-\frac{1}{2\sigma^2}\sum_{k=1}^{K} y^2[k]\right] \tag{2.15}$$

$$P(y \mid H_1) = \frac{1}{(2\pi\sigma^2)^{K/2}} exp\left[-\frac{1}{2\sigma^2}\sum_{k=1}^{K} (y[k] - s[k])^2\right] \tag{2.16}$$

Thus, the threshold γ in favour of H_1 of the Neyman-Pearson detector may be expressed as:

$$\frac{P(y \mid H_1)}{P(y \mid H_0)} > \gamma \tag{2.17}$$

By substituting Eqn. 2.15 and Eqn. 2.16 into Eqn. 2.17, the threshold γ is given as:

$$exp\left[-\frac{1}{2\sigma^2}\left(\sum_{k=1}^{K} (y[k] - s[k])^2 - \sum_{k=1}^{K} y^2[k]\right)\right] > \gamma \tag{2.18}$$

In order to remove the exponential term, a logarithm is applied at both sides. Eqn. 2.18 thus becomes:

$$-\frac{1}{2\sigma^2}\left(\sum_{k=1}^{K} (y[k] - s[k])^2 - \sum_{k=1}^{K} y^2[k]\right) > ln\gamma \tag{2.19}$$

Eqn. 2.19 may be deduced as:

$$-\frac{1}{2\sigma^2}\sum_{k=1}^{K} s^2[k] + \frac{1}{\sigma^2}\sum_{k=1}^{K} y[k]\,s[k] > ln\gamma \tag{2.20}$$

When the energy term is normalised, the test statistic for hypothesis H_0 and H_1 may be expressed as:

$$\Gamma = \sum_{k=1}^{K} y[k]\,s[k] > \gamma' \tag{2.21}$$

where $\gamma' = \sigma^2 ln\gamma + \frac{1}{2}\sum_{k=1}^{K} s^2[k]$.

The process of Neyman-Pearson detector is shown from Eqn 2.13 to Eqn. 2.21. It may be observed that the output of the matched filter is equivalent to the test statistic of the Neyman-Pearson detector. Thus, it may be concluded that the matched filter has the same performance as the the Neyman-Pearson detector.

2.2.2 Analysis of the Matched Filter

As a crucial quantity of the matched filter, the output SNR is first derived in this subsection. The expression of the possibility of detection subject to the probability of false alarm and SNR of the matched filter is derived. Based on possibility of detection equations, The plots of the probability of detection versus SNR under various scenarios are presented in the next subsection.

As the objective function, SNR will be defined first. It is well known that SNR is short for signal to noise ratio. As its name implies, with respect of matched filter, SNR can be mathematically expressed as [2][46]:

$$SNR = \frac{instantaneous\ signal\ power}{average\ noise\ power} = \frac{|\,z_s\,|^2}{Ex\{z_w^2\}} \tag{2.22}$$

The underlying assumption is that additive white Gaussian noise w with zero mean with a two-sided power spectral density of $N_0/2$ is employed. The fact that the filtered noise z_w is no long white should be noted. The symbols of z_s and z_w are the desired signal and the noise of received signals. $Ex(\cdot)$ is the expected value operator.

Recall Eqn. 2.10, the desired signal and the filtered noise may be expressed as:

$$z_s[k] = \sum_{i=1}^{K} s'[K-i]\,s[i] \tag{2.23}$$

$$z_w[k] = \sum_{i=1}^{K} s'[K-i]\,w[i] \tag{2.24}$$

Replaced z_s and z_w by Eqn. 2.23 and Eqn. 2.24, the SNR is given as:

$$SNR = \frac{|\sum_{i=1}^{K} s^{'}[K-i]\, s[i]\,|^2}{E\left[\left(\sum_{i=1}^{K} s^{'}[K-i]\, w[i]\right)^2\right]} \tag{2.25}$$

Defining

$$\mathbf{S}^{'} = \left[s^{'}[K-1]\ s^{'}[K-2]\ \ldots\ s^{'}[0]\right]^T \tag{2.26}$$

$$\mathbf{W} = [w[1]\ w[2]\ \ldots\ w[K]]^T \tag{2.27}$$

Where $[.]^T$ is transpose operation. It should be noted that the $\mathbf{S}^{'}$ and $\mathbf{W}$ are vectors for all K.

A similar manner as [2] is conducted for further reduction. Combined with Eqn. 2.26 and Eqn. 2.27, Eqn. 2.25 may be simplified as:

$$SNR = \frac{|\,\mathbf{S}^{'T} s\,|^2}{E\left\{\left(\mathbf{S}^{'T}\mathbf{W}\right)^2\right\}} \tag{2.28}$$

Expend the denominator:

$$SNR = \frac{|\,\mathbf{S}^{'T} s\,|^2}{\mathbf{S}^{'T} E\left\{\mathbf{W}\mathbf{W}^T\right\}\mathbf{S}^{'}} \tag{2.29}$$

which may be further deduced as:

$$SNR = \frac{|\,\mathbf{S}^{'T} s\,|^2}{\sigma^2 \mathbf{S}^{'T}\mathbf{S}^{'}} \tag{2.30}$$

where σ^2 is the variance of noise.

According to the Cauchy-Schwarz inequality,

$$|\,\mathbf{S}^{'T} s\,|^2 \leq |\,\mathbf{S}^{'T}\mathbf{S}^{'}\,|\,|\,s^T s\,| \tag{2.31}$$

Equality is reached when $\mathbf{S}^{'} = cs$, where c is a constant. According to the definition of matched filter, the impulse response of matched filter is a flopped in place version of original signal, thus the constant equals to one $(c = 1)$. Furthermore, the maximum output SNR of the matched filter is in the form of:

$$SNR = \frac{|\,s^T s\,|}{\sigma^2} = \frac{E}{\sigma^2} \tag{2.32}$$

where the symbol of E signifies signal energy. Thus, the maximum SNR of matched filter is the signal energy divided by the variance of noise.

Since it is assumed that a two-sided power spectral density of $N_0/2$ noise is employed, Eqn. 2.32 may be rewritten as:

$$SNR = 2\frac{E}{N_0} \tag{2.33}$$

which is a well-known analysis result of matched filter under additive white Gaussian noise circumstance. The same results may be found at Eqn. 2.17 of [51] and Eqn. 3.93 of [55], although the analysis is based on the Fourier transform.

The basic idea behind detection problem is to build connections between the probability of detection and the probability of false alarm. Therefore, the detection problem of matched filter may be soloved by the following three steps. Firstly, a probability of false alarm is defined to satisfy a special system design. Under the predefined probability of false alarm, the second step is conducted to evaluate an intermediate, the threshold. By manipulating the intermediate, the last step is performed to calculate the probability of detection as a function of the probability of false alarm and other parameters, such as signal variance, noise variance, and the number of samples. Based on the above analysis, the detection performance of matched filter under additive white Gaussian noise circumstance will be examined.

Recall Eqn. 2.10, the hypothesis H_0 and the hypothesis H_1 of Neyman-Pearson test for matched filter may be expressed as:

$$H_0 : \sum_{i=1}^{K} s^{'}[K-i]\, w[i] \tag{2.34}$$

$$H_1 : \sum_{i=1}^{K} s^{'}[K-i]\,(s[i]+w[i]) \tag{2.35}$$

where the symbols of $s[i]$, $s^{'}[K-i]$, and $w[i]$ are desired signals, the impulse response of matched filter, and white Gaussian noise. It should be noted that after filtering, the noise is no long white but Gaussian distributed.

According to the definition of matched filter, the impulse response is flipped version of original signal. Recall Eqn. 2.8, the Eqn. 2.34 and Eqn. 2.35 may be rewriten as:

$$H_0 : \sum_{i=1}^{K} s[i]\, w[i] \tag{2.36}$$

$$H_1 : \sum_{i=1}^{K} s[i]\,(s[i]+w[i]) \tag{2.37}$$

Since noise $w[i]$ is white and uncorrelated with the impulse response of matched filter and transmit signals, the expected value of the test statistic under hypothesis H_0 may be

expressed as:

$$Ex(H_0) = Ex\left(\sum_{i=1}^{K} s[i]\, w[i]\right) = 0 \tag{2.38}$$

where $Ex(\cdot)$ is expected value operation as previously defined.

In a similar manner [44], under hypothesis H_1, the expected value may be hence given as:

$$Ex(H_1) := Ex\left\{\sum_{i=1}^{K} s[i]\,(s[i]+w[i])\right\} = Ex\left\{\sum_{i=1}^{K} (s[i]\,s[i]+s[i]\,w[i])\right\} \tag{2.39}$$

Consequently, the output of Eqn. 2.39 is:

$$Ex\left\{\sum_{i=1}^{K} s[i]\,s[i]\right\} = E \tag{2.40}$$

where the symbol of E represents signal energy.

The variance of the test statistic under hypothesis H_0 may be evaluated as:

$$Var(H_0) = Var\left(\sum_{i=1}^{K} s[i]\, w[i]\right) = \sigma^2 E \tag{2.41}$$

where $Var(\cdot)$ is variance operation and σ^2 is noise variance.

Similarly, the variance of hypothesis can be calculated as:

$$Var(H_1) := Var\left\{\sum_{i=1}^{K} s[i]\,(s[i]+w[i])\right\} = \sigma^2 E \tag{2.42}$$

Therefore, the test statistic of Gaussian distributed under each hypotheses can be expressed as following:

$$H_0 : N\left(0, \sigma^2 E\right) \tag{2.43}$$

$$H_0 : N\left(E, \sigma^2 E\right) \tag{2.44}$$

Same results may be found at [16][44]. In [3], the performance analysis of binary antipodal signals with matched filters is conducted.

The probability density function (PDF) relationship between the probability of detection and the probability of false alarm is depicted in Fig. 2.6 [44]. The PDF of hypothesis H_0 and the PDF of hypothesis H_1 are represented by red-dot and green-solid lines, respectively. As the intermedia, the threshold (black-solid) is defined by the probability of false alarm. The value of signal energy is depicted by the black-dot line. It is important to note that the relevant probabilities are areas under its own PDF. For instance, the probability of

false alarm is the right side area in respect of threshold under PDF of hypothesis H_0. The probability of detection and the probability of miss detection are under PDF of hypothesis H_1. Additionally, the following formula can be achieved.

$$P_d + P_{miss} = 1 \tag{2.45}$$

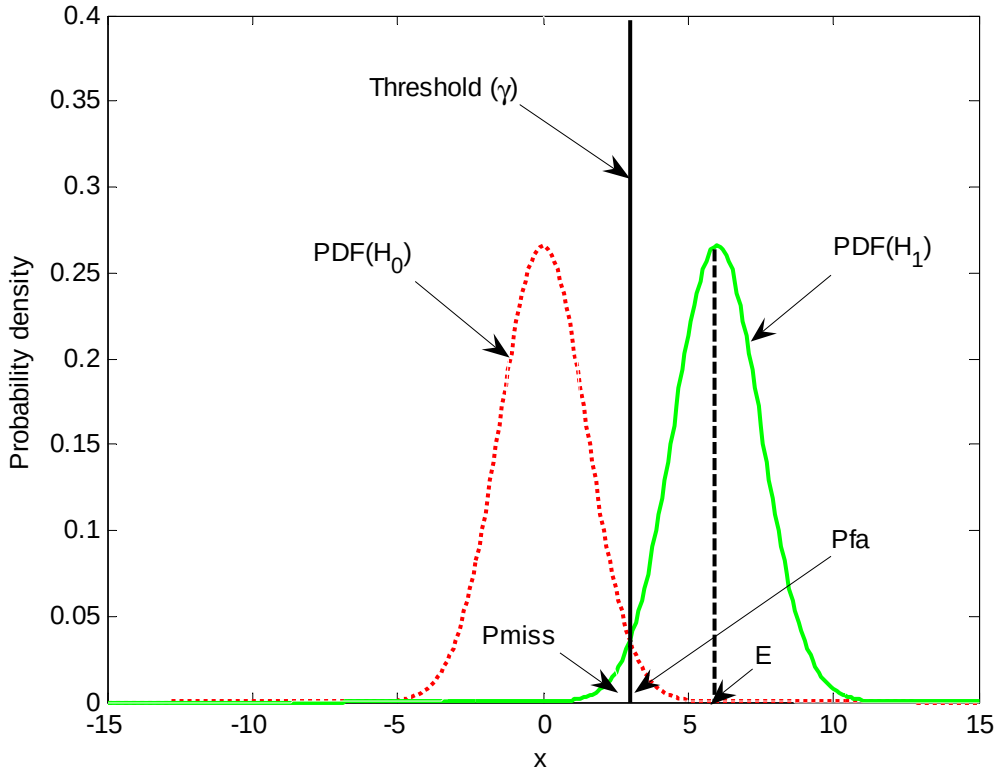

Figure 2.6: PDF relationship between probability of detection and probability of false alarm.

It may be observed that in terms of a fixed threshold, the detection performance may be improved by moving PDF of hypothesis H_1 to the right side. An efficient way is to increase signals energy or reduce noise variance, which is equivalent to increase signal to noise ratio. The expression of the probability of detection in terms of the probability of false alarm and the output SNR of the matched filter will be derived next. As previously analysed, the PDF of hypothesis H_0 is Gaussian distributed. Thus, the probability of false alarm P_{fa} may be given as:

$$P_{fa} = Pr\{T > \gamma \mid H_0\} = Q\left(\frac{\gamma}{\sqrt{\sigma^2 E}}\right) \tag{2.46}$$

As predefined above, σ^2 is the noise variance and E denotes the signal energy. The symbol of γ signifies the threshold.

$$Q(x) = \int_x^{\infty} \frac{1}{\sqrt{2\pi}} \exp\left(-\frac{t^2}{2}\right) dt = 1 - \Phi(x) \tag{2.47}$$

where $Q(x)$ is well-known to calculate the right-tail probability of normal radar variable. The symbol of $\Phi(x)$ represents the normal Cumulative Distribution Function (CDF).

As is shown in Fig. 2.6, for any probability of detection, equality holds:

$$P_d = Pr\{T > \gamma \mid H_1\} = Q\left(\frac{\gamma - E}{\sqrt{\sigma^2 E}}\right) \tag{2.48}$$

According to Eqn. 2.46, the threshold is given as:

$$\gamma = \sqrt{\sigma^2 E} Q^{-1}\left(P_{fa}\right) \tag{2.49}$$

where $Q^{-1}(\cdot)$ is the inverse function of $Q(\cdot)$.

By substituting Eqn. 2.49 into Eqn. 2.48, the probability of detection can be calculated as:

$$P_d = Q\left(\frac{\sqrt{\sigma^2 E} Q^{-1}\left(P_{fa}\right) - E}{\sqrt{\sigma^2 E}}\right) = Q\left(Q^{-1}\left(P_{fa}\right) - sqrt(SNR)\right) \tag{2.50}$$

where $sqrt(\cdot)$ returns square root values. Same results may be found at [44].

Eqn. 2.50 reveals the relationship between the probability of detection, the probability of false alarm, signal and noise variances for matched filter under additive white Gaussian noise circumstance. Based on the above analysis, detection problem may be soloved by the following steps. A probability of false alarm is defined to meet design requirements. The threshold based on the probability of false alarm is thus calculated. By manipulating the conditional PDF of the probability of detection and the detection threshold, the probability of detection subject to the probability of false alarm may be computed.

It should be noted that, the above analysis is limited to a single sample. The improvement will occur when processing N_s samples instead of a single sample for a matched filter detector, which is investigated below.

In the case of N_s samples, the SNR may be given as:

$$SNR_{N_s} = \frac{(N_s P)^2}{N_s \sigma^2} = N_s \frac{E}{\sigma^2} \tag{2.51}$$

where P is transmitting power. By exploiting N_s samples, the value of SNR V_{SNR} is multiplied by N_s $(N_s V_{SNR})$.

The processing gain by N_s samples is correspondingly given as:

$$G = 10\log_{10} N_s \; dB \tag{2.52}$$

It is important to note that a processing latency is generated as soon as multiple samples are implemented.

2.2.3 Performance of the Matched Filter Detector

In this subsection, the probability of detection by considering the SNR of the matched filter detector is first examined. The probabilities of false alarm are listed in the figure. The probability of detection versus the various values of SNR is plotted in Fig 2.7. It is evident that given a probability of false alarm, the detection performance may be improved by increasing the values of SNR. It may be observed that for a given SNR, the probability of detection will be increased by reducing the probability of false alarm. Additionly, to achieve same probability of detection, more SNR is needed for higher probability of false alarm. For instance, a comparison is conducted between systems of $P_{fa} = 1 \times 10^{-4}$ and $P_{fa} = 1 \times 10^{-6}$. In order to achieve same probability of detection (0.6), an extra SNR is needed for the system of $P_{fa} = 1 \times 10^{-6}$.

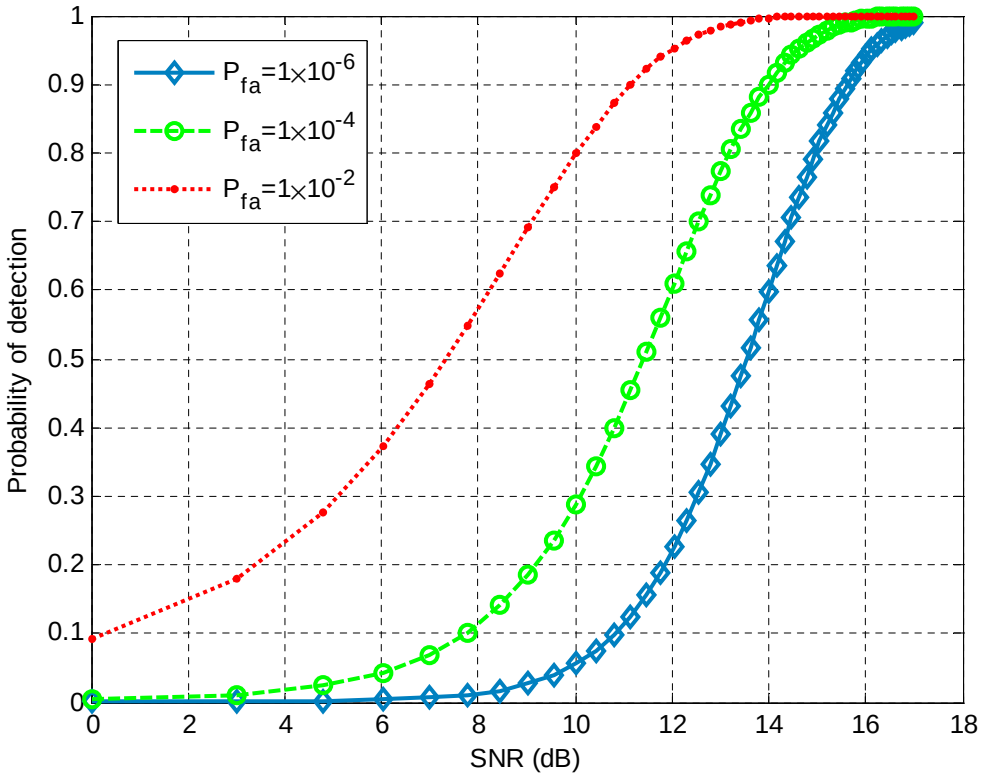

Figure 2.7: Detection performance of matched filter detector.

The corresponding probabilities of miss detection are depicted in Fig. 2.8. Same probabilies of false alarm are implemented, which are $P_{fa} = 1 \times 10^{-2}$, $P_{fa} = 1 \times 10^{-4}$, and $P_{fa} = 1 \times 10^{-6}$, respectively.

Fig. 2.9 below demonstrates the impact of different numbers (N_s) of processing samples. As expected, for a matched filter detector, the detection performance is significantly improved by processing more samples instead of a single sample. In Fig. 2.9, the values of N_s are 1, 2, 3, and 4, whereas the false alarm rate is fixed at millionth $\left(P_{fa} = 1 \times 10^{-6}\right)$.

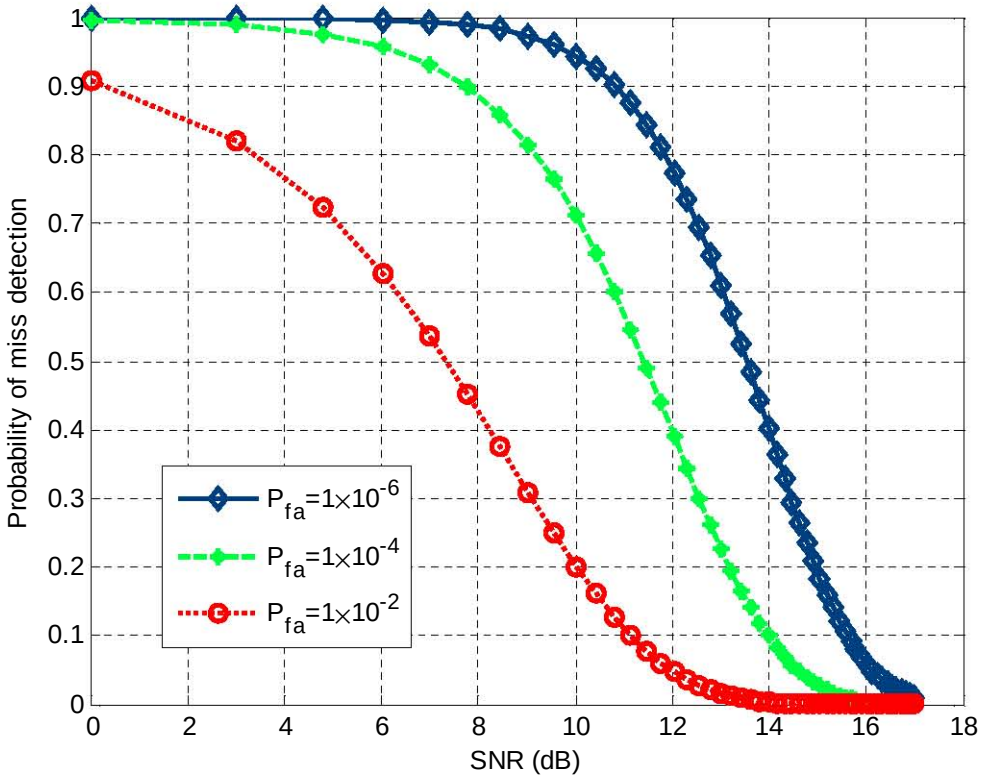

Figure 2.8: Mis-detection performance of the matched filter receiver.

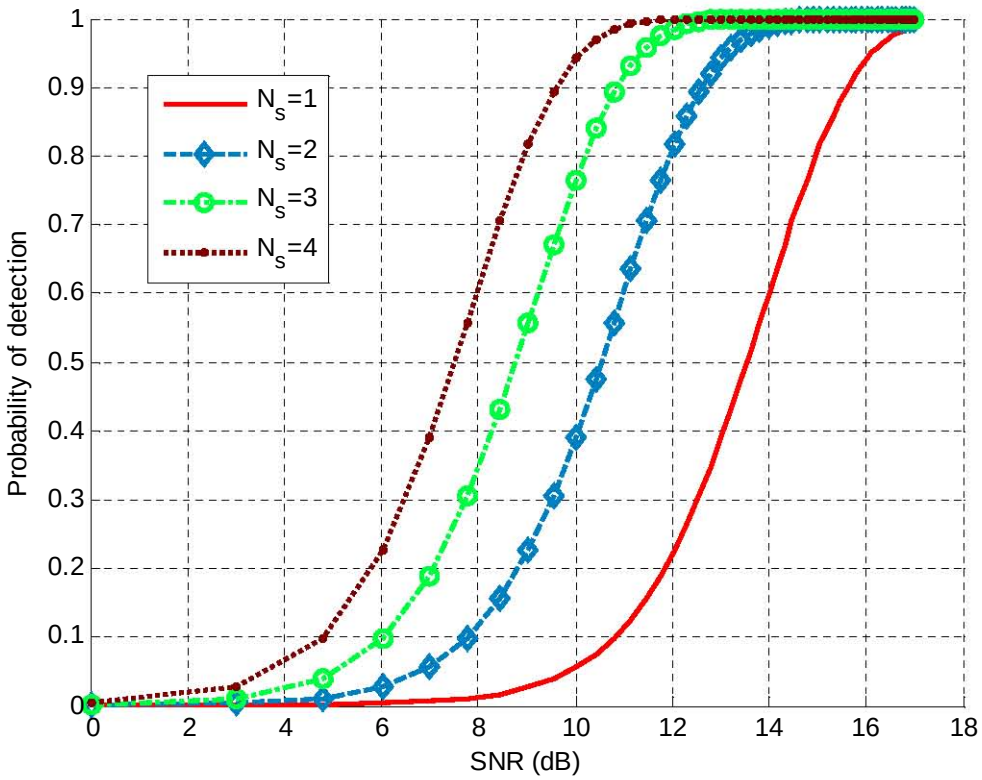

Figure 2.9: Probability of detection versus SNR in relation to different numbers of processing samples.

2.3 Ambiguity Function

It is well known that the ability of a radar system to detect or distinguish targets of interest from other objects (clutter) depends on the radar waveform. Thus, radar waveform design is a crucial subject for radar study. Ambiguity function, as a useful tool to analyse the resolution and ambiguity of the radar waveform, is studied in this section. It starts with a thorough explanation and comprehensive definition of the ambiguity function before examining the cross ambiguity function and the physical meaning of the ambiguity function. In addition, background related to the FM waveform ambiguity function are summarised, and ambiguity function surface plots in respect of time and Doppler shift are provided.

The ambiguity function is a widely used and powerful tool to analyse the properties of a radar signal waveform. In the ambiguity function surface plot, the properties of a radar waveform in respect of detection, parametric measurement accuracy, range and Doppler resolution, ambiguities and clutter rejection can be easily observed. The ambiguity function was formulated by Woodward (1953) [75]. As discussed in the matched filter section, a received signal having different Doppler frequency and time delay will be correlated with an original mirrored transmitted signal by the matched filter detector. The ambiguity function is made up of a series of correlation integrals based on the matched filter detector. Such a function describing the output of a matched filter in terms of time delay τ and Doppler frequency f_d may be mathematically represented as:

$$\chi(\tau,\ f_d) = \int_0^T s_r(t)\, s^*(t-\tau) \tag{2.53}$$

where $s_r(t)$ denotes the received signal and $s^*(t-\tau)$ is the transmitted or reference signal at delay τ. The symbol of $(.)^*$ signifies the complex conjugate operation and the integration time is represented as T.

A typical transmitted signal is in the form of:

$$s(t) = \mid u(t) \mid \exp[j2\pi f_c t] \tag{2.54}$$

where $\mid u(t) \mid$ is the magnitude of the transmitted signal, the symbol of $\mid . \mid$ denotes absolute the value of the complex number, and the carrier frequency is expressed as f_c.

It is assumed that the received signal $s_r(t)$, as stated above, is the mirrored version of the emitted signal except at time delay and Doppler frequency. Substituting Eqn. 2.54 into Eqn. 2.53, Eqn. 2.53 in respect of true time delay τ_0 is given as:

$$\chi(\tau,\ f_d) = \int_0^T u(t-\tau_0)\, u^*(t-\tau) \exp[j2\pi(f_c+f_d)(t-\tau_0)] \exp[-j2\pi f_c(t-\tau)] \tag{2.55}$$

If the effects of the true time delay and carrier frequency is not implemented($f_c = 0, \tau_0 = 0$), Eqn. 2.55 may be simply deduced as:

$$\chi(\tau,\ f_d) = \int_0^T u(t)\, u^*(t-\tau) \exp[j2\pi f_d t] \tag{2.56}$$

which is called the uncertainty function [54], whereas $|\chi(\tau,\ f_d)|^2$ is called the ambiguity function.

Some main properties are listed as follows [54]:

- The maximum value of the ambiguity function occurs at the origin, which means that the received signal is completely matched with the reference signal. With respect to the mathematical equation, it occurs only when the two signals have the same time delay and zero Doppler frequency, which is also referred to as the auto-correlation response of the waveform.

$$|\chi(\tau,\ f_d)|^2_{max} = |\chi(0,\ 0)| = (2E)^2 \tag{2.57}$$

  where the symbol of E denotes the energy of the signal.

- The time delay and Doppler frequency are symmetric along both time delay and frequency axes.

$$|\chi(\tau,\ f_d)|^2 = |\chi(-\tau,\ -f_d)|^2 \tag{2.58}$$

- The total volume is constant, which equals the maximum value of the ambiguity function. It should be noted that the integral works on all delays and Doppler frequencies.

$$\iint |\chi(\tau,\ f_d)|^2\, d_t d_{f_d} = (2E)^2 \tag{2.59}$$

- If the function $S(f)$ is the Fourier transform of the signal $s(t)$, then the ambiguity function can be calculated as:

$$|\chi(\tau,\ f_d)|^2 = \left| \int S^*(f)\, S(f-f_d) \exp[-j2\pi f t] \right|^2 \tag{2.60}$$

The proofs may be found in [51].

The ambiguity function can be calculated by calculating the term $u^*(t)\exp[j2\pi f_d t]$ subject to a given Doppler shift f_d. Then, the correlation output of $u^*(t)\exp[j2\pi f_d t]$ and $u(t)$ can be calculated.

An example of the ambiguity function is illustrated in Fig. 2.10, which depicts the ambiguity function surface plot of white Gaussian random variables with zero means and standard variance $(\sigma^2 = 1)$. According to the ambiguity function definition, a typical ambiguity function surface plot should be a 3-D plot, including the information of the Doppler shift and the time delay or equivalent distance away from antennas. The ideal ambiguity function of signal waveform is a Dirac delta function or thumbtack function. Consequently, it is expected, from the ideal signal waveform for radar systems, that the value of the ambiguity function is infinitely large at origin $(f_d = 0, \tau = 0)$, while it is zero

everywhere else. In a practical radar system, the ideal signal waveform should possess a infinite spike at $(f_d = 0, \tau = 0)$ and be near zero everywhere else. In Fig. 2.10, the output of the ambiguity function is normalized to 1. It may be observed from Fig. 2.10 that the white Gaussian distribution random variable is an ideal illuminator of opportunity relating to a passive radar system. In addition, the 2-D results of the ambiguity function for the time delay and Doppler frequency domains are presented to further demonstrate the waveform properties of Gaussian random variables. Furthermore, the AF output of white Gaussian noise is plotted on *dB* scale in Fig. 2.11.

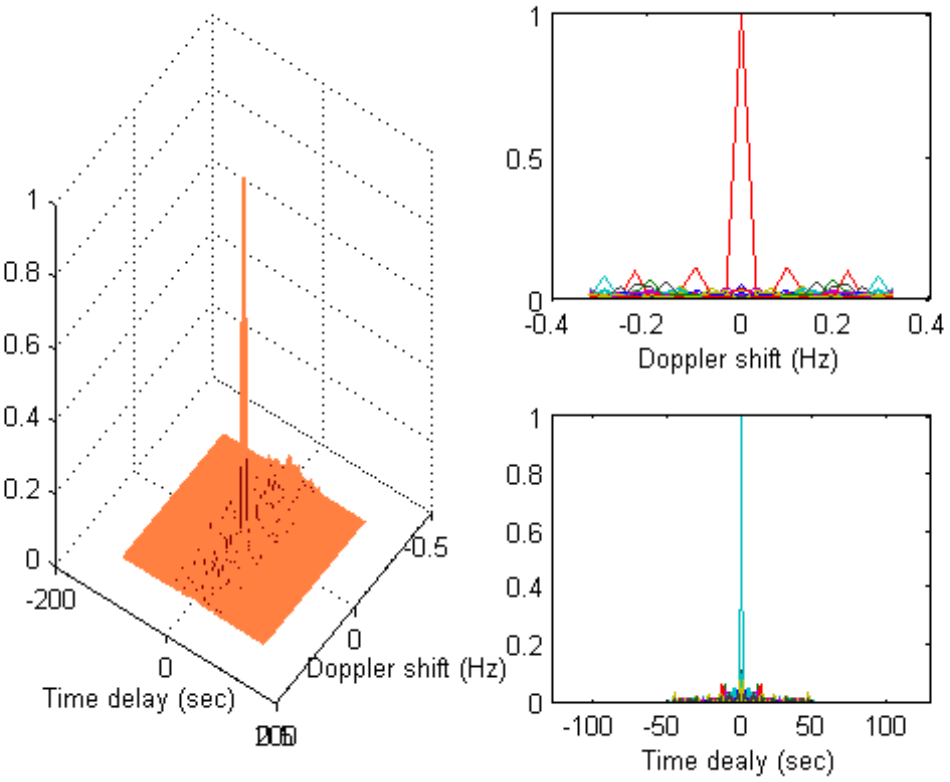

Figure 2.10: The AF surface of white Gaussian r.v.

Unlike the ambiguity function, the Cross Ambiguity Function (CAF), sometimes also called the Complex Ambiguity Function (CAF), deals with the correlation of two different signal waveforms in respect of a range of time and frequency offsets. Derived by Stein (1981) [65], a cross ambiguity function in respect of two different received signals s_1 and s_2 can be expressed as:

$$\chi(\tau,\ f_d) = \int_{-\infty}^{\infty} s_1(t)\, s_2^*(t-\tau) \exp[-j2\pi f t]\, dt \tag{2.61}$$

where τ denotes the time delay and f is the frequency offset to be searched.

Note that Eqn. 2.61 looks almost like the Fourier transform with respect to Doppler frequency, except that it is a function of range. In order to demonstrate the physical meaning of the cross ambiguity function for a radar system, $s_1(t)\, s_2^*(t-\tau)$ is replaced by $y(t)\, s^*(t-\tau)$, where $y(t)$ means the received information and $s(t-\tau)$ denotes the

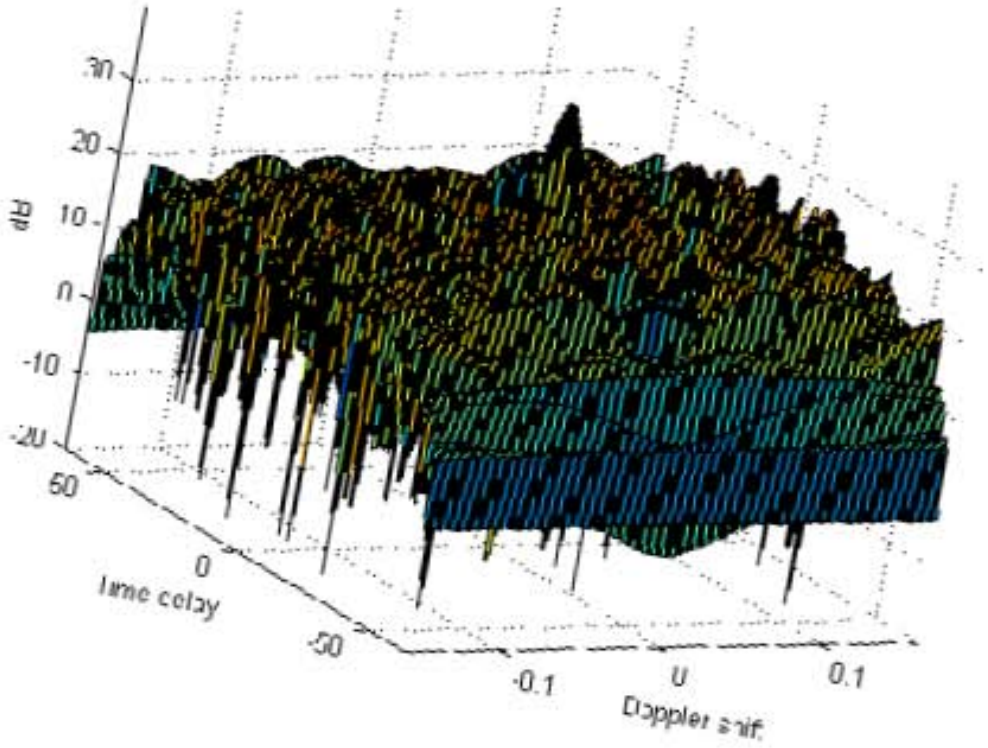

Figure 2.11: The AF output of white Gaussian r.v on dB scale.

transmitting signal at time delay τ, respectively. Two important points should be noted in this regard. The first one is that the cross ambiguity function for a radar system is the Fourier transform for the correlation product of the received signal and the transmitted signal. It is well known that the Fourier transform or Fourier analysis is an effective tool for power spectrum study, thus, the probability density of the scattering amplitudes can be measured by spectrum analysis. The second point is that, according to the theory of the matched filter, the optimal detection process is correlating the received signal with the original transmitted signal, so that the ambiguity function reveals the properties of the output of the matched filter in terms of detection, parametric measurement accuracy, range and Doppler resolution, and ambiguities. Ideally, the autocorrelation or the self-correlation of the transmitter signal should be a delta function, which means that the output of the autocorrelation of the transmitter signal should be 1 at the origin, but 0 at other place. Hence, the ideal plot of the autocorrelation of the transmitter signal should be a sharp spike at the point of origin.

Recently, passive radar systems attracted considerable attention. Unlike conventional radar systems, a passive radar detects and tracks an object of interest by exploiting the reflective signals from non-cooperative illuminators of opportunity, such as commercial FM broadcasting signals, Digital Audio Broadcasting (DAB) signals, Digital Video Broadcasting (DVB) signals, wireless communication signals, etc. By utilising non-cooperative radar transmitters, such a radar system benefits from low hardware costs, covert operation,

robustness against stealth, etc.

In this dissertation, the detection performance of a MIMO passive radar system experiencing FM broadcasting signals will be studied. Therefore, some essential background of the cross ambiguity function of such a passive radar system based on FM signals will be presented to illustrate the potential of FM signals as illuminators of opportunity. The FM theory will be studied. Besides of theory study, the results of a sinusoidal wave by frequency modulation are demonstrated to assist theory understanding. lastly, the ambiguity function surface plot of above corresponding FM signals is also presented to show the potential of FM signals as an ideal illuminator of opportunity for passive radar systems.

FM is widely used in the field of broadcasts radio. As an analogue modulation, FM conveys information signals over a sinusoidal carrier wave. The modulation is done by using its instantaneous frequency, in which the frequency of the carrier wave is modulated. FM can be also referred to as Phased Modulation (PM) because PM is the time integral of FM modulation signals. The FM transmitted signal in respect of carrier amplitude A_c and carrier frequency f_c can be represented as:

$$y(t) = A_c \cos\left(2\pi f_c t + 2\pi f_\triangle \int_0^t s(\tau)\, d\tau\right) \tag{2.62}$$

where $f_\triangle$ denotes the frequency deviation, which is defined as the maximum frequency shift away from the carrier frequency f_c in one direction. $f_\triangle$ is also called the frequency sensitivity, which measures the signal transmitted over the given bandwidth. $s(t)$ is the information signal, of which the amplitude is restricted to 1 ($|\, s(t)\, | \leq 1$).

Normally, a baseband modulated signal may be approximated as a sinusoidal wave with a frequency f_s. The integral of such a sinusoidal wave can thus be given as:

$$s(t) = \frac{A_s \cos(2\pi f_s t)}{2\pi f_s} \tag{2.63}$$

A_s is the amplitude of the information signal, which is below 1.

Therefore, the FM transmitted transmitting signals given in the condition of Eqn. 2.63 could be further simplified as:

$$y(t) = A_c \cos\left(2\pi f_c t + \frac{f_\triangle}{f_s}\cos(2\pi f_s t)\right) \tag{2.64}$$

The FM signals based on the above analysis are illustrated in Fig. 2.12. The original signal is a sinusoidal wave with frequency 50 Hz The carrier frequency for FM in this case is 200 Hz. The frequency deviation is 10 Hz, which means that the maximum frequency away from the carrier frequency in one direction is 10 Hz.

Now considering a simple passive bistatic radar system with one transmitter and one receiver and exploiting FM broadcasting signals, the corresponding direct signal from the transmitter can be simply expressed as:

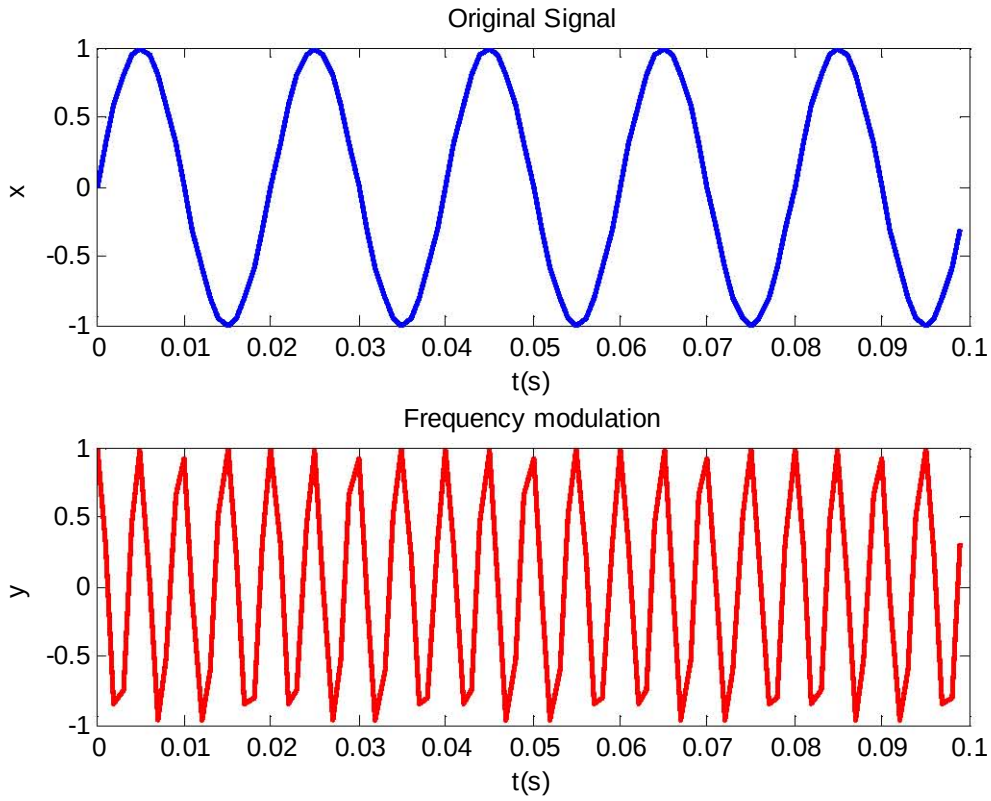

Figure 2.12: The frequency modulation signal.

$$R = \sqrt{E}AS + W \tag{2.65}$$

where R is the received signal, E denotes the transmitted signals energy, $\sqrt{E}$ is thus the transmitted signals power, the symbol of A signifies the amplitude, S represented the FM transmitted signal, and W indicates the channel noise, which has white Gaussian distribution.

The ambiguity function surface plot of the above FM signals is shown in Fig 2.13. It can be seen from this figure that a thumbtack plot may be achieved that is similar to the white Gaussian distribution random variables. Consequently, the FM illuminator of opportunity is regarded as the Gaussian or equivalent Gaussian random variables. In fact, according to the Central Limit Theorem (CLT), the received signal without a target for a passive radar system by exploiting FM illuminators of opportunity utilises Gaussian random variables. The detailed derivation will be presented in Chapter 3. From Fig. 2.13, we can conclude that FM broadcasting signal is an ideal illuminator of opportunity for passive radar systems. Lastly, the AF output of FM signals on dB scale is presented in Fig. 2.14.

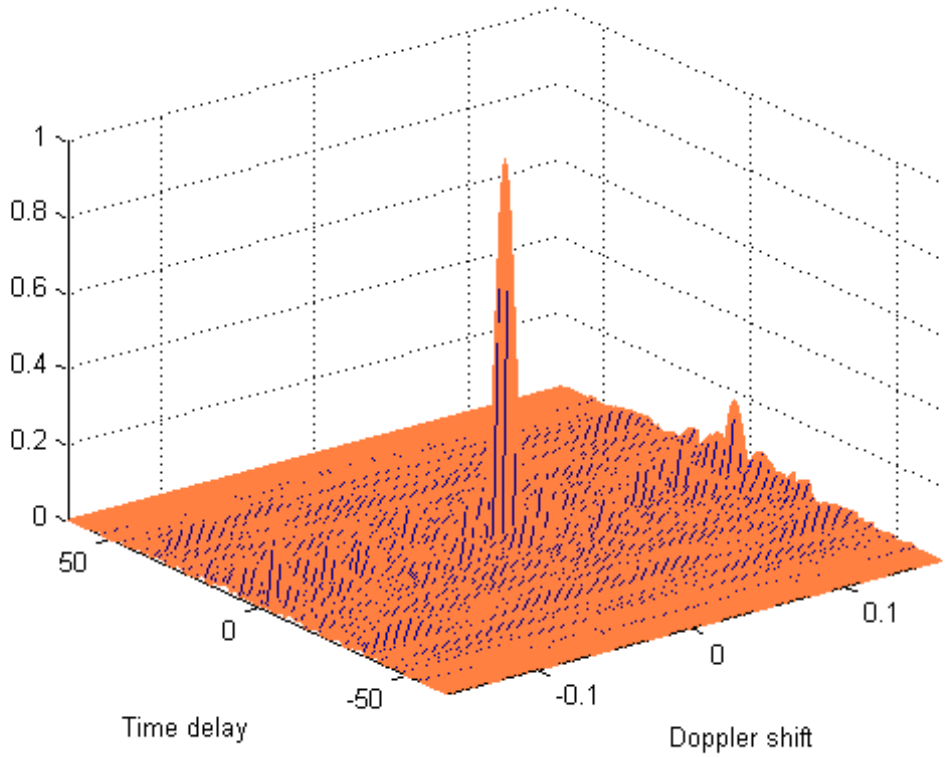

Figure 2.13: The ambiguity function of FM signals.

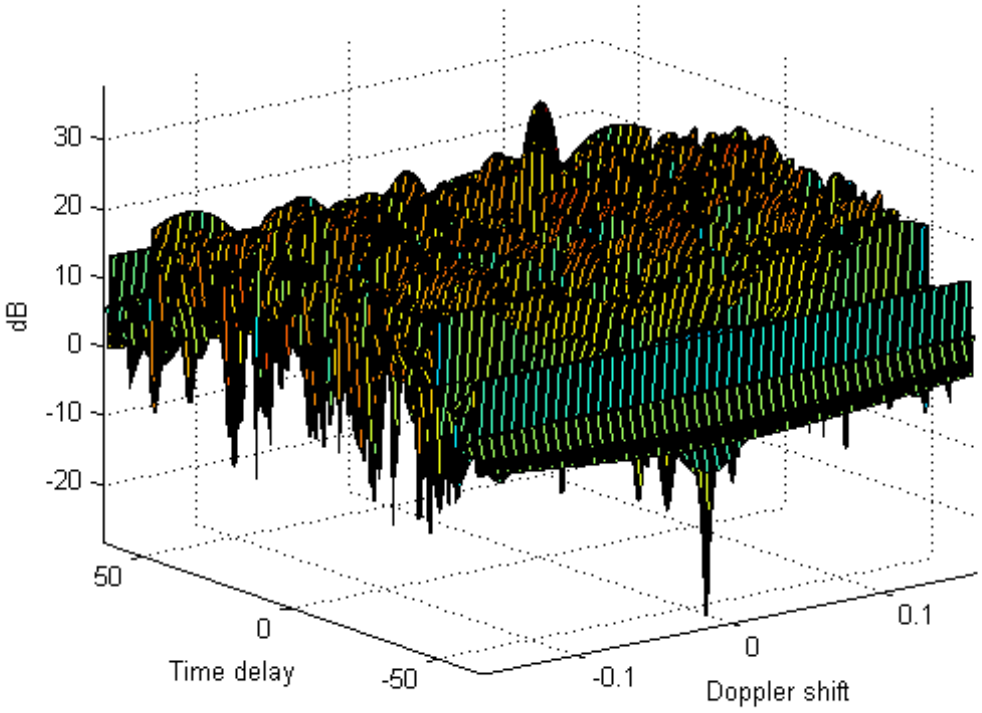

Figure 2.14: The ambiguity function output of FM signals on *dB* scale.

2.4 Literature Review

In this section, selected papers on the detection performance of MIMO radar systems are reviewed.

As a fundamental principle, the principle of detection for a radar system attracted considerable interest since radar has been invented. A comprehensive understanding of detection principle for a radar system may be found in [47]. Originally published in 1968, [47] is one of the great time-tested classics in the field of detection theory. The detection theory of Gaussian signals in white Gaussian noise is introduced in details. Furthermore, the detection theories of slowly fluctuating point targets, Doppler-spread targets, and channel range-spread targets are also presented. The book of [21] is also one of classic test books. The following topics are covered in detail. [21] begins with relating math fundamentals, such as probability theory, random processes, and statistical decision theory. Optimum radar detection is then introduced. Both nonfluctuating model and fluctuating models detection based on multiple observations are presented. Based on the radar equation, cumulative detection of both stationary and moving targets is further presented. In addition, an interesting topic is also given to reduce testing time, which thus can achieve more efficient detection.

The concept of MIMO as applied to a single transmitter and receiver radar was investigated by Fishler et al [28]. Motivated by the potential of MIMO techniques to overcome channel fading in a communication system, Fishler et al adapted the concept of MIMO to a radar system, with the aim of dealing with similar issues, namely, the fluctuations of targets. In conventional radar systems, fluctuations of targets are responsible for degrading performance. In contrast, the proposed MIMO radar exploits independently transmitted signals from the widely spaced transmit antennas to achieve better RCS estimation of the underlying targets, which consequently improves the performance of a radar system. In Fishler et al's paper [28], such a MIMO radar system model was described. Due to the space limits of a conference paper, the focus of the analysis was on the direction finding (DF) performance of the proposed MIMO radar system. The numerical results in terms of the Cramer-Rao bound are presented, which show that the MIMO technique may dramatically improve the performance of a radar system in terms of DF accuracy.

Fishler et al further studied and analysed the detection performance of MIMO radar systems in their work [29, 30]. Paper [29], which was also a conference paper, is a concise version of paper [30], where the detection performance of MIMO radar systems was studied by Fishler et al. A novel concept, viz. statistical MIMO radar, was introduced, which can also be found in other work by Haimovich et al [35]. By utilising the classic Neyman-Pearson hypothesis test, the optimal detector for statistical MIMO radar systems was developed and the simulated results of the optimal detector were presented. The advances of statistical MIMO radar in terms of detection emerged when it was compared with conventional phased array radar systems, multiple input single output (MISO) radar systems. As the basis of statistical MIMO radar systems, the concept of widely spaced

antennas is numerically defined in [30].

The comparison between this novel multiple-antenna radar and conventional multiple-antenna radar is inevitable. A well-known paper regarding comparison between MIMO radar and phased arrary radar was presented in [18]. The comparison was carried out on the following 5 aspects: waveforms, transmit antenna, transmit antenna gain, SNR, and maximum useful area of range-Doppler space. As an advanced wireless communication technique, MIMO has been proved a promising solution for next generation wireless communication to increase channel capacity and decrease bit error ratio [8][70]. On the other hand, phased array radar is a mature and developed multiple-antenna technique for radar systems. The comparison is more or less unfair for MIMO radar systems. It should be noted that unlike phased array radar, the way to improve the performance of MIMO radar is to utilise angular diversity or space diversity but not coherent gain, which is a novel approach to implement multiple-antennas on a radar system. Furthermore, combined with phased array radar systems, MIMO-phased radar was proposed in [38] by exploiting MIMO radar with collocated antennas. This novel system aims to enjoy advantages of angular or space diversity from MIMO technique on one hand, without sacrificing the main advantages of phased array radar systems on the other hand. The effectiveness of the proposed combined MIMO and phased radar systems may be observed from numerical results.

It should be noted that in papers [28][30], only Swerling I model targets are employed. It is well known that the basic work on the detection of fluctuating targets has been done by Peter Swerling [66]. The fluctuating targets may be further characterised into four categories. In respect of case I and case III, the fluctuating targes are summarised as slow fluctuation, which are scan-to-scan fluctuating. The amplitude distribution can be recognized as well-known Rayleigh random distribution. Whereas the cases of Swerling II and Swerling IV are characterised as fast pulse-to-pluse fluctuating targets, which represents that the targets whose return is independent from pulse to pulse. Based on the PDF of a radar RCS, the probability of detection of a fluctuating target is calculated in [23]. As a function of estimate of the stationary mean, correlation function, and PDF, the RCS amplitude distribution of a complex target is modeling. By utilising chi-squared and Kolmogorov-Smirnov nonparametric test, under the null hypothesis, it has been shown that the data follow a particular theoretical distribution. With a knowledge of classical detection statistics, the probablity of detection for a complex target can be calculated. Drumheller, David M extended Swerling fluctuating models to Chi-square models [24]. In addition, Rice and Log-normal fluctuating tagets detection are presented in [19][20].

Acting as a catalyst, papers [29, 30] attracted the attention of more and more scholars who were interested in the field of MIMO radar. Sammartino et al, for example, extended MIMO radar systems by using real target models [61]. Unlike [30], which only examined the Swerling case I. Sammartino et al [61], also looked at the spherical and Swerling case III. In addition to studying MIMO radar systems, the real target models were also applied

to two other multiple antennas radar systems,viz. netted radar and re-phased netted radar. A more concrete Rice target detection study of MIMO radar systems was presented by Tang et al in [68]. Based on Stein's lemma, an optimum detector for the Rice targets of MIMO radar systems was developed by exploiting the concept of relative entropy. Some interesting results were achieved. In the low SNR region, the Rice target detection of MIMO radar depends on the number of receive antennas. In the high SNR region, the improvement of the detection performance depends on the product of the number of transmit antennas and the number of receive antennas. Another detection study of MIMO radar systems based on relative entropy can be obtained from Tang et al [67].

Subsequently, the detection of a target, composed of a finite number of small scatterers, was examined by Du et al [26]. As special configurations, the system models presented in [30] were extended to a general case without placing a limitation on the locations of antennas. The theoretical probability of detection expression was derived to predict the performance of MIMO radar systems, which is a meaningful guideline to avoid time-consuming simulations in practice. At the IEEE international radar conference 2009, Du et al, extended the target model to a more realistic case [25].

The detection performance of MIMO radar systems with clutter effects may be obtained from Sammartino et al in [15, 60]. Based on the Spherically Invariant Random Vector (SIRV), a novel MIMO detector was introduced by Chong et al in the non-Gaussian clutter environment [15]. Gamma and Weibull clutter models, for example, were applied to MIMO radar systems. The theoretical performance of the new detector was investigated, which was verified by Monte Carlo simulations. It was showed by simulation results that the detection performance of MIMO radar may be improved dramatically by the new detector. In [60], for instance, the effects of K-distributed clutter on the detection performance of MIMO radar systems were examined. The simulation results showed that the detection performance may be improved significantly by increasing the number of antennas.

Inspired by the development of passive radar systems, some attempts were made to apply the concept of MIMO to passive radar systems. By using third party transmit antennas, for example, a passive radar system possesses many advantages, such as low cost of operation and maintenance, covert operation, rapid updates etc. A MIMO passive radar based on FM radio transmit antennas was thus investigated by Krzysztof Kulpa and Mateusz Malanowski in [45], where the MIMO passive radar is used to increase surveillance volume. A paper by Jeong et al [40] examined the performance of MIMO radar systems embedded in the Wideband Code Division Multiple Access (W-CDMA) network. A W-CDMA rake receiver was developed for MIMO passive radar systems. Since W-CDMA is a successful commercial 3G wireless communication system, this novel mechanism of integrating radar with W-CDMA is more flexible and convenient.

In addition, some novel types of radar systems were developed based on MIMO radar. In [22][76], Wu et al extended the existing MIMO radar systems with Orthogonal Frequency

Division Multiplexing (OFDM) waveforms. An overwhelming advance from MIMO OFDM radar is that it can meet a deficit of demanding capacity for MIMO radar systems. Another reason is that the proposed MIMO OFDM radar may be a promising type of MIMO passive radar that uses digital illuminators of opportunity. A MIMO radar experiences frequency diversity, introduced in [79]. It can be observed that such frequency diversity may significantly reduce the target's fluctuations.

In contrast, unlike the above MIMO radar systems with orthogonal waveforms, a concept paper of MIMO radar systems with coherent pulse detector was investigated by A. Sheikhi and A. Zamani in [62]. By exploiting temporal coherent pulse, the proposed MIMO radar systems overcome the difficulties of the classic phased array radar systems in terms of parameter identifiability, flexibility of transmit beampattern design, degree of freedom, tracking ability, jammer rejection, etc. The coherent detection performance in respect of MIMO radars may be also obtained by A. Sheikhi and A. Zamani in [63], where Constant False Alarm Rate (CFAR) and Generalized Likelihood Ratio Test (CLRT) detectors were developed. The superiority of MIMO radars over the conventional phased array radars with regard to coherent processing may be observed. Besides of temporal coherent pulse, an adaptive detector based on GLRT was also proposed. The detection performance of MIMO radars with coherent pulses was examined by Qu et al in [58]. It is worth noting that the detection performance of MIMO radars with coherent pulses in Swerling case I targets overcomes that of Swerling case II targets, while, normally, the performance of a radar system in Swerling case II targets is better than that of a radar system in Swerling case I targets.

In reality, it is hard to receive either fully correlated or independent signals from different antennas. Therefore, a more realistic case of partially correlated scattering from the target has been examined in [6]. The GLRT detector for target detection was proposed based on the maximum likelihood estimates of the unknown parameter. Target detection and identification by using canonical correlation and subspace partitioning was proposed by Wei in [73]. The maximum canonical correlation between the targets set and the observations and coefficients of the canonical vector have been utilised to identify and detect targets. In addition, the study on the correlation and optimization of waveform for MIMO radar systems was conducted by K. W. Forsythe [32]. Two types of waveform optimization were examined based on static radar systems. By exploiting space-time coding, it has been proved by X. Song et al, the cross correlation of waveform for MIMO radar systems may be significantly reduced [77]. The performance degradation in resolving spatially close returns can be attributed to the correlation among waveforms. In [77], space-time coding, also known as a MIMO technology, was implemented to migrate effects of cross correlation. The effectiveness of space-time coding may be observed from numerical results.

2.5 Summary

In this chapter, the background of this dissertation was introduced. The Doppler relationship for a single transmitter and receiver bistatic radar system was examined. Defined as the time rate or change of the total path length of the scattered signal, the Doppler frequency is determined by the projected velocity component of the target along the bistatic bisector. Simulation results under various scenarios were presented. To assess weather it is an efficient detector, the matched filter theory was examined. The mathematical forms of the probability of detection subject to the probability of false alarm and the values of SNR were derived based on the theory of matched filter detection. Both non-fluctuating targets and fluctuating targets were implemented. Both analysis and simulation results of detection and mis-detection are provide. The derived expression was verified by the simulation results. In addition, the processing gain of multiple samples for a matched filter detector was examined. The ambiguity function of the FM signals was studied. It is evident from the simulation results that such an illuminator of opportunity is an ideal passive source of information for a radar system. Lastly, selected papers studying detection abilities of MIMO radar systems were reviewed.

Chapter 3

Detection Performance in respect of Stationary Targets

As it is well known, a radar system transmits electromagnetic energy to detect targets. Some of this energy is reflected off of targets or called scatterers within the search volume, which is referred to as a radar return. The probability of detection is the probability that a sample amplitude of the radar return exceeds the predefined threshold voltage. The variations within a target's RCS is responsible for lowering the probability of detection. It was found by Swerling [66] that the detection performance of a radar system may be significantly degraded by the fluctuations of a target's RCS. In order to commemorate his contribution, the models of fluctuation targets were named after Swerling. Phased array radar was proposed to increase the received target signal energy, in which either transmit or receive antennas are placed close together to maximise the coherent signal processing gain.

Inspired by the development of MIMO techniques in the field of wireless communication, the notion of MIMO radar was first introduced in the proceedings of the IEEE international radar conference 2004. It is well known that detection and estimation are the two key problems of radar systems, although these are not only limited to radar systems but also extend to communication systems. As a promising method of overcoming fading during transmission, MIMO or space-time coding concepts were adapted to radar systems to address the problems of the reflected signal fluctuations. As an alternative approach, MIMO radar exploits the angular diversity of targets to reduce the effects of targets' fluctuation. It is evident from the simulation results by Fishler. et al [29] that the performance of a radar system in terms of detection, estimation, navigation, etc can be significantly improved by such angular diversity.

In order to generate angular or spatial diversity, as is the case in communication systems, the spacing of antennas is crucial in MIMO radar systems. It is well known that, in MIMO communication systems, the multiple antennas must be widely spaced in order to transmit independent signals. When the concept of MIMO from a communication system is applied to a radar system, it is also the objective of MIMO radar systems to achieve

spatial (angular) diversity, where the widely separated antennas can measure the RCS of a target from different angles and consequently provide a better understanding of the target of interest.

This chapter is organised as follows. In the first section below, the detection performance of MIMO radar systems is examined. It thus looks at comparative studies between MIMO radar and phased array radar systems in order to illustrate their respective properties. The second section develops a practical distributed MIMO radar configuration in terms of bandwidth limitation. The closed-form probability calculations of detection based on OR, MAJ, and AND rules are computed and simulation results under various scenarios are presented. In the last section, by exploiting illuminator of opportunity, the MIMO passive radar system based on FM signals is proposed. The simulation results of such a MIMO passive radar system is provided as a function of different values of SNR, various numbers of antennas, different integration times, etc.

3.1 Detection Performance of MIMO Radar Systems

The detection probability of MIMO radar systems is analysed and evaluated in this section. This analysis may be divided into the following parts, which are listed as follows:

- A MIMO radar system model is depicted. The closed-form expression of the probability of detection is derived, and it is verified by the simulation results.
- Comparative studies between MIMO and phased array radar systems are carried out.
- The robustness to clutter between of MIMO and phased array radar systems are examined and compared.

3.1.1 MIMO radar probability of detection calculations

Without loss of generality, a MIMO radar system with M transmit antennas and N receive antennas is employed. It is assumed that a narrow-band signal is emitted by the ith transmit antenna $\left(\sqrt{E/M}s_i(t)\right)$, where E is the total energy. The orthogonal waveform $s_i(t)$ satisfies:

$$\int_0^T s_i(t)\, s_j^*(t)\, dt = \delta_{ij} = \begin{cases} 0 & i \neq j \\ 1 & i = j \end{cases} \tag{3.1}$$

where the symbol of $(\cdot)^*$ denotes the conjugate operation.

The received signals are of the form:

$$r(t) = \sqrt{\frac{E}{M}}\alpha s(t-\tau) + w(t) \tag{3.2}$$

where $r(t)$ represents the received signal. The target is modelled as Swerling type I, hence α are independent and identically distributed (i.i.d.) complex Gaussian random variables with zero mean, which may be expressed as $\alpha \sim CN\left(0, \sigma^2 I_{MN}\right)$. I_{MN} is the identity matrix with size MN by MN $(MN \times MN)$. As mentioned before, $s(t-\tau)$ is the transmitted signal. The symbol of $w(t) \sim CN\left(0, \sigma_w^2 I_{MN}\right)$ indicates AWGN. It should be noted that there are M orthogonal waveforms due to M independent transmit antennas.

In order to ensure the angular or spatial diversity, it is crucial that the antennas are widely separated. In [30][76], the minimum distance among antennas is derived, and it is of the form:

$$d \geq \frac{\lambda R}{D} \tag{3.3}$$

where λ denotes the wavelength of the signal waveform, R represents the distance between the target of interest and the antenna, and D is the effective size of the target. The λ/D indicates the beamwidth of the energy backscattered from the target towards the transmitter. Eqn. 3.3 means that when the inter-element spacing in the transmit antenna array is greater than the target beamwidth coverage at distance R, the target then presents different aspects to adjacent transmit antennas. This minimum distance is the measure to distinguish MIMO radar from conventional multiple-antenna radar, phased array radar. If the distance among antennas is below or fails to obey this measure. A high correlation between signals either transmitted or received by an array will thus occurs. Conversely, the MIMO technique improves detection performance of a radar system by exploiting the independence between signals at the array elements. Therefore, throughout the dissertation, the minimum distances among antennas obey Eqn. 3.3 strictly.

The Neyman-Pearson hypothesis of MIMO radar may be expressed as:

$$X = \begin{cases} H_0: \ w(t) \\ H_1: \ \sqrt{\frac{E}{M}}\alpha s(t-\tau) + w(t) \end{cases} \tag{3.4}$$

H_0 denotes the null hypothesis and the symbol of H_1 signifies the alternative hypothesis, which means that the target exists at delay τ.

The distribution of the test statistic is of the form [26][30][35]:

$$\| X^2 \| \sim \begin{cases} H_0: \ \frac{\sigma_w^2}{2}\chi_{2MN}^2 \\ H_1: \ \left(\frac{E}{2M}\sigma_\alpha^2 + \frac{\sigma_w^2}{2}\right)\chi_{2MN}^2 \end{cases} \tag{3.5}$$

Where χ_{2MN}^2 represents a chi-square random variable with $2MN$ degrees of freedom. The symbols of σ_α^2 and σ_w^2 represent the variance of fluctuation of a target's RCS and noise, respectively. Due to Swerling I targets implemented, α is sampled from complex Gaussian random variables $\left(\alpha \sim CN\left(0, \sigma^2 I_{MN}\right)\right)$. The variance of α is affected by the transmitted signal power.

Therefore, the optimal detector in terms of the Neyman-Pearson test is given by:

$$\| X^2 \| \begin{array}{l} > H_0 \\ < H_1 \end{array} \gamma_{MIMO} \tag{3.6}$$

where γ_{MIMO} is the threshold, depending on the value of the probability of false alarm. The corresponding probability of the false alarm is given as:

$$P_{fa} = P\left(\frac{\sigma_w^2 \chi_{2MN}^2}{2} > \gamma_{MIMO}\right) \tag{3.7}$$

Thus, the threshold γ_{MIMO} may be computed as:

$$\gamma_{MIMO} = \frac{\sigma_w^2}{2} F_{\chi_{2MN}^2}^{-1}\left(1 - P_{fa}\right) \tag{3.8}$$

where $F_{\chi_{2MN}^2}^{-1}$ represents the inverse cumulative distribution function of a chi-square random variable with $2MN$ degrees of freedom.

Furthermore, the probability of detection for MIMO radar systems is of the form:

$$P_d = P\left(\frac{E}{2M}\sigma_\alpha^2 + \frac{\sigma_w^2}{2}\right)\chi_{2MN}^2 > \gamma_{MIMO} \tag{3.9}$$

Substitute Eqn. 3.8 into Eqn. 3.9, and thus the probability of detection is given as [30][35]:

$$P_d = 1 - F_{\chi_{2MN}^2}\left(\left(\frac{\sigma_w^2}{\frac{E}{M}\sigma_\alpha^2 + \sigma_w^2}\right) F_{\chi_{2MN}^2}^{-1}\left(1 - P_{fa}\right)\right) \tag{3.10}$$

The probability of detection in respect of the values of SNR is plotted in Fig. 3.1. Three different numbers of antennas for MIMO radar systems have been employed, two by two, five by five, and eight by eight systems, respectively. A two by two (2×2) system consists of two transmit antennas and two receive antennas. The probability of false alarm is fixed at millionth $\left(P_{fa} = 1 \times 10^{-6}\right)$, which means that the false alarm is only allowed to happen once over million data. The results from left to right are eight by eight, five by five, and two by two systems, respectively. As expected, by exploiting angular or spatial diversity, the detection performance of MIMO radar systems may be significantly improved by increasing the number of antennas. For example, take two by two and five by five systems as an example, with respect to the same performance $(P_d = 0.5)$, about two dB diversity gain is provided by the five by five MIMO radar system over the two by two MIMO radar system.

Fig. 3.2 depicts the probability of mis-detection versus SNR. As is the case with MIMO in wireless communication fields, in Fig. 3.2, a linearly scaled y-axis is replaced by a logarithmically scaled y-axis. A three by three MIMO radar system is compared with a four by four MIMO radar system. The probability of false alarm is fixed at millionth,

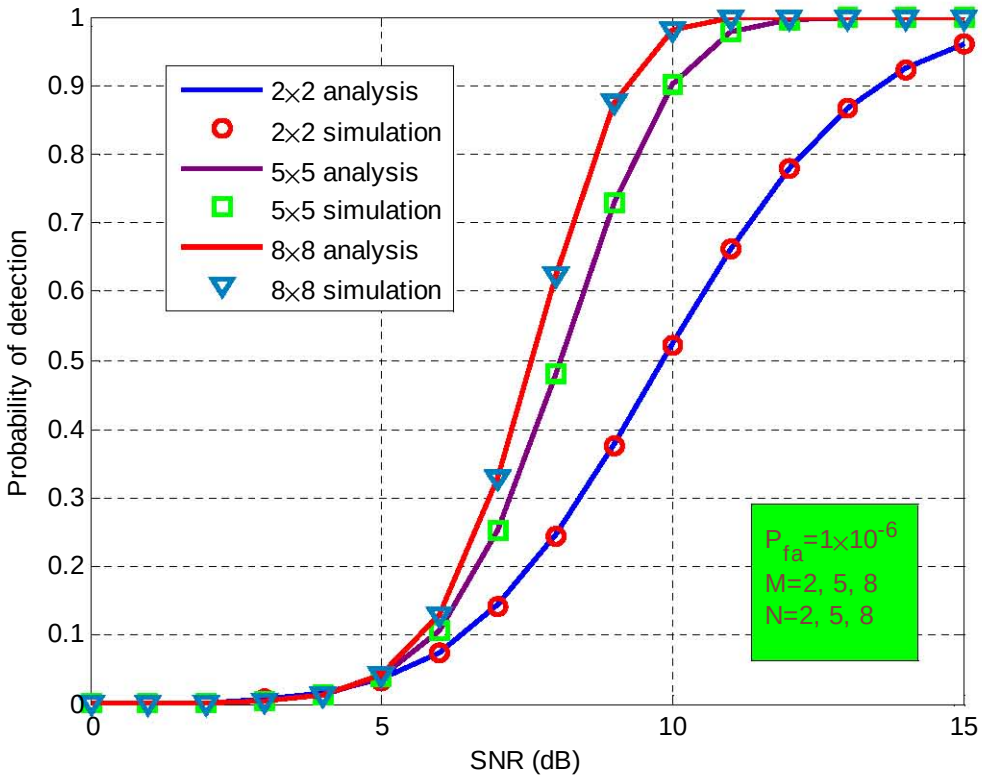

Figure 3.1: Detection performance of MIMO radar systems.

as was the case in the previous example. The red-dot results and the blue-solid results are those obtained with the three by three and four by four systems, respectively. The potential of MIMO radar system in terms of detection performance is clearly shown in Fig. 3.2. There is about a 1.5 dB diversity gain from the four by four MIMO radar system when the probability of mis-detection equals one percent $\left(P_{miss} = 1 \times 10^{-2}\right)$.

The last result presented in this sub-section is the Receive Operating Characteristic (ROC) plot of the MIMO radar systems, which demonstrates the relationship between the probability of detection and the probability of false alarm. Also known as Relative Operating Characteristic, a ROC curve demonstrates the sensitivity of true rate versus false rate. With respect to a radar system, a classical ROC curve indicates the sensitivity between the probability of detection and the probability of false alarm. A MIMO radar system made up of two transmit antennas and two receive antennas is employed to illustrate the ROC performance. The values of SNR are one and three $(SNR = 1dB, 3dB)$ and the probability of false alarm varies uniformly from zero to one $\left(P_{fa} \sim (0-1)\right)$. The number of transmit and receive antennas are five $(M = N = 5)$, as is shown in x-axis. A common sense may be observed that more SNR is needed to realize the same probability of detection when a lower probability of false alarm is required.

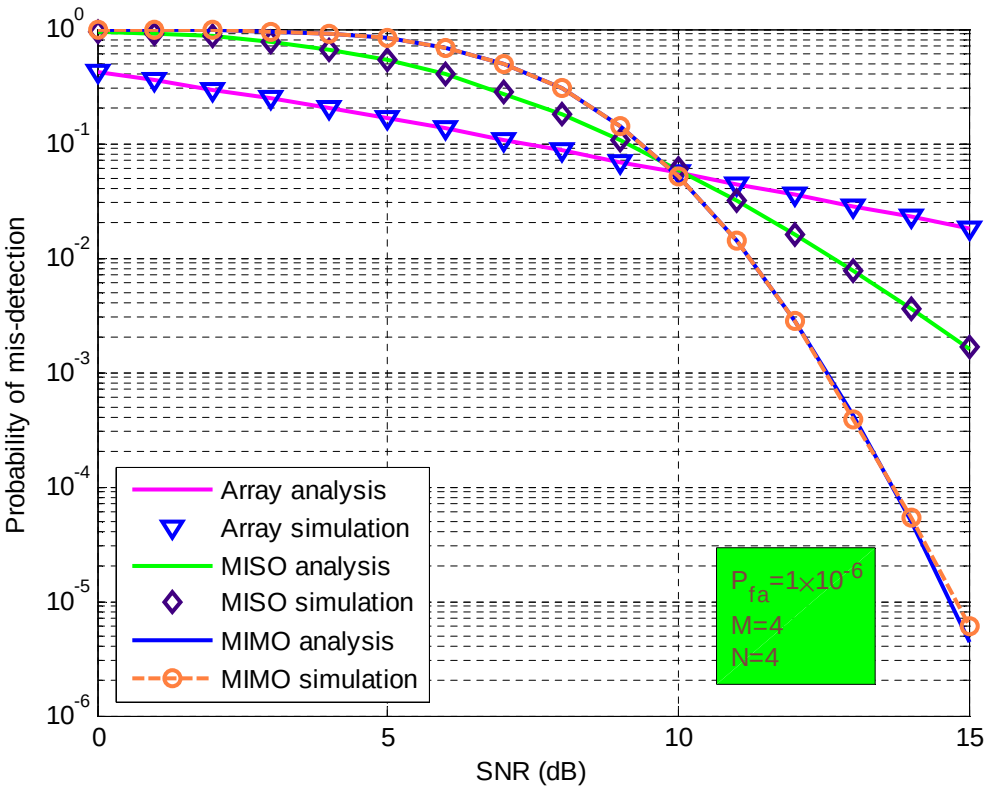

Figure 3.2: Probability of mis-detection of MIMO radar systems.

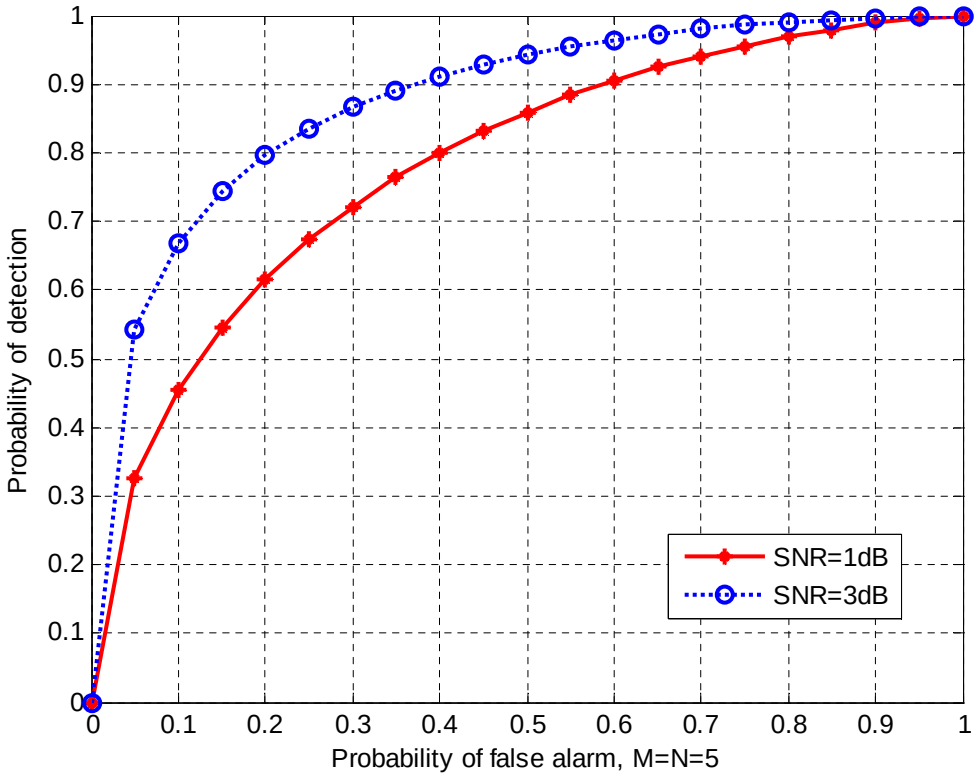

Figure 3.3: ROC performance on various SNR.

3.1.2 Comparison between MIMO and phased array radar systems

To create a fair comparison, a phased array radar system with M transmit antennas and N receive antennas is implemented. It is also assumed that the narrow-band signal is emitted by the ith transmit antenna $\left(\sqrt{E/M}s_i(t)\right)$, where the symbol of E denotes the total energy. The orthogonal waveform $s_i(t)$ may be represented same as Eqn.3.1. It should be noted that with respect to both MIMO and phased array radar systems, the total transmit power is normalised to one. Since, as stated previously, there are M transmit antennas and N receive antennas for MIMO and phased array radar systems, the transmit power of each element is equal.

After passing through the matched filter, the output of the matched filter is of the form:

$$r(t) = \sqrt{\frac{E}{M}}\alpha\varphi(x,y)^H \varphi\left(x^{'},y^{'}\right)\psi(x,y)^H \psi\left(x^{'},y^{'}\right)s(t-\tau)+w(t) \tag{3.11}$$

where $\psi(x,y)$ and $\varphi(x,y)$ indicate the relative position between transmit antennas and targets, receive antennas and targets, respectively. The symbols of $\varphi\left(x^{'},y^{'}\right)$ and $\psi\left(x^{'},y^{'}\right)$ are relative beamformers from transmit and receiver position to targets, respectively. $(.)^H$ denote Hermitian transform operations. The symbol of $w(t)$ represents the noise. With respect to phased array radar systems, the understanding of a target of interest will be reinforced by altering the relative phase of signal fed to each antenna. The symbols of $\psi(x,y)$ and $\varphi(x,y)$ describe position relative parameters, such as angles between either transmit or receive antennas and targets. As is well known, in phased array radar systems, the processing gain is achieved when the steer toward direction of beamformer from the receiver equals the angle of the target between the receiver $(x,y) = \left(x^{'},y^{'}\right)$. This processing gain of the phased array radar system when the beamformer steers to the target may be mathematically expressed as [30][31]:

$$\varphi(x,y)^H \varphi\left(x^{'},y^{'}\right) = N \tag{3.12}$$

$$\psi(x,y)^H \psi\left(x^{'},y^{'}\right) = M \tag{3.13}$$

This means that the maximum transmit and receive diversity gains for the phased array radar systems are M and N, respectively. It should be noted that the fading coefficient α of a target plays key role to achieve this maximum processing gain. Compared with phased array radar, MIMO radar is easily to overcome this fade [30].

Thus, the Neyman-Pearson test statistic of the phased array radar systems may be represented as [30]:

$$\| X^2 \| \sim \begin{cases} H_0 : \frac{\sigma_w^2 N}{2}\chi^2_{(2)} \\ H_1 : \left(\frac{EMN^2}{2}\sigma_\alpha^2 + \frac{\sigma_w^2 N}{2}\right)\chi^2_{(2)} \end{cases} \tag{3.14}$$

Compared with the MIMO radar systems, the degrees of freedom of the chi-square distribution are reduced from $2MN$ to 2. Same methodology as the MIMO radar systems is implemented to derive the probability of false alarm herein. This gives rise to the following form of the probability of false alarm:

$$P_{fa} = P\left(\frac{\sigma_w^2 N \chi^2_{(2)}}{2} > \gamma_{array}\right) \tag{3.15}$$

Therefore, the threshold for the phased array radar system is calculated by:

$$\gamma_{array} = \frac{\sigma_w^2 N}{2} F^{-1}_{\chi^2_{(2)}}\left(1 - P_{fa}\right) \tag{3.16}$$

The probability of detection for the phased array radar system given a certain probability of false alarm is in the form of:

$$P_d = 1 - F_{\chi^2_{(2)}}\left(\frac{\sigma_w^2}{\sigma_w^2 + EMN\sigma_\alpha^2} F^{-1}_{\chi^2_{(2)}}\left(1 - P_{fa}\right)\right) \tag{3.17}$$

Another interesting multiple antenna radar configuration was proposed by Fishler. et al [30], namely the Multiple Input Single Output (MISO) radar system. As its name implies, it comprises multiple transmit antennas and a single receive antenna, which is regarded as a hybrid of a MIMO and a phased array radar system. The optimal detector is of the form:

$$\| X^2 \| \begin{array}{l} > H_0 \\ < H_1 \end{array} \gamma_{MISO} \tag{3.18}$$

where γ_{MISO} is the threshold to ensure the requirement of the probability of false alarm.

The same derivation method is implemented as was used for the MIMO and the phased array radar systems [30]. The probability of false alarm, the threshold, and the probability of detection are of the form, respectively:

$$P_{fa} = P\left(\frac{\sigma_w^2 N \chi^2_{2M}}{2} > \gamma_{MISO}\right) \tag{3.19}$$

$$\gamma_{MISO} = \frac{\sigma_w^2 N}{2} F^{-1}_{\chi^2_{2M}}\left(1 - P_{fa}\right) \tag{3.20}$$

$$P_d = 1 - F_{\chi^2_{2M}}\left(\frac{\sigma_w^2}{\sigma_w^2 + \frac{EN\sigma_\alpha^2}{M}} F^{-1}_{\chi^2_{2M}}\left(1 - P_{fa}\right)\right) \tag{3.21}$$

The differences among the MIMO, phased array, and MISO radar systems lie in the degrees of freedom of chi-square random variables. They are $2MN$, 2, and $2M$, respectively. Since both MIMO and MISO have same number of transmit antennas, it could be an in-

teresting topic to compare detection performance between MIMO and MISO radars with digital beamforming receivers.

The detection performances of MIMO, MISO, and phased array radar systems are illustrated in Fig. 3.4. Two transmit antennas and four receive antennas were employed for both MIMO and phased array radar systems. To ensure a fair comparison, as is previously defined, the total transmit powers are equal for three systems. Furthermore, two transmit antennas were also used to the MISO radar system. The probability of false alarm is fixed at ten thousandth $\left(P_{fa} = 1 \times 10^{-4}\right)$. It is evident from Fig. 3.4 that, in the high SNR region, the detection performance of the MIMO radar systems is better than that of the phased array radar systems, while in the low SNR region, the performance of the phased array radar systems in terms of detection is better than that of the MIMO radar systems. This means that the phased array radar is better at detecting smaller targets, whereas the MIMO radar is better at detecting and tracking larger targets. Recognised as a hybrid of MIMO and phased array radar systems, not surprisingly, the performance of the MISO radar systems lies between MIMO and phased array radar systems [49].

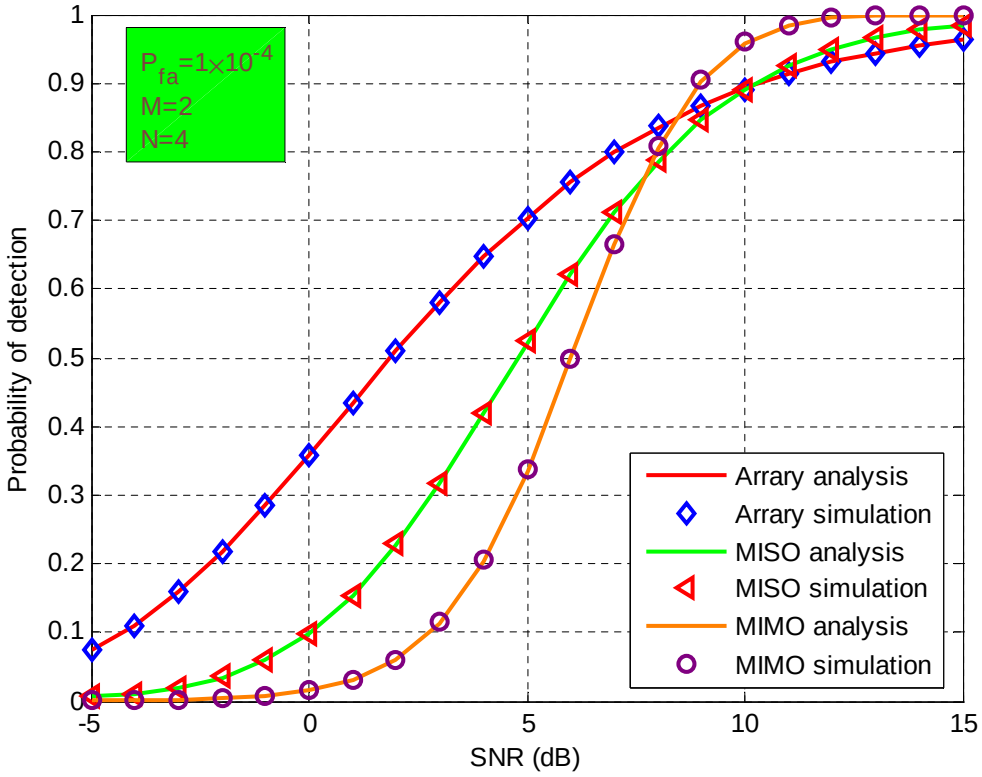

Figure 3.4: Comparative detection performance of MIMO, MISO, and phased array radar systems.

The mis-detection performances of MIMO, MISO, and phased array radar systems are shown in Fig. 3.5. Four transmit antennas and four receive antennas were used for both the MIMO and phased array radar systems. Four transmit antennas were used for the MISO radar system too. The probability of false alarm is set at ten thousandth $\left(P_{fa} = 1 \times 10^{-4}\right)$.

It is clear from the figure that the performance of the MIMO radar systems is better when the SNR is increasing.

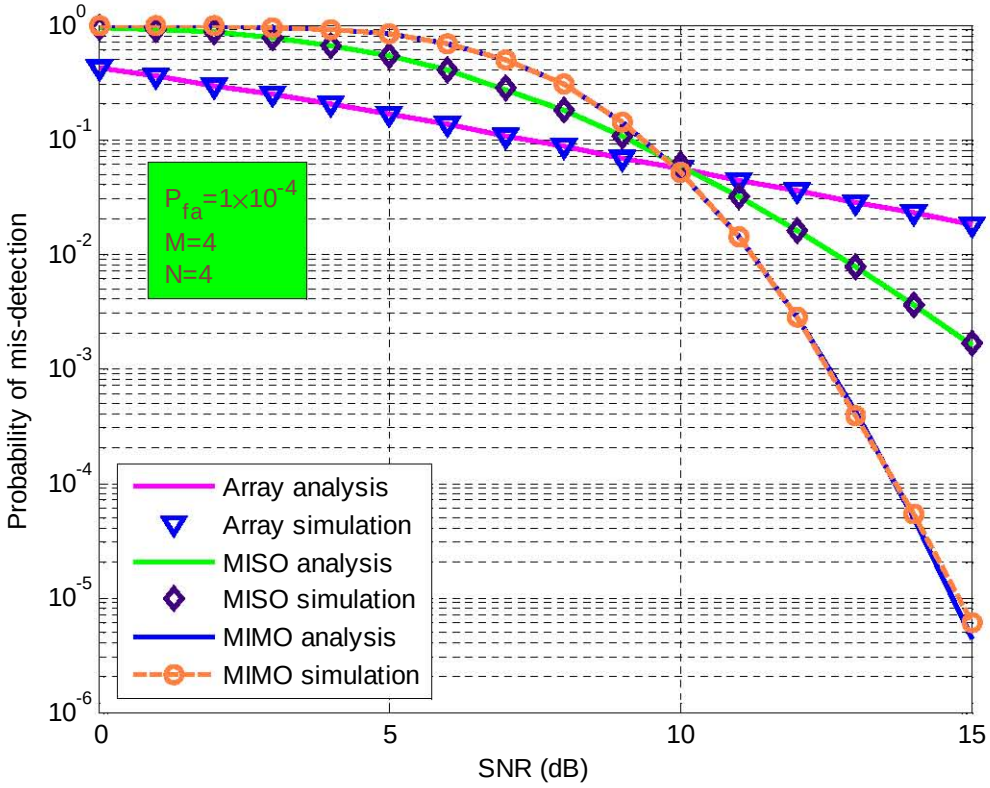

Figure 3.5: Miss detection performance of MIMO, MISO, and phased array radars.

In Fig. 3.6, the impact of different numbers of antennas on the detection performance is examined. As expected, more diversity gain is generated by using more antenna for both MIMO and phased array radar systems. In Fig. 3.6, the number of the transmit antennas is set at two $(M = 2)$, while the number of the receive antennas increases from two to ten $(N = 2, 3, ..., 10)$. The probability of false alarm is fixed at millionth $\left(P_{fa} = 1 \times 10^{-6}\right)$. The value of SNR equals nine dB $(SNR = 9dB)$. The curvature of the simulation results shows that, by exploiting MIMO techniques, more diversity gain may be achieved for a multiple-antenna radar system. An interesting conclusion can be found from Fig. 3.6, namely, that MIMO radar systems are more sensitive to changes in the number of antennas. In fact, it will be shown in the following sections that the MIMO radar systems are more sensitive to the changes of parameters due to the higher degrees of freedom in terms of chi-square distribution random variables.

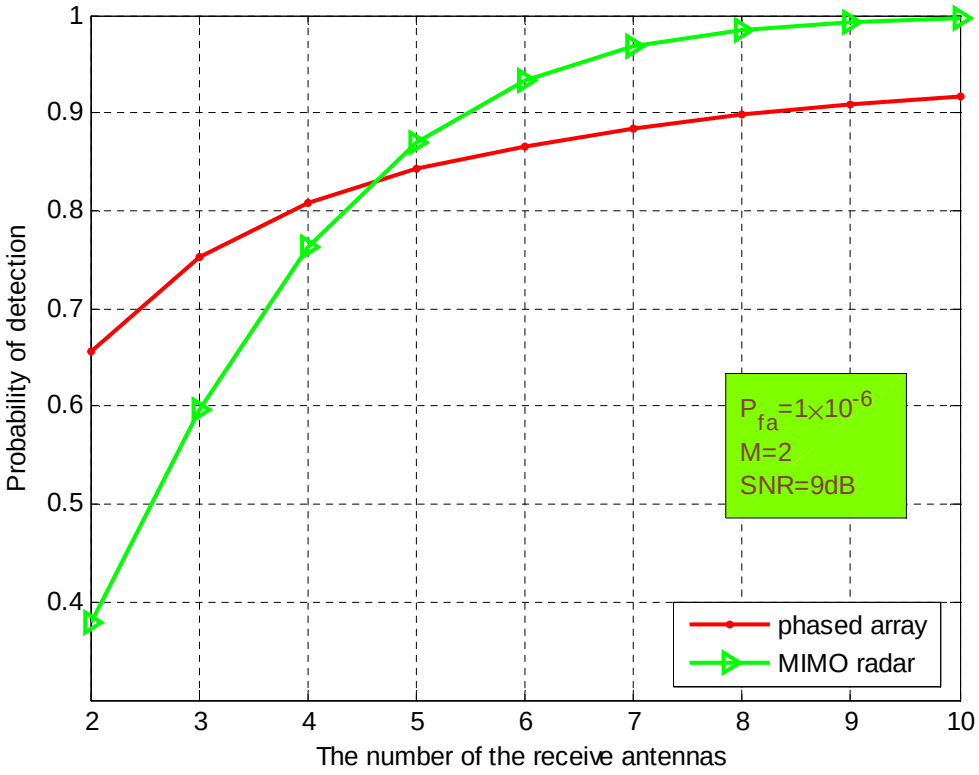

Figure 3.6: The impact of different number of receive antennas on the detection performance.

3.1.3 Robustness of the MIMO radar systems to clutter

So far , none of the results have taken clutter into account. However, in practice, clutter is inevitable. It could be unwanted echoes returned from buildings, mountains, sea, rain, even animals. It is well known that such clutter can cause serious performance losses in radar systems. In this subsection, the effects of clutter on the detection performance of MIMO radar systems will be thus examined. By comparing these with phased array radar systems, the potential of the MIMO radar systems to reduce the effects of clutter is shown.

Without loss of generality, a MIMO radar system with M transmit antennas and N receive antennas is employed. As in the previous subsections, it is assumed that a narrow-band signal is emitted by the ith transmit antenna $\left(\sqrt{E/M}s_i(t)\right)$, where E is the total energy. In the presence of clutter, the received signals are thus of the form:

$$r(t) = \sqrt{\frac{E}{M}}\alpha s(t-\tau) + \sqrt{\frac{E}{M}}\alpha_c s(t-\tau) + w(t) \tag{3.22}$$

The same definitions are employed as in the previous subsections. $r(t)$ represents the received signals. Since Swerling type I targets are employed throughout the thesis, the symbol of α can be modelled as identically distributed zero-mean complex Gaussian random variables $\left(\alpha \sim CN\left(0, \sigma^2 I_{MN}\right)\right)$, and I_{MN} is identity matrix with size MN by MN $(MN \times MN)$. $w(t) \sim CN\left(0, \sigma_w^2 I_{MN}\right)$ indicates AWGN. The symbol of α_c denotes the clutter. The intention of this dissertation is not to introduce new models of clutter but to demonstrate the robustness of MIMO radar systems to clutter. Therefore, a simple Gaussian distribution clutter is implemented $\left(\alpha_c \sim CN\left(0, \sigma_c^2 I_{MN}\right)\right)$, which in order to lead to a closed-form expression of the probability of detection. By comparing the results of the MIMO and phased array radar systems, it is shown that the MIMO radar can reduce the effects of clutter more effectively than that of phased array radar systems.

The Neyman-Pearson hypothesis of the MIMO radar systems in the presence of clutter may be denoted as:

$$X = \begin{cases} H_0: \sqrt{\frac{E}{M}}\alpha_c s(t-\tau) + w(t) \\ H_1: \sqrt{\frac{E}{M}}\alpha s(t-\tau) + \sqrt{\frac{E}{M}}\alpha_c s(t-\tau) + w(t) \end{cases} \tag{3.23}$$

where H_0 and H_1 indicate that the target either does not exist or does exist at delay τ , respectively.

Similar derivation manner as previous subsection, thus, the distribution of the test statistic is given as:

$$\| X^2 \| \sim \begin{cases} H_0: \left(\frac{E}{2M}\sigma_c^2 + \frac{\sigma_w^2}{2}\right)\chi_{2MN}^2 \\ H_1: \left(\frac{E}{2M}\left(\sigma_\alpha^2 + \sigma_c^2\right) + \frac{\sigma_w^2}{2}\right)\chi_{2MN}^2 \end{cases} \tag{3.24}$$

where χ_{2MN}^2 represents a chi-square random variable with $2MN$ degrees of freedom.

By exploiting the optimal detection, the corresponding probability of false alarm in respect of MIMO radar systems in the presence of clutter can be expressed as:

$$P_{fa} = P\left(\left(\frac{E\sigma_c^2}{2M} + \frac{\sigma_w^2}{2}\right)\chi^2_{2MN} > \gamma_{MIMO}\right) \tag{3.25}$$

Thus, the threshold γ_{MIMO} may be denoted as:

$$\gamma_{MIMO} = \left(\frac{E\sigma_c^2}{2M} + \frac{\sigma_w^2}{2}\right) F^{-1}_{\chi^2_{2MN}}\left(1 - P_{fa}\right) \tag{3.26}$$

where $F^{-1}_{\chi^2_{2MN}}$ represents the inverse cumulative distribution function of a chi-square random variable with $2MN$ degrees of freedom.

Furthermore, the probability of detection for MIMO radar systems is stated as:

$$P_d = P\left(\frac{E}{2M}\left(\sigma_\alpha^2 + \sigma_c^2\right) + \frac{\sigma_w^2}{2}\right)\chi^2_{2MN} > \gamma \tag{3.27}$$

By substituting Eqn. 3.26 into Eqn. 3.27, the probability of detection is given as:

$$P_d = 1 - F_{\chi^2_{2MN}}\left(\left(\frac{\frac{E}{M}\sigma_c^2 + \sigma_w^2}{\frac{E}{M}\sigma_\alpha^2 + \frac{E}{M}\sigma_c^2 + \sigma_w^2}\right) F^{-1}_{\chi^2_{2MN}}\left(1 - P_{fa}\right)\right) \tag{3.28}$$

On the other hand, the received signals of the phased array radar systems may be represented as:

$$X = \begin{cases} H_0: \sqrt{\frac{E}{M}}MN\alpha_c s(t-\tau) + w(t) \\ H_1: \sqrt{\frac{E}{M}}MN\alpha s(t-\tau) + \sqrt{\frac{E}{M}}MN\alpha_c s(t-\tau) + w(t) \end{cases} \tag{3.29}$$

where the symbols of $\alpha \sim CN\left(0,\sigma^2\right)$, $\alpha_c \sim CN\left(0,\sigma_c^2\right)$, and $W \sim CN\left(0,N\sigma^2\right)$ signify the complex amplitude, clutter, and noise, respectively.

The Neyman-Pearson test statistic of the phased array radar systems radar systems when there is clutter circumstance is thus given as:

$$\| X^2 \| \sim \begin{cases} H_0: \left(\frac{EM^2N^2\sigma_c^2}{2M} + \frac{\sigma_w^2 N}{2}\right)\chi^2_{(2)} \\ H_1: \left(\frac{EM^2N^2\left(\sigma_c^2+\sigma_\alpha^2\right)}{2M} + \frac{\sigma_w^2 N}{2}\right)\chi^2_{(2)} \end{cases} \tag{3.30}$$

The degrees of freedom in respect of the chi-square distribution are two.

As same method was used in the phased array radar without clutter, the probability of false alarm, the threshold, and the probability of detection of the phased array radar systems when faced with clutter may be expressed as, respectively:

$$P_{fa} = P\left(\frac{\left(EMN^2\sigma_c^2 + \sigma_w^2 N\right)\chi^2_{(2)}}{2} > \gamma_{array}\right) \tag{3.31}$$

$$\gamma_{array} = \left(\frac{EMN^2\sigma_c^2 + \sigma_w^2 N}{2} \right) F^{-1}_{\chi^2_{(2)}} \left(1 - P_{fa}\right) \tag{3.32}$$

$$P_d = 1 - F_{\chi^2_{(2)}} \left(\left(\frac{EMN\sigma_c^2 + \sigma_w^2}{EMN\left(\sigma_\alpha^2 + \sigma_w^2\right) + \sigma_w^2} \right) F^{-1}_{\chi^2_{(2)}} \left(1 - P_{fa}\right) \right) \tag{3.33}$$

The detection performance versus Signal to Clutter Ratio (SCR) is presented in Fig. 3.7. Four by four systems for both the MIMO and the phased array radars were implemented. The probability of false alarm is fixed at millionth $\left(P_{fa} = 1 \times 10^{-6}\right)$. The values of SNR vary from 6 dB to 15 dB by 3dB. The detection performance of the MIMO radar systems is shown as blue-solid lines, whereas the detection performance of the phased array radar systems is plotted as red-dot lines. It may be observed from Fig. 3.7 that the detection performance of the MIMO radar systems is significantly improved by increasing the SNR. Conversely, the detection performance of the phased array radar is slightly affected by the variance of SNR. In other words, the same increment of SNR may bring more diversity gain to the MIMO radar systems. As stated in the previous section, the MIMO radar systems are more sensitive to the changes of parameters.

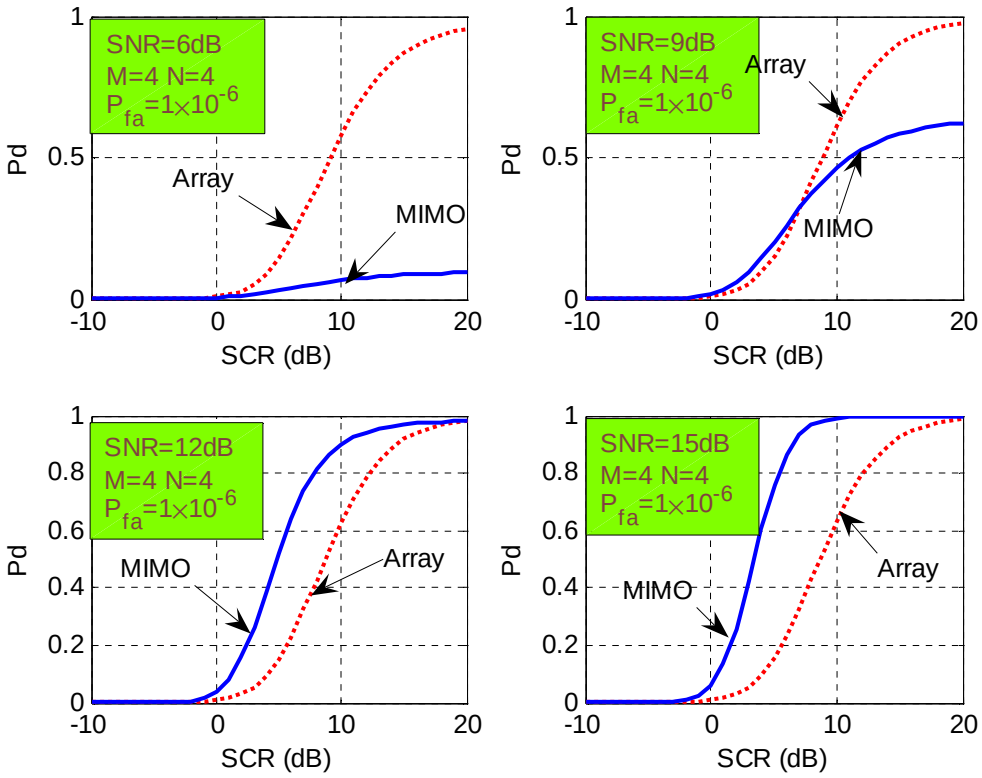

Figure 3.7: Detection performance versus SCR.

Fig. 3.8 describes the comparison detection performances of MIMO and phased array radar systems versus SNR. The number of transmit and receive antennas is five $(M = N = 5)$. The probability of false alarm is set at millionth $\left(P_{fa} = 1 \times 10^{-6}\right)$ as in the previous test. The values of SCR vary uniformly from five to twenty by five. The

same trend as in Fig. 3.7 could be found in Fig. 3.8. MIMO radar systems are thus sensitive to changes in parameters, whereas, phased array radar systems are unaffected by changes in parameters. Sometimes, though, they perform better.

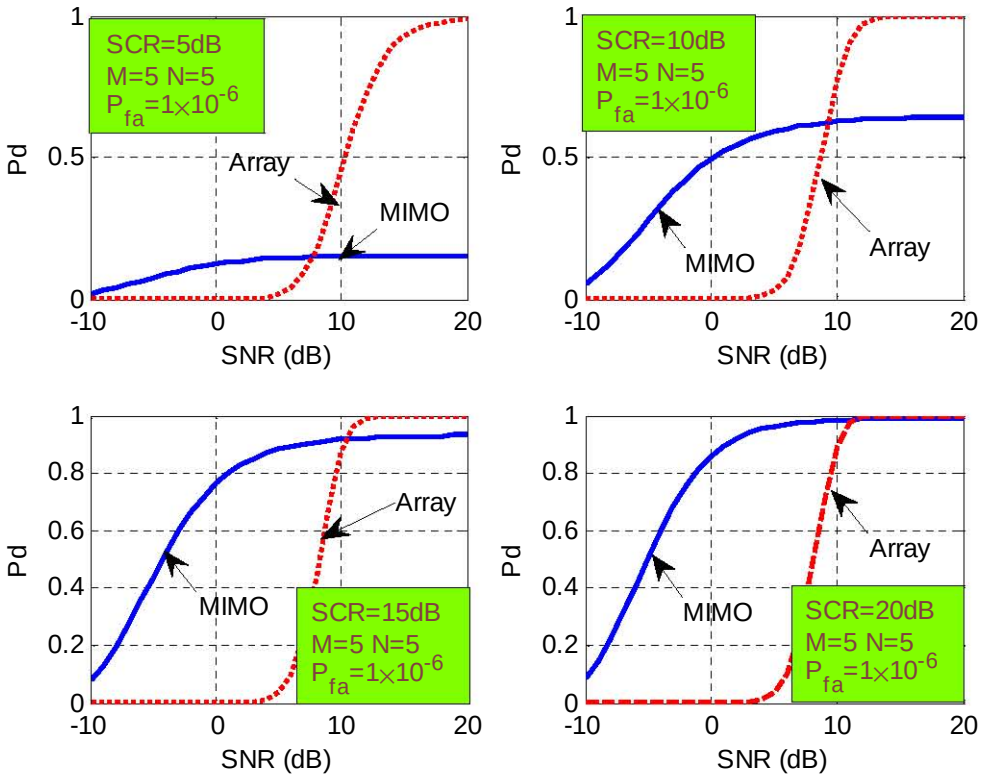

Figure 3.8: Probability of detection versus SNR in the presence of clutter.

It is observed that MIMO radar systems are more sensitive to the change of parameters than that of phased array radar systems. Under clutter circumstance, same SNR or SCR increment may produce more processing gain to MIMO radar systems than that of phased array radar systems. It should also be mentioned that the modelling of clutter here is static and needs to be further explored [7]. Other forms of clutter will modify the detection results here. For instance, real clutter, in particular sea clutter, has time correlation. It should be noted that the aim of this subsection is to prove the robustness of MIMO radar systems to the clutter compared with phased array radar systems. In addition, clutter viewed by different transmit-receive pairs has a largely unknown dependence on bistatic angle, but might exhibit correlation. i.e. a large scatter might tend to be strong in all bistatic views. It is assumed here that the target backscatter is uncorrelated with angle.

3.2 Distributed Detection of MIMO Radars

The optimal detector under the Neyman-Pearson hypothesis raises the question of how to characterise more practical and sub-optimal schemes. It is well known that the optimal detector is impractical due to bandwidth limitations of the interlinks. In this section, therefore, a practical low-bandwidth consumption distributed MIMO radar system is developed in which a finite number of decision messages is sent to the fusion centre [9]. Compared with optimal MIMO radar systems, clearly, there is a performance loss from distributed MIMO radar systems. In practice, however, the distributed MIMO radar system is nonetheless a meaningful configuration in terms of bandwidth limitation.

As is shown in Fig. 3.9, a fusion centre has been added compared with MIMO radar systems to process data from each branch. It has been proved that compared with a single antenna radar system, a multiple-antenna distributed radar network results in a larger coverage area. This is due to the fact that each antenna transmits a detective pulse and receives a radar return due to this transmitted detective pulse as well as the transmitted pulses from rest antennas in this distributed radar network [39][53]. It has been an issue in terms of multitarget identification since monostatic radar systems. As is well known, multitarget may be distinguished by Capon method [33]. Multitarget identification study in a MIMO radar enviroment could be found in [41]. It has been found that with respect to MIMO radar systems, the targets angles from different transmit antennas and receive antennas may be ultised with received signals to improve accuracy of locations of multiple targets. It should be noted that synchronization of this MIMO radar system play key role to increase received SNR. The impact of synchronization on received SNR may be found in [39]. After receiving a binary decision from each branch, the final decision will be made depending on the different distributed algorithms.

There are three classical decision rules, namely, OR rule, AND rule, and MAJ rule [78]. The above three distributed detection algorithms will be investigated in MIMO radar systems.

3.2.1 OR Rule

The OR rule is defined as follows: if one detection result of the total number of branches is positive, the final decision is positive. If the fusion centre adopts the OR rule, the total mis-probability is the product of the individual miss probabilities. Therefore, the detection probability of a distributed MIMO radar system with the OR rule may hold as :

$$P = 1 - (1 - P_d)^{MN} \tag{3.34}$$

It is important to note that the probability of false alarm of the fusion centre is also the product of the individual probabilities of false alarm.

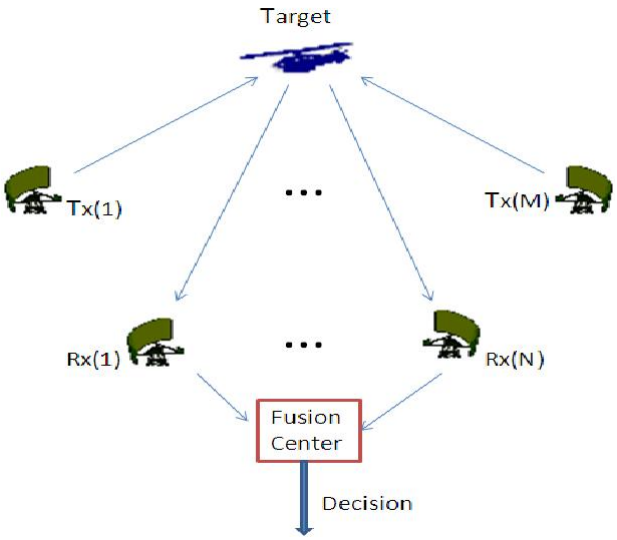

Figure 3.9: The process flow of the distributed MIMO radar systems.

3.2.2 AND Rule

In contrast to the OR rule, the AND rule means that a positive decision is only made when each sub-branch achieves a positive decision. Hence, the detection probability of this MN out of MN MIMO radar system is of the form:

$$P = (P_d)^{MN} \tag{3.35}$$

3.2.3 MAJ Rule

MAJ is short for majority logic. As its name implies, if x out of total MN sub-branch selected as reference branches to declare the decision for distributed MIMO radar systems, the positive decision is only made when all the x branches obtain positive decisions. Obviously, the number x lies among one to MN $(X \sim (1-MN))$. When x equals one, the system becomes into OR distributed system, and if x equals MN, then the system is equivalent to AND distributed system. The performance of MAJ distributed detection thus lies between OR and AND rules. The detection performance of the MIMO radar systems under the MAJ rule is of the form:

$$P = \sum_{i=x}^{MN} \begin{pmatrix} MN \\ i \end{pmatrix} (P_d)^i (1-P_d)^{MN-i} \tag{3.36}$$

3.2.4 Detection Performance of Distributed MIMO Radar Systems

The detection performance of a distributed MIMO radar system without clutter is presented in Fig. 3.10. The probability of false alarm is fixed at ten thousandth $\left(P_{fa} = 1 \times 10^{-4}\right)$. There are two transmit antennas and two receive antennas at each side. Compared with optimal detector, there is clearly an expected performance gap. Despite this performance

loss, as is expected, the OR rule provides the best performance among all the fixed rules. Therefore, the OR rule is the rule most widely used in the literature and in practice.

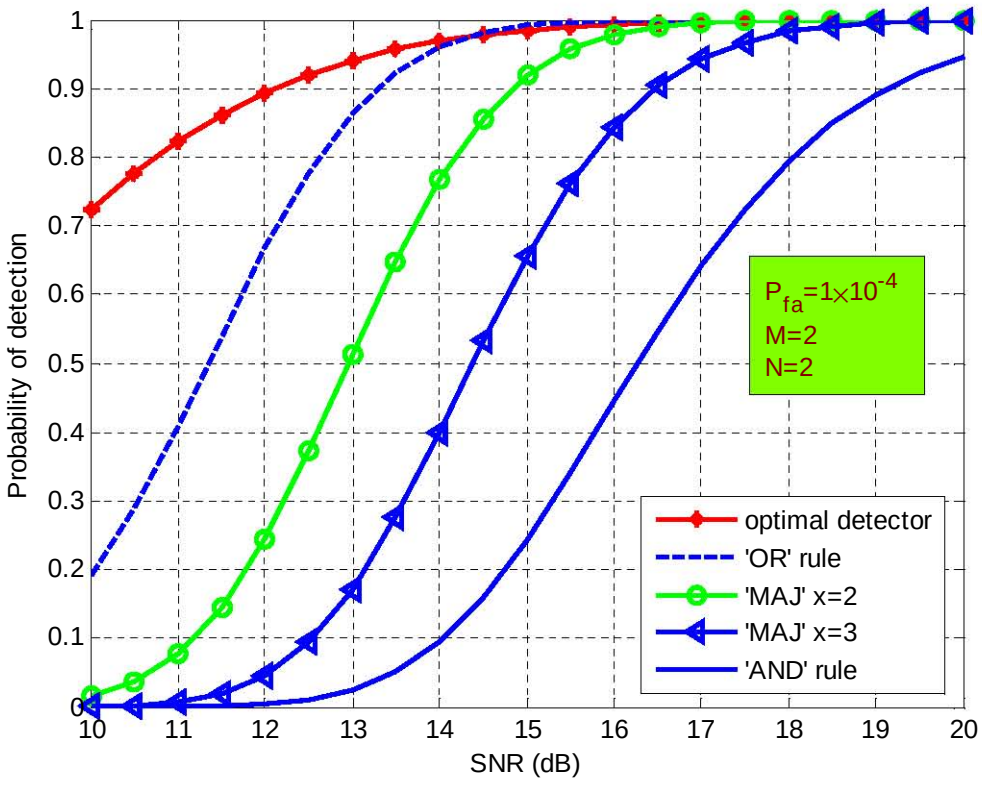

Figure 3.10: Distributed detection performance.

The detection probability curves of a two by two (2×2) MIMO radar system in the presence of clutter versus SCR is plotted in Fig. 3.11. The SNR is fixed at twenty dB $(SNR = 20dB)$, and the probability of false alarm is ten thousandth $\left(P_{fa} = 1\times 10^{-4}\right)$. The detection performance of the OR rule sub-optimal scheme is much better than that of the other two systems.

We will now examine the detection performance of the proposed distributed MIMO radar system with the same order of diversity but with different numbers of transmit antennas or receive antennas. For example, instead of examining a system comprising two transmit antennas and two receive antennas, one transmit antenna with four receive antennas, and a system with four transmit antennas and one receive antenna are examined. Without loss of generality, the OR rule is applied to the MIMO radar system with the fixed probability of false alarm at ten thousandth $\left(P_{fa} = 1\times 10^{-4}\right)$.

Since clutter, when viewed multistatically, has a largely unknown dependence on bistatic angle, although it might exhibit correlation over transmit or receive pairs. i.e. a large scatterer might tend to be strong in all bistatic views, it triggers a fixed diversity MIMO radar system, which could achieve different detection performances with different numbers of antennas. The target backscatter, except for very small targets, is likely to be uncorrelated with angle, as assumed in this dissertation.

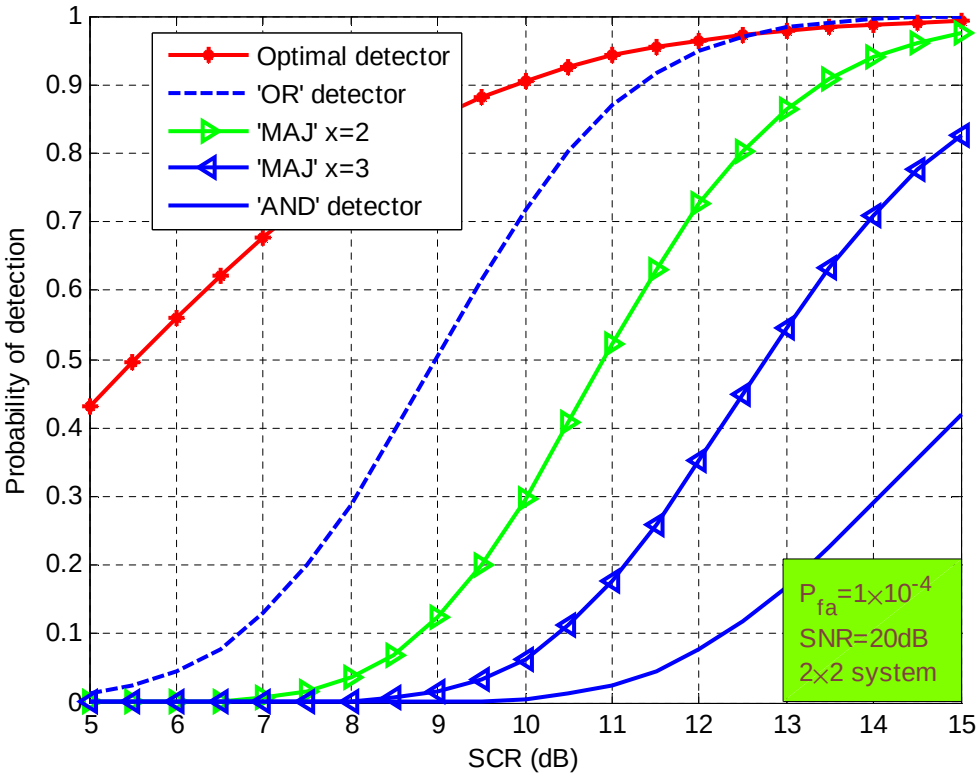

Figure 3.11: Detection performance versus signal to clutter ratio.

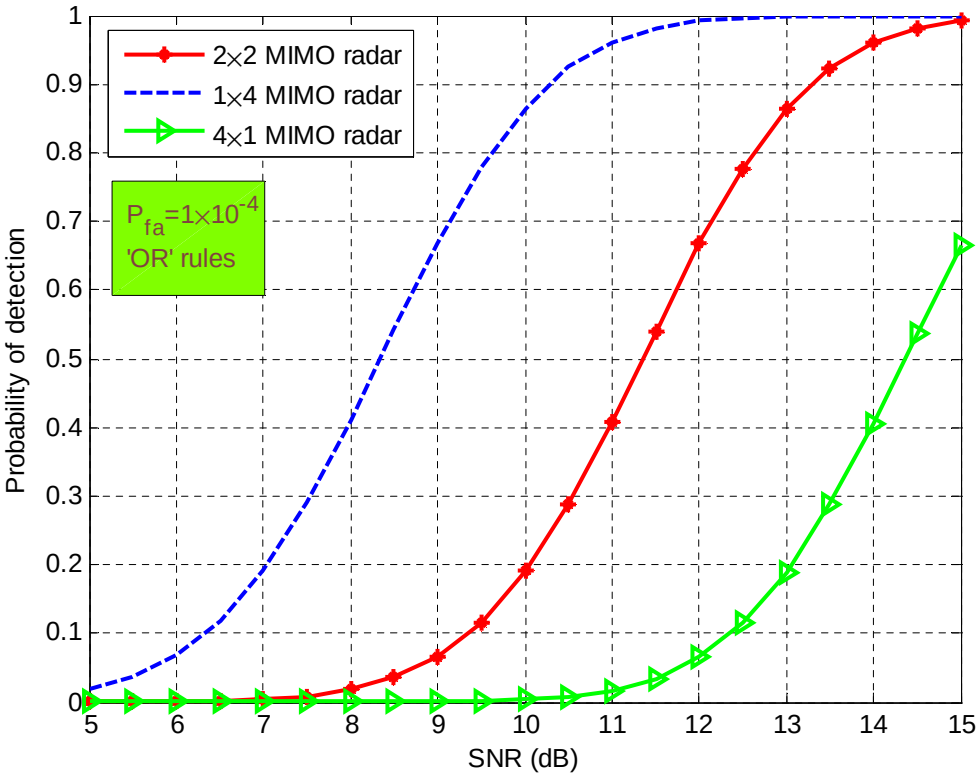

Figure 3.12: The impact on the different number of antennas with same order of diversity.

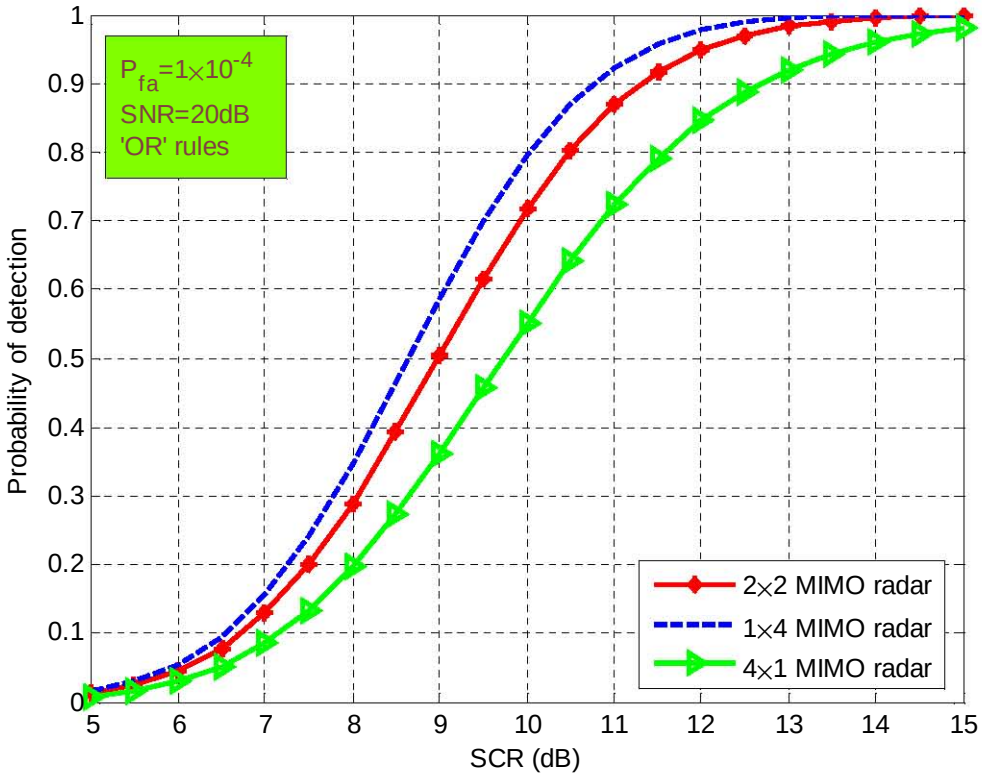

Figure 3.13: The impact on the different number of antennas in the presence of clutter.

3.3 MIMO Passive Radar Detection based on the FM signals

Based on the Neyman–Pearson hypothesis, the detection problem for a radar may be solved by two steps. The first step manipulates the conditional PDFs of measurements $(P(H_0), P(H_1))$, so as to obtain sufficient statistic PDFs, in some cases, however, there is no closed-form expression. The second step calculates the probability of detection P_d of such a radar system by the threshold, which can be evaluated after the predefined value of the probability of false alarm (P_{fa}). The same two-step method will be implemented in this chapter. The key problem is to derive the PDFs of measurements for MIMO passive radar systems.

As assumed in Chapter 2, the received signal without a target of a single transmitter and single receiver passive radar system based on FM illuminator of opportunity may be modelled as Gaussian random variables. If this assumption is valid, the statistic of MIMO passive radar system experiencing FM signals with targets can be consequently summarized as Chi-square random variables, as was the case in previous sections. Thus, this section starts with the PDF derivation of the received signal without target for a single transmitter and single receiver passive radar system in respect of FM illuminators of opportunity. Afterwards, the results will be adapted to MIMO passive radar systems under the null hypothesis. The value of the threshold is then applied to the alternative hypothesis

to calculate the probability of detection for a MIMO passive radar system with respect to FM illuminators of opportunity. Lastly, the simulation results under various scenarios are presented to verify the derivations.

3.3.1 Derivation of the Probability Density Function of Null Hypothesis

As direct calculation of PDF of the self ambiguity function is a daunting task, some reasonable assumptions about received signals are predefined in order to arrive at a theoretical model. It is assumed that the signal's spectrum is white and the received signals are uncorrelated. The purpose of these two assumptions is to ensure that the real components of the signal and the imaginary component of the signal are independent. Furthermore, the transmitting signal and channel noise are independent of each other.

As discussed in Chapter 2, the power spectrum can be calculated by means of the ambiguity function. On the other hand, the probability density may be calculated by manipulating the spectrum density function. Thus, the probability density can be analysed by using the ambiguity function. The received signal without any target may be represented as:

$$R(k) = \left| \sum_{t=0}^{N_f-1} x(t) \exp\left(\frac{-j2\pi kt}{N_f}\right) \right|^2 \; k = 0, 1, ..., N_f - 1 \tag{3.37}$$

Using the same definitions as the Discrete Fourier Transform (DFT) [4], N_f denotes the block size of transform or it refers to the number of Fourier frequencies. The symbol of $x(t)$ signifies the relating signal, here equalling $s_d(t-\tau)\,y(t)$, where the symbol of $s_d(t)$ denotes the direct transmitting signal and $y(t)$ is the received signal without target $(y(t) = s_d(t) + w(t))$. j is the imaginary unit $\left(j^2 = -1\right)$.

The complex variable $x(t)$ may be expanded as [69]:

$$x(t) = x_i(t) + j * x_q(t) \tag{3.38}$$

It is well known that $\exp\left(\frac{-j2\pi kt}{N_f}\right) = \cos\left(\frac{-2\pi kt}{N_f}\right) + j\sin\left(\frac{-2\pi kt}{N_f}\right)$. Thus, rearranging Eqn. 3.37 and Eqn. 3.38, yields:

$$\begin{aligned} R(k) = \Bigg| & \sum_{t=0}^{N_f-1} \left(x_i(t) \cos\left(\frac{2\pi kt}{N_f}\right) + x_q(t) \sin\left(\frac{2\pi kt}{N_f}\right) \right) \\ & + j \sum_{t=0}^{N_f-1} \left(x_q(t) \cos\left(\frac{2\pi kt}{N_f}\right) - x_i(t) \sin\left(\frac{2\pi kt}{N_f}\right) \right) \Bigg|^2 \end{aligned} \tag{3.39}$$

The symbols of $A(k)$ and $B(k)$ denote the real and imaginary components, respectively, thus $R(k) = A(k)^2 + B(k)^2$.

As is stated by the central limit theorem, a sufficiently large number of independent random variables, each with finite mean and variance, can be approximately modelled as normally distributed random variables [10]. $A(k)$ and $B(k)$ are Gaussian distributed random variables with zero mean, as claimed in work [69] by Shan (2007). Since both $A(k)$ and $B(k)$ are long enough, if $A(k)$ and $B(k)$ can be proved to be independent, then $\sqrt{R(k)}$ is a Gaussian distribution. The correlation of $A(k)$and $B(k)$ can be expressed as:

$$\begin{aligned} corr(A(k),B(k)) &= E(A(k),B(k)) \\ E\sum_{t=0}^{N_f-1}\left(x_i(t)\cos\left(\frac{2\pi kt}{N_f}\right)+x_q(t)\sin\left(\frac{2\pi kt}{N_f}\right)\right) \\ \times\sum_{t=0}^{N_f-1}\left(x_q(t)\cos\left(\frac{2\pi kt}{N_f}\right)-x_i(t)\sin\left(\frac{2\pi kt}{N_f}\right)\right) \end{aligned} \tag{3.40}$$

Under the condition $k=0,1,...,N_f-1$, the above equation equals zero [69]. Thus $\sqrt{R(t)}$ is the Gaussian distributed random variable with zero mean. Since the variance of $A(k)$ and $B(k)$ may be calculated as:

$$\sigma_{A(k)} \sim N\left(0,\sigma^2\sqrt{\sum_{t=0}^{N_f-1}2\cos^2\left(\frac{2\pi kt}{N_f}\right)}\right)+N\left(0,\sigma^2\sqrt{\sum_{t=0}^{N_f-1}2\sin^2\left(\frac{2\pi kt}{N_f}\right)}\right) \tag{3.41}$$

$$\sigma_{B(k)} \sim N\left(0,\sigma^2\sqrt{\sum_{t=0}^{N_f-1}2\cos^2\left(\frac{2\pi kt}{N_f}\right)}\right)+N\left(0,\sigma^2\sqrt{\sum_{t=0}^{N_f-1}2\sin^2\left(\frac{2\pi kt}{N_f}\right)}\right) \tag{3.42}$$

$N\left(\mu,\sigma^2\right)$ indicates the Gaussian distribution random variable with mean μ and variance σ^2. According to the central limited theorem [36][37], the mean and variance of the new generated Gaussian distribution random variable are the sum of each independent Gaussian random variable $\left(\mu=\mu_0+\mu_1+...+\mu_N,\sigma^2=\sigma_0^2+\sigma_1^2+...+\sigma_{N,}^2\right)$. Thus the above equations can be further deduced as:

$$\sigma_{A(k)} \sim N\left(0,\sigma^2\sqrt{2N_f}\right) \tag{3.43}$$

$$\sigma_{B(k)} \sim N\left(0,\sigma^2\sqrt{2N_f}\right) \tag{3.44}$$

The accuracy of these derivations is verified in Fig 3.14, in which a standard normal distribution $x(t)$ is implemented and the block size of DFT varies from 512 to 2560. It is evident that there is good agreement between analysis and simulation results.

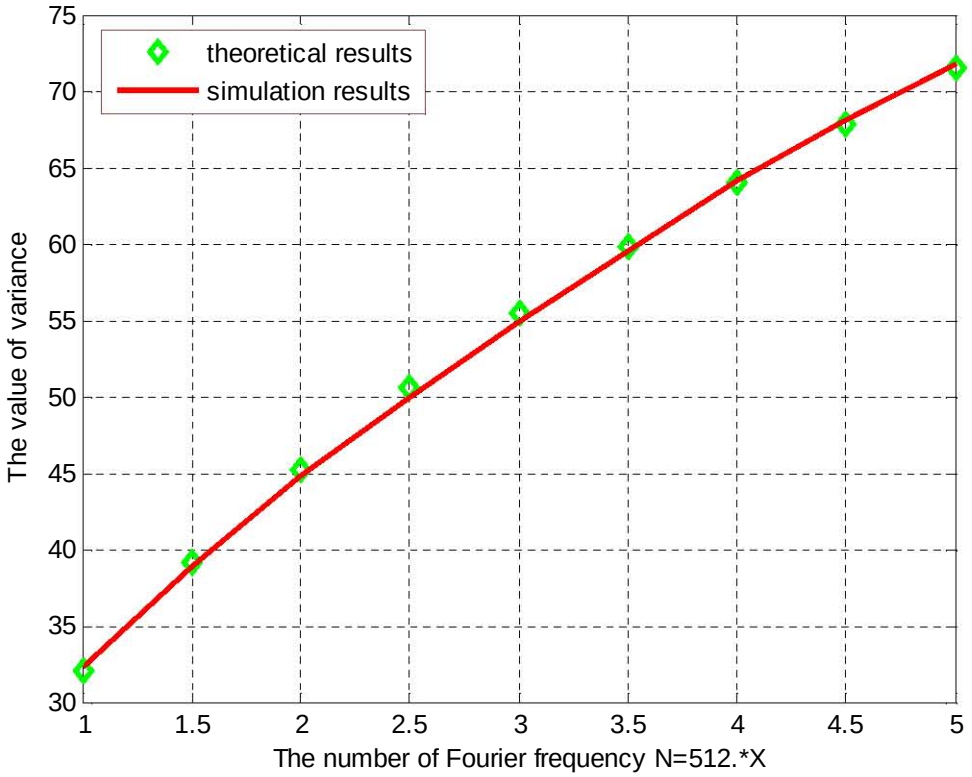

Figure 3.14: The accuracy of derivations.

Under the above agreement, the PDF of the received signal by normalising $A(k)$ and $B(k)$ as standard normal distribution random variables may be derived, since it is well known that the sum of the squared standard normal distribution random variables can be modelled as chi-square random variables. Scaling $A(k)$ and $B(k)$ by the factor $\frac{1}{\sigma^2\sqrt{2N_f}}$, $\frac{1}{\sigma^2\sqrt{2N_f}}A(k)$ and $\frac{1}{\sigma^2\sqrt{2N_f}}B(k)$, standard normal random variables then become $\left(\frac{1}{\sigma^2\sqrt{2N_f}}A(k), \frac{1}{\sigma^2\sqrt{2N_f}}B(k) \sim N(0,1)\right)$. Consequently, the PDF of the squared received signal is a chi-square random variable with two degrees of freedom.

$$\frac{1}{2N_f\sigma^4} \mid \chi(\tau, f_d) \mid^2 = \frac{1}{2N_f\sigma^4}R(k) \sim \chi_2^2 \tag{3.45}$$

where $\mid \chi(\tau, f_d) \mid^2$ is the ambiguity function of the received signal. f_d is the Doppler frequency, which is replaced by k in the DFT term.

In the case of a MIMO passive radar system under null hypothesis, the above derivation can be extended in a straightforward manner:

$$H_0 : \chi_{2MN}^2 \tag{3.46}$$

where M and N are the number of transmit antennas and receive antennas, respectively. The degrees of freedom for the chi-square distribution in the case of MIMO passive radar system are consequently extended from 2 to $2MN$.

Consequently, given a probability of false alarm for a MIMO passive radar system, a similar threshold as that of the MIMO radar system may be achieved, which takes the form of:

$$\gamma_{passive} = \frac{\sigma_p^2}{2} F_{\chi^2_{2MN}}^{-1}\left(1 - P_{fa}\right) \tag{3.47}$$

It should be noted that the variance of the MIMO passive radar σ_p^2 is different from that of MIMO radar systems discussed in the previous sections.

3.3.2 Probability Density in the Presence of a Target

Unlike received signals without a target, the received signal for a MIMO passive radar system under the alternative hypothesis may be expressed as:

$$y(t) = s_d(t) + s_r(t) + w(t) \tag{3.48}$$

where $s_d(t)$ and $w(t)$, the same as the case without a target, refer to the direct signal and channel noise. The difference from the only noise case is brought by the reflected signal by a target, which is denoted as $s_r(t)$ in Eqn. 3.48.

In order to formulate the probability density of the received signal with a target for the MIMO passive radar system, substituting Eqn. 3.48 into 3.37, yields:

$$R(k) = \left| \sum_{t=0}^{N_f-1} y(t)\, s_d(t-\tau) \exp\left(\frac{-j2\pi kt}{N_f}\right) \right|^2 \; k = 0, 1, ..., N_f - 1 \tag{3.49}$$

A close look at Eqn.3.49 and Eqn. 3.37 shows that the only difference is the inner term $s_r(t)$, therefore, the Eqn.3.49 may be deduced as:

$$\sqrt{R(k)} = A(k) + B(k) + \sum_{t=0}^{N_f-1} s_r(t)\, s_d(t-\tau) \exp\left(\frac{-j2\pi kt}{N_f}\right) \tag{3.50}$$

$$\sqrt{R(k)} \approx A(k) + B(k) + 2\alpha\sigma^2 N_f \tag{3.51}$$

where the symbol of α is the complex amplitude of the reflected signal. Consequently, σ_α^2 denotes the reflected power of the target of interest, which is very small compared with the direct signal in practice. Given the normalised $A(k)$ and $B(k)$, if we square $\sqrt{R(k)}$, it will lead to a summation of the squared independent non-zero mean Gaussian random variables, which are referred to as non-central chi-square distribution random variables [69].

In order to compute the non-central parameter, the non-zero mean or the constant needs need to computed first [5]. As analysed before, the symbols of $A(k)$ and $B(k)$ denote the real and imaginary parts, respectively. Thus, the received signals may be expressed as:

$$R(k) = \left(A(k) + 2\alpha\sigma^2 N_f\right)^2 + B(k)^2 \tag{3.52}$$

Then, the constant is given as $4\alpha^2\sigma^4 N_f^2$. As obtained from Eqn. 3.43 and Eqn. 3.44, the variance of $R(k)$ is $2\sigma^4 N_f$. Therefore, the non-central coefficient is given as [5]:

$$\lambda = \frac{4\alpha^2\sigma^4 N_f^2}{2\sigma^4 N_f} = 2\alpha^2 N_f \tag{3.53}$$

In practice, instead of single sample processing in one block, multiple samples are employed to improve the performance of the system. Assuming the sampling frequency f_s, which denotes the bandwidth in the FM system, and the observation time T, which also indicates the integral time, the above equation may be adjusted as:

$$\lambda = 2\alpha^2 f_s T \tag{3.54}$$

where the product of $f_s T$ reveals the total processing samples in the time length T.

In the case of MIMO passive radar systems, the degrees of freedom increase from 2 to $2MN$. Consequently, the non-central parameter for the MIMO passive radar system becomes:

$$\lambda_{MIMO} = 2\alpha^2 f_s TMN \tag{3.55}$$

The standard form of the non-central chi-square distribution random variables for MIMO passive radar systems may be expressed correspondingly as [5]:

$$f_x(x; 2MN; \lambda_{MIMO}) = \frac{1}{2}\exp^{-(x+\lambda_{MIMO})/2}\left(\frac{x}{\lambda_{MIMO}}\right)^{2MN/4-1/2} I_{2MN/2-1}\left(\sqrt{\lambda_{MIMO} x}\right) \tag{3.56}$$

The mean and variance of such non-central chi-square random variables are of the form:

$$\mu = 2MN + 2\alpha^2 f_s TMN \tag{3.57}$$

$$\sigma^2 = 2\left(2MN + 2 \times 2\alpha^2 f_s TMN\right) \tag{3.58}$$

The alternative hypothesis of MIMO passive radar systems may be calculated as:

$$H_1 : \left(\frac{E}{2M} + \frac{\sigma_p^2}{2}\right)\chi^2_{non(2MN)} \tag{3.59}$$

where the symbol of E is total transmitting power and $\chi^2_{non(2MN)}$ denotes the non-central chi-square distribution random variables with $2MN$ degrees of freedom.

Therefore, the probability of detection for a MIMO passive radar system based on the FM broadcasting signals subject to the probability of false alarm is given as:

$$p_d = 1 - F_{\chi^2_{non(2MN)}}\left(\frac{\sigma_p^2}{\frac{E}{M}+\sigma_p^2}\right)\left(F^{-1}_{\chi^2_{2MN}}\left(1-P_{fa}\right)\right) \tag{3.60}$$

Generally, the closed-form solution for these complex mathematical calculations does not exist. Some empirical approximations exist for the manual calculation though [16]. One popular example of this is the Albersheim equations [59].

3.3.3 Detection Performance of MIMO passive radar systems based on FM waveform

In this section, the detection performance of MIMO passive radar systems is investigated. Considering the practical environment, the carrier frequencies of commercial FM sound-broadcasting band are allocated between 87.5 MHz and 108 MHz, and there are 204 channels, each of 100 KHz bandwidth. Thus, throughout this section, the sampling frequency is assumed to be 100 KHz ($f_s = 100,000Hz$).

The impact on the reflected or scattering power is illustrated in Fig. 3.15. A four by four MIMO radar system is implemented, which means that there are four transmit antennas and four receive antennas. The integral time is 1 second and the probability of false alarm is millionth $\left(P_{fa} = 1 \times 10^{-6}\right)$. The values of scattering power to the directed signal ratio in this example are -46 dB, -50 dB, -60 dB, and -70 dB, respectively. It is interesting to notice that the impact of the reflected power is descending when the values of power are decreasing. In fact, the detection performance plot will be approximately overlapped even when lower scatter power than -70 dB is engaged, which raises an issue relating to the minimum detectable scattering power. In practice, signals are buried in the noise, which are sometimes not detectable since their powers are too small, which brings a trade-off study between the product of time-bandwidth (f_sT) and the number of antennas. It is obvious that a bigger number of antennas can produce more angular diversity, or spatial diversity, as discussed in previous sections. Conversely, increasing the product of time-bandwidth is another solution. Normally, the sampling rate or the bandwidth for FM broadcasting is fixed in each country. Thus, the detection performance of such a passive radar system in respect of minimum detectable signals may be improved by extending the integral or observation time length.

In Fig. 3.16 below, the detection performance of a MIMO passive radar system with regard to different integral time is demonstrated. In contrast to the above case, a 2 by 2 MIMO passive radar system is implemented here. The probability of the false alarm rate is the same as in the last example $\left(P_{fa} = 1 \times 10^{-6}\right)$. The value of the SNR is set at 5 dB, and the values of Reflected to Direct signal power Ratio (RDR) vary from -55 dB to -35 dB. The integral times are 0.5 sec, 1 sec, and 2 sec, respectively. As expected, the detectable

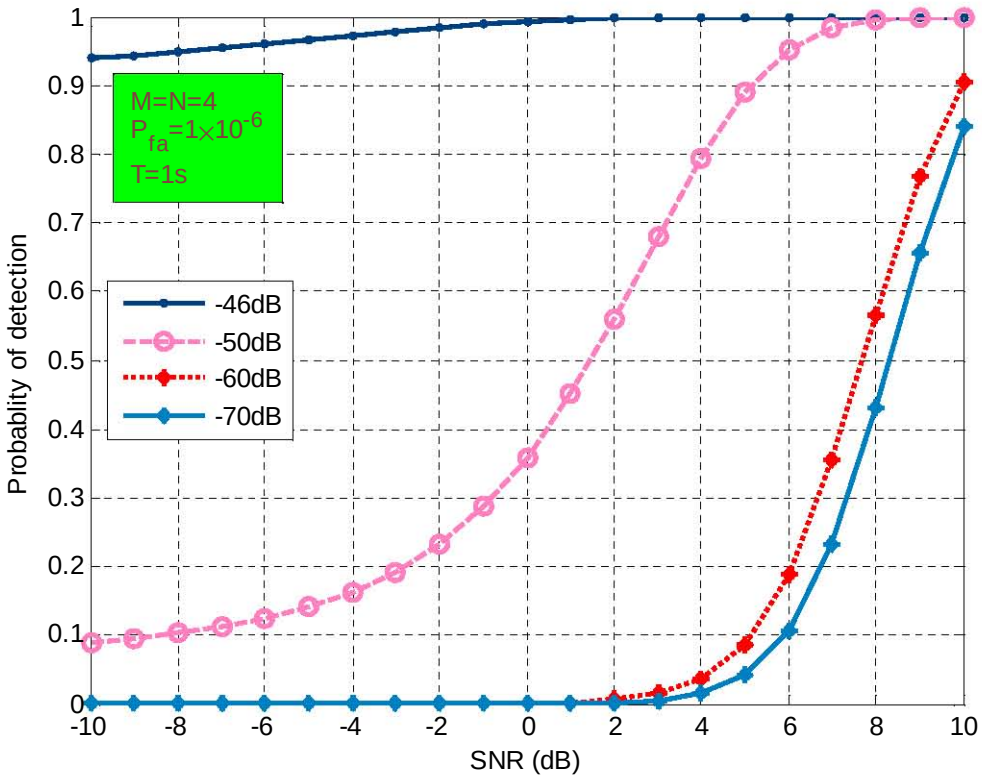

Figure 3.15: Detection performance against different reflected power.

range of a MIMO passive radar system may be significantly extended by exploiting more observation time. However, it should also be noted that the detection efficiency can-not be improved by extending integral time. It is inevitable, from Fig. 3.16, that curvature is affected by different integral time.

The ROC plot is depicted in Fig. 3.17, two different MIMO passive radar systems are engaged, in which one is a 3 by 3 MIMO passive radar system and another one is a 5 by 5 MIMO passive radar system. The values of SNR are qualified at 5 dB and 10 dB and the reflected to direct signal noise ratio is fixed at -50 dB for both systems. Based on the above analysis, the detection performance of MIMO passive radar systems is a function of the product of time-bandwidth, SNR, RDR, and the number of antennas.

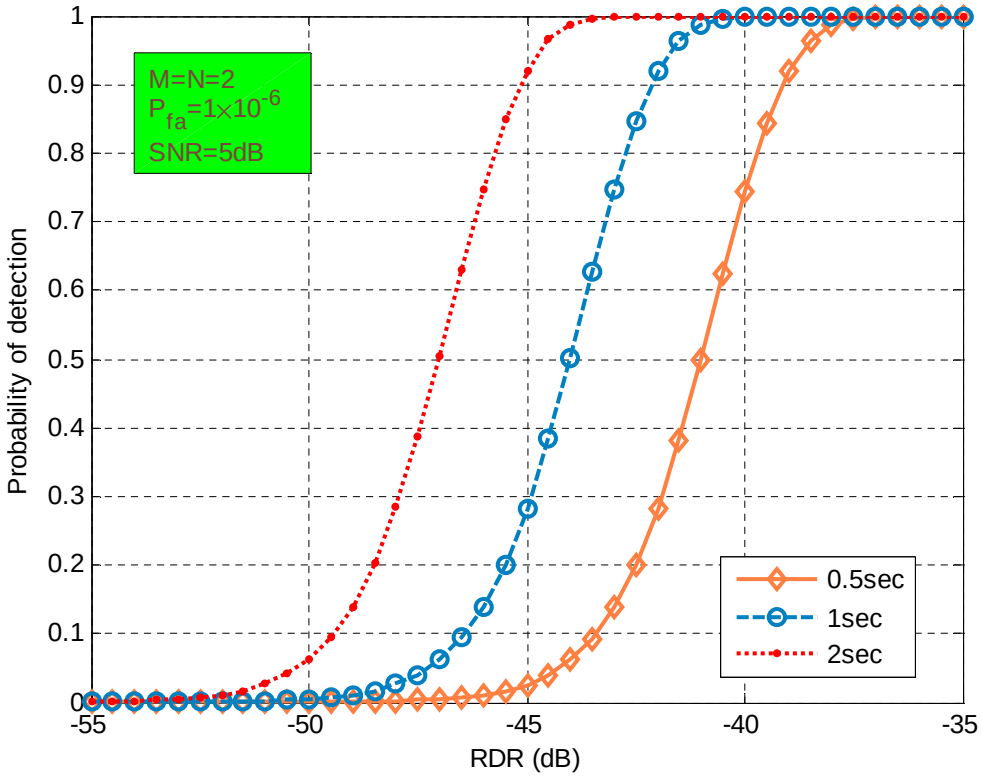

Figure 3.16: Impact of the integration time length on the detection performance.

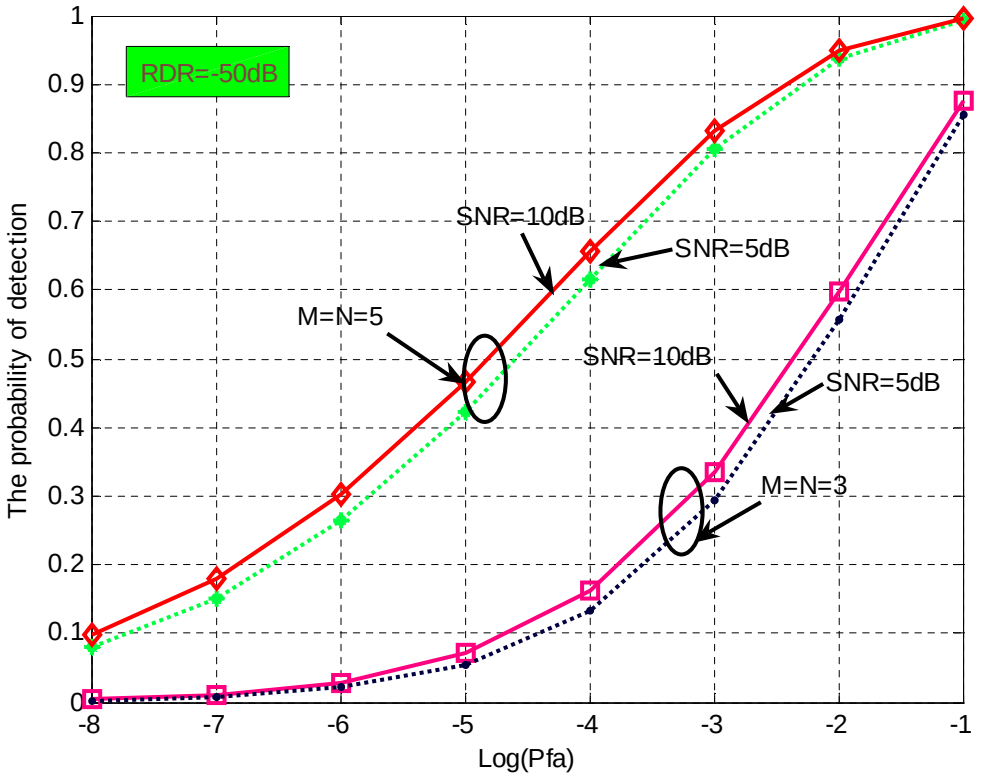

Figure 3.17: ROC of MIMO passive radar systems.

3.4 Summary

In this chapter, the detection performance in respect of stationary targets of a novel multiple antennas radar system, namely, a MIMO radar system, was examined. The detection performance of various MIMO radar systems was analysed and simulated. The closed-form expression for the probability of detection was computed and verified by simulation results.

Firstly, in order to achieve a better understanding of such a MIMO radar system, a comparison was presented between MIMO radar systems and phased array radar systems. In addition, the comparison included a hybrid system between MIMO radar systems and phased array radar systems, namely, MISO radar system.

Secondly, the robustness of MIMO radar systems to clutter was investigated. By comparing these results with those relating to phased array radar systems, it was found that MIMO radar systems are more sensitive to the change of parameters, such as SCR, SNR, and the number of antennas. The same increment of SNR or SCR may produce more processing gain to a MIMO radar system than that of a phased array radar system.

Thirdly, due to bandwidth limitations, a more practical distributed MIMO radar system was proposed. In this sub-optimal scheme, only part of the decision message instead of all the decision messages was sent to the fusion center to meet the low-bandwidth requirement. Three classical distributed algorithms were applied to MIMO radar systems, which were OR rule, AND rule, and MAJ rule, respectively. Simulation results shows that, as the most commonly used in the literature and practice, OR rule sub-optimal scheme performs better that those of the other two sub-optimal scenarios.

Lastly, since passive radar systems attract considerable attention due to its low hardware cost, covert operation, robustness against stealth, etc by exploiting non-cooperative illuminators of opportunity, a MIMO passive radar system based on FM waveform was proposed. By using Neyman-Pearson hypothesis, an optimal receiver for the MIMO passive radar was developed. The detection performance as a function of various parameters was presented.

Chapter 4

Detection of Moving Targets

In practice, radar researchers are more interested in detecting and tracking moving targets than stationary targets, such as buildings, tree, mountains, etc. This chapter thus addresses detection performance issues of MIMO radar systems in respect of moving targets. As discussed above, Doppler shift is the standard velocity measurement of moving targets. Therefore, this chapter begins by presenting Doppler frequency calculations for MIMO radar systems. It should be noted that the targets and antennas are assumed to perform in the same dimension, which means that the velocities of targets are simply 2-dimensional. As stated in the previous chapters, the principle of radar detection is to induce and summarise the relationship between the probability of false alarm, the threshold, and the probability of detection. The probability of false alarm as a function of threshold is thus analysed. Some results are plotted in respect of the probability of false alarm versus the threshold. The probability of detecting moving targets of MIMO radar systems is then examined. Both simulation and analysis results under various scenarios are presented.

4.1 Doppler Frequency Calculation for a MIMO Radar System

In Chapter 2, a simple Doppler shift relationship for a bistatic radar system was described. It was found that, as a means of measuring the change in velocity, the Doppler frequency for a bistatic radar system lies on the projected velocity component of the target along the bistatic bisector. It is well known that the Doppler frequency caused by the moving targets is responsible for performance variances in a radar system. As this chapter aims to predict the detection performance for the moving targets of a MIMO radar system, therefore, in this section, the Doppler relationship study is extended into a more complex radar system, which is made up of multiple transmit antennas and multiple receive antennas. As in Chapter 2, however, the Doppler frequency calculation is restricted to the stationary transmit and receive antennas, while moving targets are employed.

Without loss of generality, a MIMO radar system with M transmit antennas and N receive antennas is employed. These were placed wide apart, as in [30]. Advocated by Willis (1995) in [74], a well-known understanding of the Doppler shift of a bistatic radar configuration is the time rate or change of the total path length of the scattered signal. In the case of a MIMO radar system, the same principle is employed. The Doppler frequency is extended to a summation from different transmit-receive antenna pairs. For example, as shown in Fig. 4.1, for a MIMO radar system of two transmit antennas and two receive antennas, the total Doppler frequency is a summation of four different antenna pairs.

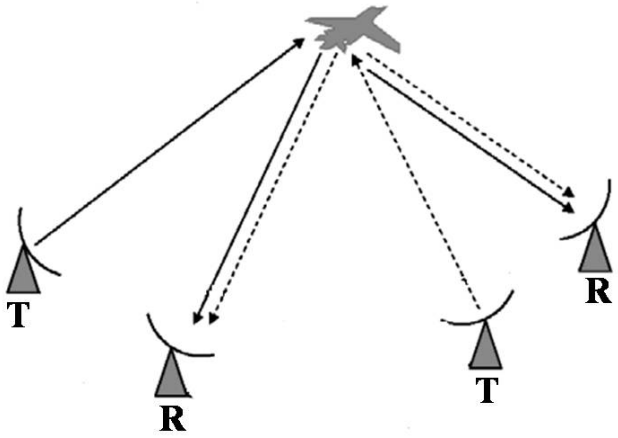

Figure 4.1: The moving target scheme of a MIMO radar system.

As discussed in Chapter 2, in the case of stationary transmit and receive antennas, the Doppler frequency can be determined by the projected velocity component of the target along the bistatic bisector. Thus, the Doppler frequency for the 2-dimensional velocity may be calculated as:

$$f_D = \frac{|V|}{\lambda} cos\theta \tag{4.1}$$

where $|V|$ denotes the amplitude of velocity, the symbol of θ signifies the moving direction, and λ represents the wavelength, which may be expressed as:

$$\lambda = \frac{c}{f_c} \tag{4.2}$$

The symbol of c is the speed of light and f_c stands for the carrier frequency.

Now, two special cases to demonstrate the Doppler frequency relationship for a MIMO radar system are examined. In the first case, a target is traveling at a constant speed with uniformly varying direction, whereas in the second case, a target is traveling in a constant direction at various velocities. A simple scheme with two transmit antennas and a single receive antenna is employed. In the first case of constant speed ($|V| = 200\,(m/s)$), the direction with respect to the first transmit-receive pair varies uniformly from 0 to 90 degrees, whereas, the direction with respect to the second transmit-receive pair varies uniformly from -90 to 0 degrees. In the second case of constant direction ($\theta_1 = 60^o, \theta_2 = 30^o$), the

velocity varies uniformly from 100 m/s to 200 m/s. The relating Doppler shift relationship is illustrated below:

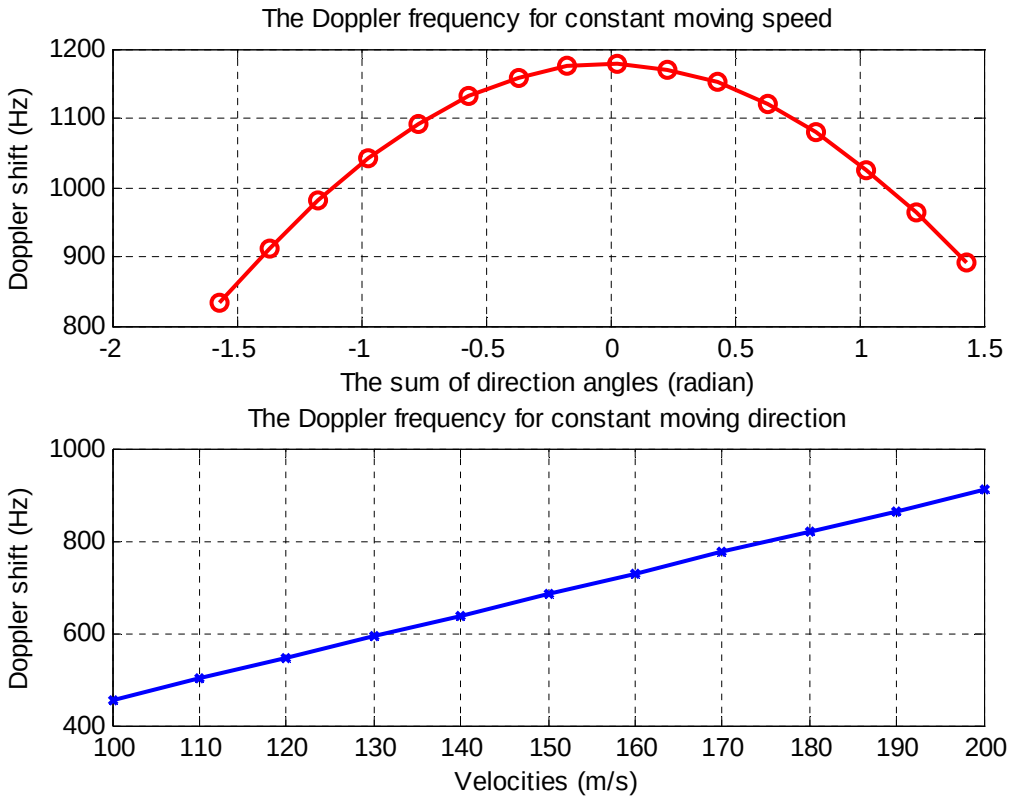

Figure 4.2: The Doppler shift relationship for a two by one MIMO radar system.

In Fig. 4.2, the carrier frequency is set at 1 GHz. As shown in Fig. 4.2, the Doppler effect is bigger when the moving speed is larger and the Doppler frequency is determined by the projected velocity component of the moving targets along the x-axis. In the case of 3-dimensional velocity, as discussed in Chapter 2, another parameter, namely, the angle difference between transmit and receive antennas, needs to be introduced to demonstrate the relatively 3-dimensional motion between objects and antennas.

4.2 Detection of Moving Targets

The Neyman-Pearson criterion is typically employed in radar detection to derive expressions for the probability of false alarm, the threshold, and the probability of detection, which is the most powerful test specifies a procedure to test an alternative hypothesis against a null hypothesis. When this is incorporated into radar detection problems, the probability of detection can be maximised by using the Neyman-Pearson test for a given probability of false alarm less than or equal to a particular value. The Neyman-Pearson hypothesis will thus be implemented in detecting moving targets and to analyse the internal relationship between the probability of false alarm, the threshold, and the probability of detection.

The probability of false alarm for a MIMO radar system is calculated in Subsection 4.2.1. In Subsection 4.2.2, the detection performance of moving targets for a MIMO radar system is mathematically demonstrated. Necessary derivations are provided. Lastly, in Subsection 4.2.3, the detection performance under various scenarios of moving targets for MIMO radar systems is presented.

4.2.1 The Probability of False Alarm

Signals processed by radars are inherently corrupted by unwanted clutter and system thermal noise. With respect to moving targets, the echo signals returned from the target of interest are thus impaired by the interference caused by the Doppler shift. The basis of distinguishing targets from other reference objects is to choose wisely when setting a fixed amplitude threshold level, which is required to be greater than noise mean level, while, conversely, also being less than the expected magnitude of the returned signal. Consequently, any signal, whose amplitude is over the threshold, will be claimed as a detected target. As stated before, however, it is possible that a noise peak will be greater than the threshold, thus leading to a false detection, which is referred to as a false alarm. The ratio of the number of false alarms over the total number of samples is known as the probability of false alarm.

Under the null hypothesis, the received signals are noises only, and they may be expressed as:

$$H_0 : \ w(t) \tag{4.3}$$

Without loss of generality, the noise is modelled by means of identically distributed zero-mean Gaussian random variables with variance σ_w^2, as in previous chapters. In the case of multiple antennas, $w(t)$ is the sum of a number (MN) of identically distributed Gaussian variables, where M is the number of transmit antennas and the symbol of N signifies the number of receive antennas. As assumed before, samples are independent. Therefore, $w(t)$ may be modelled as zero-mean Gaussian random variables with MN variance $\left(w(t) \sim N\left(0, \sigma_w^2 I_{MN}\right)\right)$, where I_{MN} is the identity matrix with size MN by MN $(MN \times MN)$.

In the case of MIMO radar systems, the distribution of the test statistic may be represented in the following manner:

$$H_0 : \ \frac{\sigma_w^2}{2} \chi_{2MN}^2 \tag{4.4}$$

where the symbol of χ_{2MN}^2 denotes the chi-square distribution with $2MN$ degrees of freedom. The Probability of Density Function (PDF) is of the form:

$$p_{\chi_{2MN}^2} = \frac{1}{2^{MN}\Gamma(MN)} x^{MN-1} \exp^{-x/2} \tag{4.5}$$

where $\Gamma(.)$ denotes the Gamma function.

Thus, with regarding toThe ROC plot as a function of range is represented in Fig. 4.11. Not surprisingly, more SNR is needed to realize a high quality. In this simulation example, the range is thus fixed at 2.5×10^8 m. the MIMO radar system, the probability of false alarm as a function of the threshold may be given as:

$$P_{fa} = F\left(\frac{\sigma_w^2 \chi_{2MN}^2}{2} > \gamma_{MIMO}\right) \tag{4.6}$$

The symbol of $F(.)$ signifies the cumulative distribution function. Consequently, the threshold given the probability of false alarm may be expressed as:

$$\gamma_{MIMO} = \frac{\sigma_w^2}{2} F_{\chi_{2MN}^2}^{-1}\left(1 - P_{fa}\right) \tag{4.7}$$

where $F^{-1}(.)$ means the inverse CDF.

In the case of phased array radars, the corresponding distribution of the test statistic is of the form:

$$H_0 : \frac{\sigma_w^2 N}{2} \chi_2^2 \tag{4.8}$$

where the degrees of freedom of the chi-square distribution are reduced from $2MN$ to 2.

Consequently, the PDF of the chi-square distribution in the case of phased array radars may be deduced as:

$$p_{\chi_2^2} = \frac{1}{2\Gamma(1)} \exp^{-x/2} \tag{4.9}$$

The corresponding probability of false alarm as a function of the threshold is given as:

$$P_{fa} = F\left(\frac{\sigma_w^2 N \chi_2^2}{2} > \gamma_{array}\right) \tag{4.10}$$

Therefore, the threshold is in the form of:

$$\gamma_{array} = \frac{\sigma_w^2 N}{2} F_{\chi_2^2}^{-1}\left(1 - P_{fa}\right) \tag{4.11}$$

Compared with MIMO radar configurations, the degrees of freedom for the chi-square distribution are reduced from $2MN$ to 2. Conversely, the variance of noise varies from σ_w^2 to $\sigma_w^2 N$, where N is the number of receive antennas.

Lastly, with respect to MISO radar systems, a hybrid of MIMO and phased array radar systems, the corresponding distribution of the test statistic may be expressed in the following manner:

$$H_0 : \frac{\sigma_w^2 N}{2} \chi_{2M}^2 \tag{4.12}$$

The corresponding PDF of chi-square distribution for MISO radar systems may be expressed as:

$$p_{\chi^2_{2M}} = \frac{1}{2^M \Gamma(M)} x^{M-1} \exp^{-x/2} \tag{4.13}$$

The degrees of freedom for the MISO radar scheme are M, which means that it lies between MIMO and phased array radar systems.

Thus, the CDF of the probability of false alarm as a function of the threshold is of the form:

$$P_{fa} = F\left(\frac{\sigma_w^2 N \chi^2_{2M}}{2} > \gamma_{MISO}\right) \tag{4.14}$$

Consequently, the threshold of MISO radar systems given a certain probability of false alarm is of the form:

$$\gamma_{MISO} = \frac{\sigma_w^2 N}{2} F^{-1}_{\chi^2_{2M}}\left(1 - P_{fa}\right) \tag{4.15}$$

As a hybrid of MIMO and phased array radar system, the degrees of freedom for the chi-square distribution are M. Conversely, the variance of noise is extended to $\sigma_w^2 N$, which is the same as in phased array radar systems.

The probability of false alarm as a function of the threshold for MIMO MISO and phased array radar systems is depicted in Fig. 4.3. The number of transmit and receive antennas are 2 and 3, respectively. Compared with MISO and phased array radar systems, in order to achieve the same probability of false alarm, the threshold of MIMO radar systems must be relatively lower, which shows the potential of MIMO radar system in terms of detection issues. The probability of false alarm versus the threshold for a MIMO radar system with various numbers of antennas is charted in Fig. 4.4. As expected, when the number of antennas is incrementally increased it also increases the degrees of freedom of chi-square distribution, and then there are higher requirements with regard to the threshold level. The systems engaged are 2by2, 2by3, and 3by3, respectively.

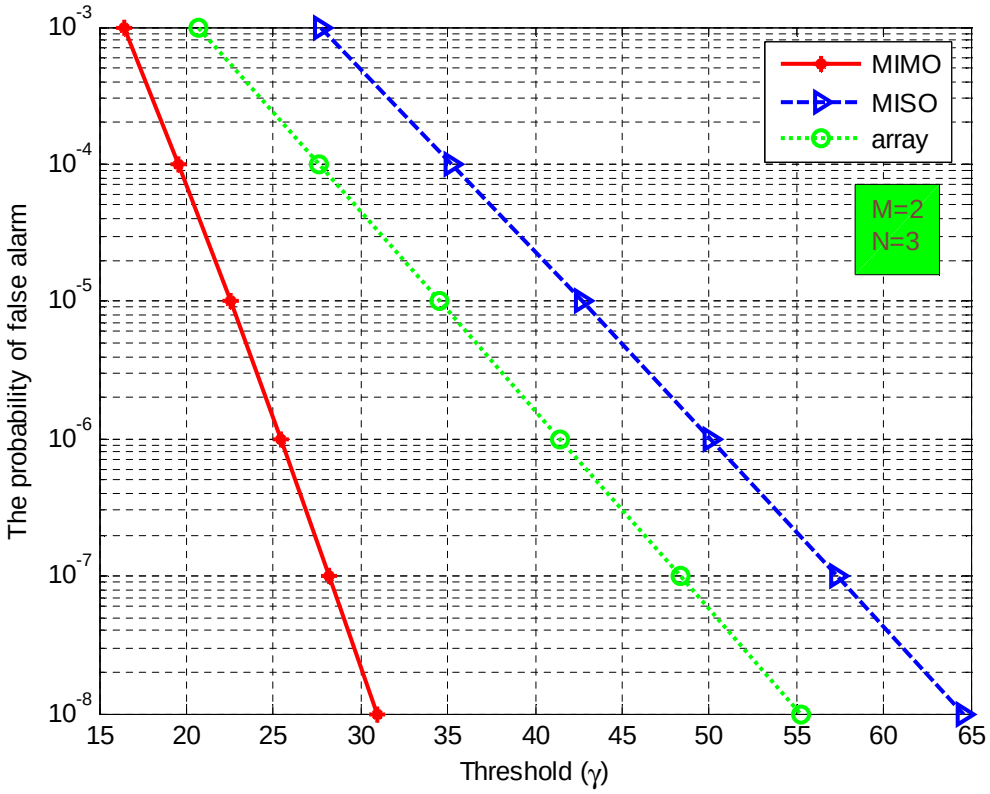

Figure 4.3: The probability of false alarm vs threshold.

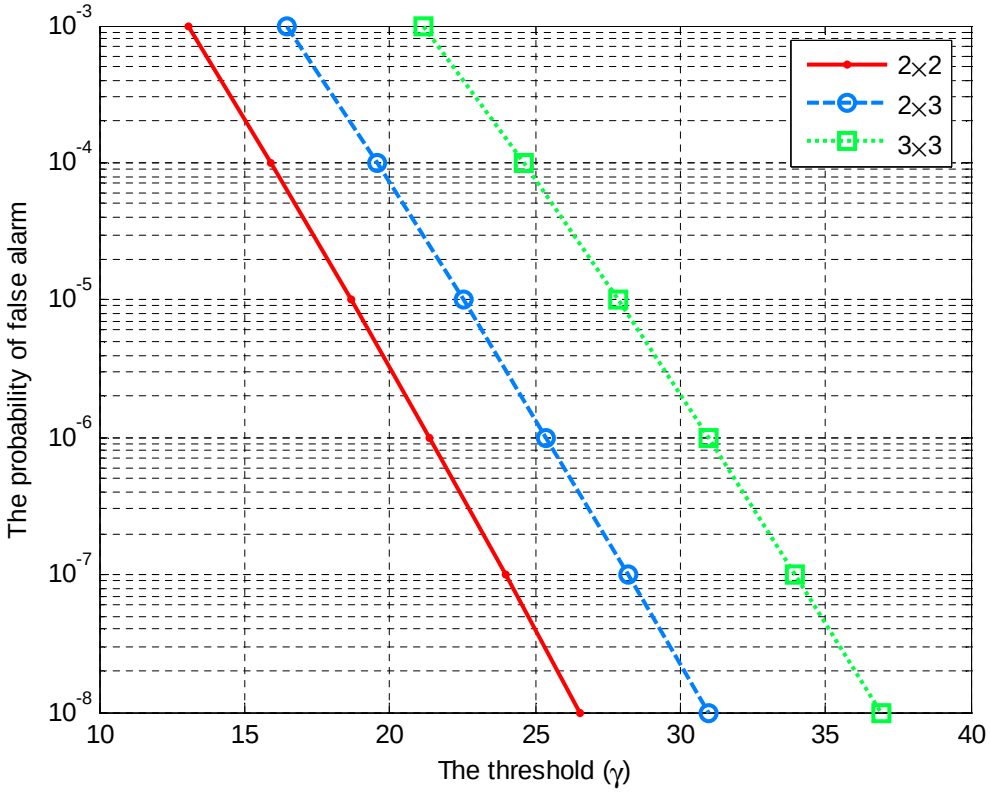

Figure 4.4: The impact of different number of antennas on threshold.

4.2.2 Detection Performance of Moving Targets

In the radar receiver, if the power of the received signals is greater than a certain threshold, the system will declare that a target has been detected. In Chapter 3, the detection performance for MIMO radar systems is analysed and examined in respect of stationary targets. The situation in respect of stationary targets is ideal, as the signal is perfectly known by receiver. In practice, however, targets are more likely to be moving. This creates issues with regard to the detection of signals with unknown parameters. The detection of moving targets with unknown velocity may also be included in this category.

In terms of the Neyman-Pearson test, under the alternative hypothesis, the received signals consist of targets and noise, which may be expressed in the following manner:

$$H_1 : \sqrt{\frac{E}{M}}\alpha s(t-\tau) + w(t) \tag{4.16}$$

Using the same definitions as in Chapter 3, symbols of E, M, and $W(t)$ denote the total transmit power, the number of transmit antennas, and system noise, respectively. In the case of Swerling I fluctuating targets, α may be modelled as identically distributed zero-mean complex Gaussian random variables $\left(\alpha \sim CN\left(0, \sigma^2 I_{MN}\right)\right)$. With respect to the non-fluctuating targets, the signal amplitude A_m may be represented as a function of SNR [27]:

$$A_m = \sqrt{2\sigma_w^2 SNR} \tag{4.17}$$

where σ_w^2 is the variance of noise.

In the case of stationary targets, as discussed in Chapter 3, the orthogonal transmit signals $s(t)$ are of the form:

$$\int_0^T s_i(t)\, s_j^*(t)\, dt = \delta_{ij} = \begin{cases} 0 & i \neq j \\ 1 & i = j \end{cases} \tag{4.18}$$

As is well known, the optimal receiver calculates the probability of detection by comparing the above statistic with the threshold. If the threshold is exceeded, the system will declare that a target has been detected, otherwise, it will declare that no target has been detected.

In practice, a radar waveform consists of two parts. The first part is a sinusoidal wave carrier with a certain frequency and amplitude according to different radar applications. The second part refers to the modulations used, such as amplitude modulation, frequency modulation, and phase modulation. A typical radar signal may be written as:

$$s(t) = A_m(t)\cos\left(2\pi f_c t + \theta\right) \tag{4.19}$$

where the symbol of f_c indicates the carrier frequency. θ is the initial phase, which is

uniformly distributed over $[0, 2\pi]$ and independent from signal to signal. The symbol of $A_m(t)$ denotes the amplitude of the signal, in the case of Swerling I fluctuating targets, which may be modelled as complex Gaussian distribution random variables, whereas, non-fluctuating targets, can be calculated by using a given SNR $\left(A_m = \sqrt{2\sigma_w^2 SNR}\right)$. Therefore, the probability of detection in respect of the unknown initial phase for a radar system may be calculated by averaging over the initial phase θ.

In the case of moving targets, the signal may be rewritten as:

$$s(t) = A_m(t)\cos(2\pi f_s t + 2\pi f_d t + \theta) \tag{4.20}$$

where the Doppler frequency is denoted by the symbol f_d.

If the Doppler frequency and initial phase are known at the receiver and if they remain constant during the observation time, then the factor $\cos(2\pi f_s t + 2\pi f_d t + \theta)$ will be a constant, which may be simply denoted by the symbol C_{on}. The detection issues in respect of this example may be calculated by combining Eqn. 3.10, Eqn. 3.17, and Eqn. 3.21 with factor C_{on}. Consequently, the probability of detection for MIMO, phased array, and MISO radar systems may be expressed in the following manners:

$$P_{d(MIMO)} = 1 - F_{\chi^2_{2MN}}\left(\left(\frac{\sigma_w^2}{\frac{EC_{on}^2}{M}\sigma_\alpha^2 + \sigma_w^2}\right) F^{-1}_{\chi^2_{2MN}}\left(1 - P_{fa}\right)\right) \tag{4.21}$$

$$P_{d(array)} = 1 - F_{\chi^2_2}\left(\frac{\sigma_w^2}{\sigma_w^2 + EC_{on}^2 MN\sigma_\alpha^2} F^{-1}_{\chi^2_2}\left(1 - P_{fa}\right)\right) \tag{4.22}$$

$$P_{d(MISO)} = 1 - F_{\chi^2_{2M}}\left(\frac{\sigma_w^2}{\sigma_w^2 + \frac{EC_{on}^2 N\sigma_\alpha^2}{M}} F^{-1}_{\chi^2_{2M}}\left(1 - P_{fa}\right)\right) \tag{4.23}$$

If the parameters of the Doppler frequency and initial phase are not known for the receiver, the probability of detection may be computed by means of two steps. The unknown initial phase θ may be averaged over 2π. The result may be further averaged over the incremental phase caused by the unknown Doppler frequency $\varphi = 2\pi f_d T$. As indicated in the definition of the probability of detection, a target will be detected if the received power is greater than a certain threshold. In the case of MIMO radar systems, the probability of detection may be represented as:

$$P_{d(MIMO)} = \int_{Th}^{\infty}\int_{0}^{2\pi} p\left(H_1^2 \mid \theta\right) \tag{4.24}$$

The symbol of $p\left(H_1^2 \mid \theta\right)$ signifies the PDF of test statistic in the favour of alternative hypothesis under the condition of θ. The closed-form solutions do not exist for such integrals. Some approximations may be found in [11][17][21][59].

With respect to a moving target without constant moving speed, it is mere to acquire the instantaneous values of the Doppler frequency and phase of signals. Thus, here, we

propose a cumulative detection measurement for moving targets based on the average velocity and observation time.

As is well known, for a radar system, one can obtain SNR as a function of range and RCS by manipulating the radar range equation. Given a target, since the RCS of the target is fixed, the values of SNR vary correspondingly for different locations of the target of interest. Keeping this in mind, thus, as an intermediary, SNR may be calculated by using the effective range. The probability of detection as a function of the target's range can be further calculated by the values of SNR.

Serving as a theoretical study, a simple scheme is implemented in this work. Each transmit-receive antenna pair is assumed to be an independent bistatic radar, and each pair experiences the same coefficient, such as transmitting antenna power gain, receiving antenna power gain, received peak power, transmitted peak power, etc. For a bistatic radar system, the range measurement is defined as the product of transmitter-to-target range and receiver-to-target range. Furthermore, it is assumed that compared with the distance among antennas, the traveling distance of moving targets is big enough to remove the effects of space between the antennas, which means that the change of range may be computed by the product of velocity and observation time.

A well-known range equation for the bistatic radar may be expressed in the form of:

$$SNR = \frac{P_T G_T G_R \lambda^2 \sigma_B F_T^2 F_R^2}{(4\pi)^3 k T_s B_n \kappa^2 L_T L_R} \tag{4.25}$$

Table 4.1: Definitions.

P_T	transmitted power
G_T	transmit antenna power gain
G_R	receive antenna power gain
λ	transmitted wavelength
σ_B	radar cross section
F_T	propagation parameter for transmitter-target path
F_R	propagation parameter for receiver-target path
k	Boltzmann's constant, $1.3807 \times 10^{-23} JK^{-1}$
T_s	receiver noise temperature
B_n	receiver noise bandwidth
κ	range product
L_T	transmit system losses
L_R	receive system losses

The Boltzmann constant is the physical constant, which indicate energy at the individual particle level when the temperature is observed at the collective or bulk level.

A reduced range equation of bistatic radar system is expressed in the following manner:

$$SNR = \frac{P_T G_T G_R c^2 \sigma_B}{(4\pi)^3 f_c^2 \kappa^2} \tag{4.26}$$

where c denotes the speed of light and f_c indicates the carrier frequency. With regard to the effect of the Doppler frequency, the carrier frequency may be calculated as $f_c = f_c + f_d$. The rest remaining parameters are the same as defined above.

It is assumed that the range difference for a bistatic radar system may be simply computed by the product of average moving speed and observation. Thus, the above equation may be further rewritten as:

$$SNR = \frac{P_T G_T G_R \lambda^2 \sigma_B F_T^2 F_R^2}{(4\pi)^3 k T_s B_n (VT)^2 L_T L_R} \tag{4.27}$$

In the case of multiple antennas, each transmit-receive pair is independent from others. Therefore, the total SNR is a summation of the independent transmit-receive pairs. The corresponding probability of detection may be calculated by using Eqn. 3.10, Eqn. 3.17, and Eqn. 3.21. The simulation results will be presented in the next section.

4.2.3 Monte Carlo Simulations

The detection performance of moving targets for multiple antennas radar systems will be examined in this section. The detection performance of instantaneous Doppler frequency is examined first, and thereafter the cumulative probability of detection for moving targets.

The main involved parameters in the first part are listed as following:

Table 4.2: Simulation parameters.

M	number of transmit antennas	2
N	number of receive antennas	2
SNR	signal to noise ratio	-5~20dB
V	velocity	100m/s
F_c	carrier frequency	10GHz
θ	the initial phase	$\pi/18$
c	speed of light	3×10^8m/s
P_{fa}	the probability of false alarm	1×10^{-6}
θ_i	moving direction	$\theta_i = \frac{i}{MN}\pi$
F_r	Pulse Repetition Frequency (PRF)	1MHz

Without indicating on the simulation plots, the default parameters are listed above.

The probability of detection for various multiple antennas radar systems is illustrated in Fig. 4.5. The Doppler frequency may be calculated by manipulating Eqn. 4.1. It should be noted that the absolute value of Doppler frequency is implemented in this dissertation. The meaning of positive and negative values of Doppler frequency indicate the moving direction, thus, it will not affect the detection performance. It can be seen from Fig. 4.5 that there is good agreement between the simulation results and the theoretical results. As expected, in the high SNR region, MIMO radar systems outperform the traditional multiple antenna radar systems, namely, phased array radar systems. As a hybrid of

MIMO and phased array radar systems, the detection performance of the MISO radar configuration lies between MIMO and phased array radar systems.

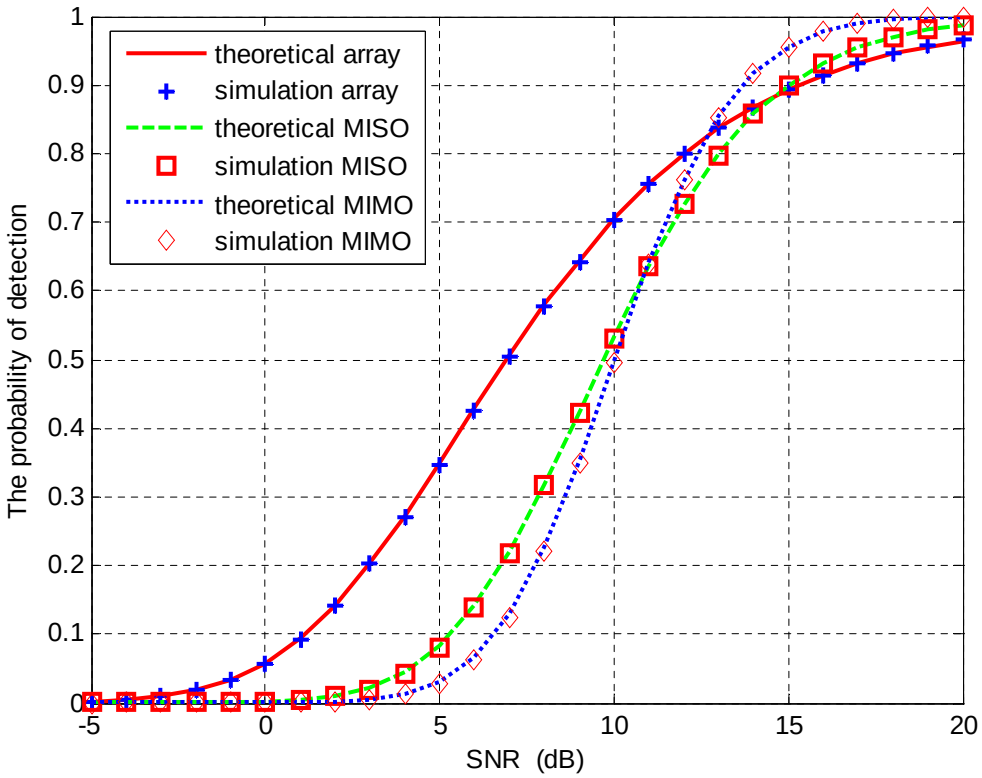

Figure 4.5: Detection performance of MIMO, MISO, and phased array radar systems.

The impact of diversity gain on the detection performance of MIMO radar systems is illustrated in Fig. 4.6, which plots the detection performance of a moving target of interest versus SNR. In this example, the MIMO and phased array radar systems are 2by2 and 4by4, respectively. It is evident, from Fig. 4.6, that the detection performance may be significantly improved by the diversity or spatial gain provided by multiple antennas. It may be observed that the analysis is verified by the simulation results. Additionally, for high quality service, for instance, the required probability of detection is above ninety percent, which means that MIMO radars are better than phased array radar systems under such circumstances.

The comparative study between static and moving targets for a MIMO radar systems is conducted in Fig. 4.7. Besides default parameters, the comparison is performed between two MIMO radar systems, which are two by two and two by five radar systems, respectively. The initial phase is defined as $\pi/6$. It may be clearly observed from Fig. 4.7 that there is a detection performance loss attributed to Doppler frequency between static and moving targets. Take two by five MIMO radar systems as an example, there is about 1 dB loss when the probability of detection equals 0.6.

The detection performances of various values of Doppler shift are summarised in Fig. 4.8. The Doppler frequency is normalised by the PRF, which may be expressed as f_d/f_r.

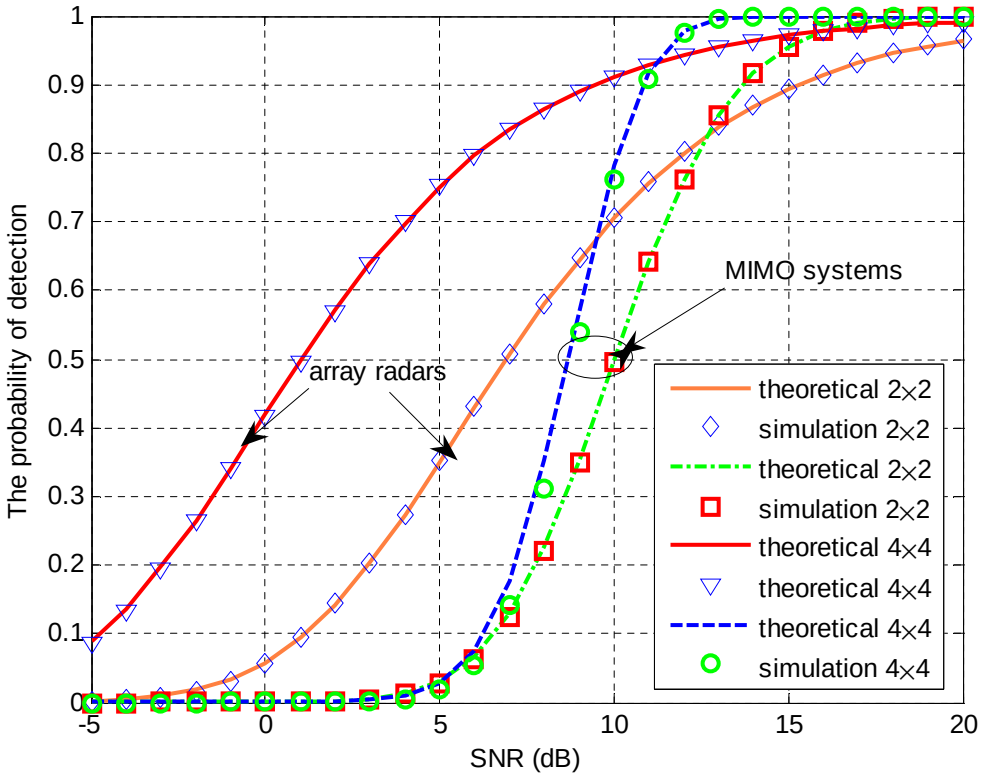

Figure 4.6: Impact of different number of antennas on the detection performance.

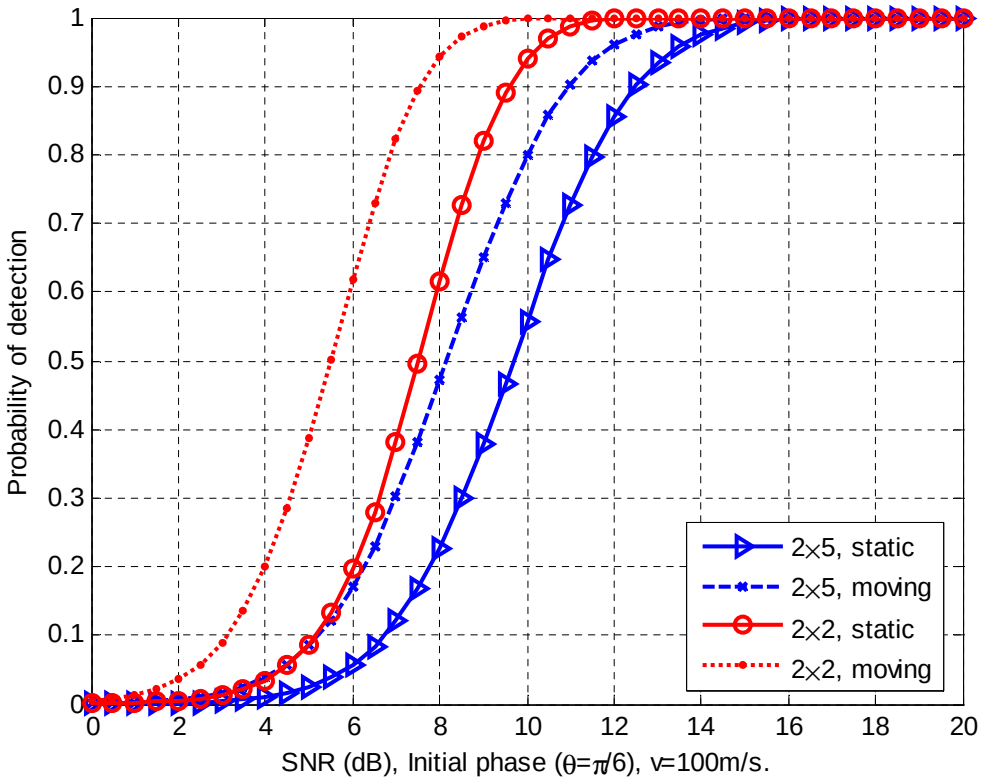

Figure 4.7: Comparison between static and moving targets for MIMO radar system.

A thorough definition may be found in [13]. The total phase for the input signal varies uniformly from 0 degree to 90 degrees in increments of 10 degrees. It can be seen that moving targets cannot be detected even for very large SNR when the total phase is too large, which means that each SNR is appointed a maximum detectable velocity. The total phase is made up of two parts, as stated before, namely, the initial phase and the contribution of Doppler frequency. Since $cos(x)$ is mono-decreasing between 0 degree and 90 degrees, the corresponding probability of detection is decreasing too. If the initial phase is assumed to be zero, thus, when the phase equals to 90 degrees, the corresponding Doppler frequency equals 250 kHz. According to Eqn. 4.1,

$$f_d = \frac{v}{c} f_s \tag{4.28}$$

It may be obtained:

$$v = 7.5 \times 10^4 \, (m/s) \tag{4.29}$$

which means that under the above detectable speed, a greater SNR is needed to detect faster targets.

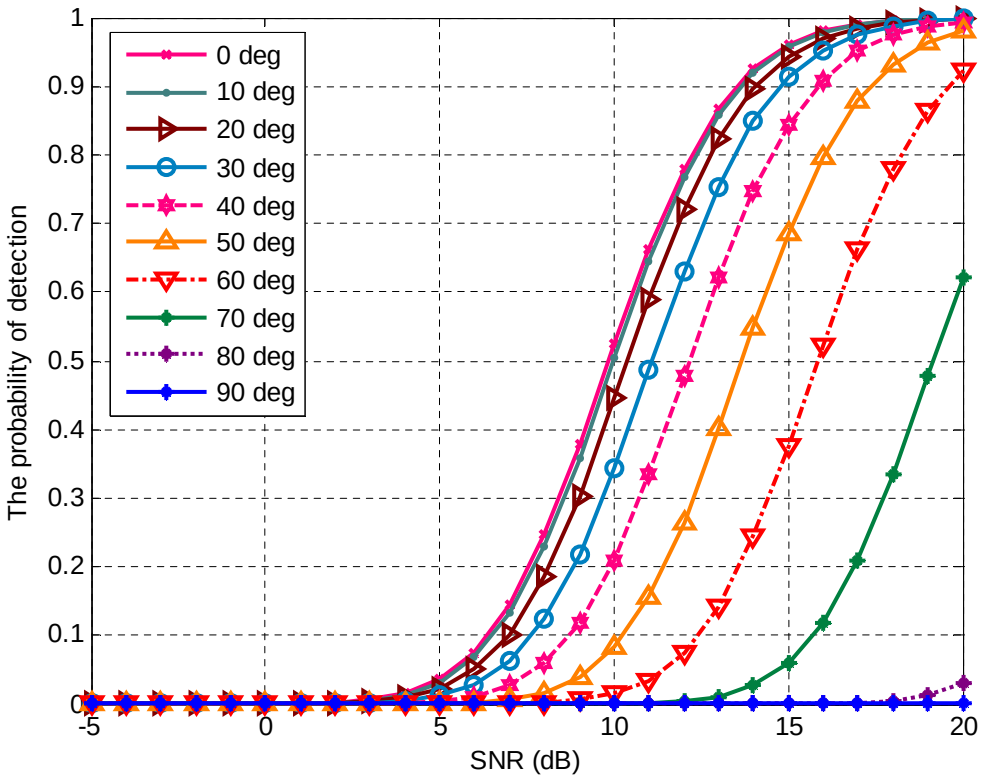

Figure 4.8: Detection performance on various total phase.

The ROC performance of both MIMO and phased array radar systems is ploted in Fig. 4.9, in which the relationship between the probability of detection and the probability of false alarm is depicted. As expected, MIMO radar systems outperform phased array radar

systems with high SNR. Conversely, though in the low SNR region, phased array radar systems perform better than MIMO radar systems.

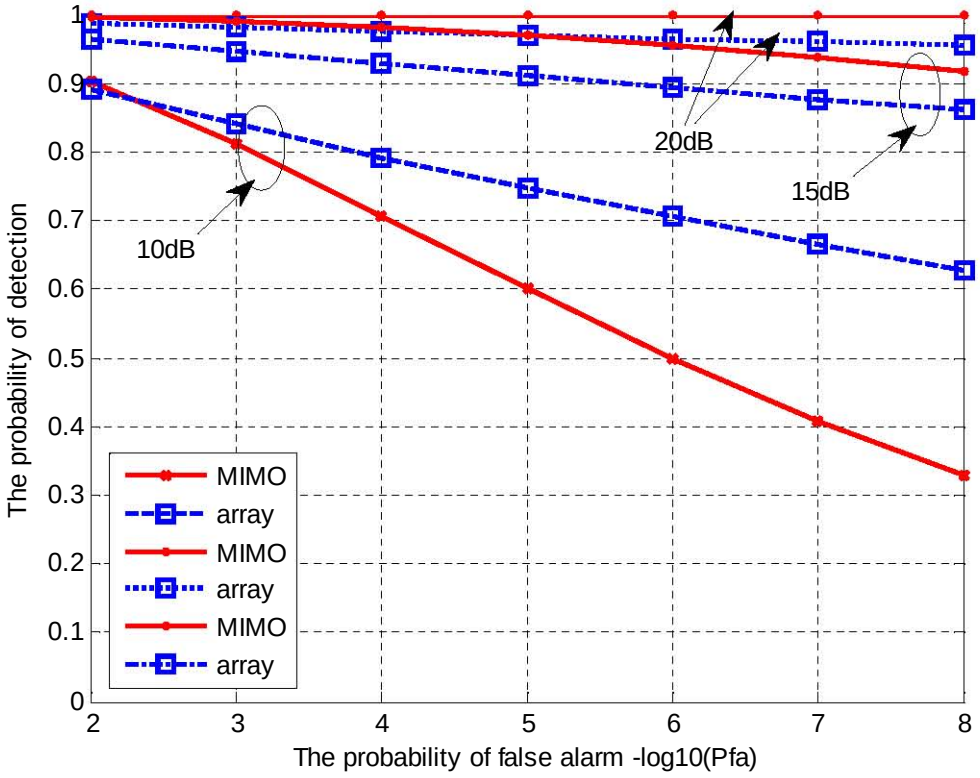

Figure 4.9: ROC of MIMO and phased array radar systems.

The second part of this section presents the cumulative probability of detection for moving targets in respect of the range change. The involved parameters are listed as following:

Similarly as the last part of this section, the default parameters will be implemented without special indication.

Based on Eqn. 4.25, Fig. 4.10 demonstrates SNR as a function of range. It is well known that the value of SNR given a target will be reduced by the increment of range. The Fig 4.10 illustrates the internal relationship between SNR and range for a MIMO radar system. Three different targets are engaged. The RCS for each target is 10 dBsm, 15 dBsm, and 20 dBsm, respectively. The remaining simulation parameters are listed in Table. 4.3. It is clearly shown that the value of SNR decreases by increasing range. It is interesting to observe that the curvatures for these three simulation results look similar, which means that for a given radar system, the impact of range to the value of SNR is fixed.

It should be noted that it may have many other forms in respect of radar range equations. The aim of this dissertation is to introduce a cumulative detection method for moving targets based on the average moving speed due to the fact that it is difficult to know instantaneous details of moving targets. For instance, the time-bandwidth product and Doppler processing may also bring extra gain to a radar system. In this work, it is thus

Table 4.3: Simulation parameters.

M	number of transmit antennas	2
N	number of receive antennas	2
Pt	transmitted power	30 dBW
Gt	transmit antenna gain	30 dB
Gr	receive antenna gain	30 dB
RCS	radar cross section	10, 15, 20 dBsm
$\bar{v}$	average speed of target	100 m/s
c	speed of light	3×10^8 m/s
P_{fa}	the probability of false alarm	1×10^{-6}
k	maximum range	9×10^7m
F_c	carrier frequency	10 GHz
F_t	transmit path propagation factor	-5 dB
F_r	receive path propagation factor	-5 dB
Bo	boltzmann constant	$1.3807 \times 10^{-23} JK^{-1}$
Bn	bandwidth of noise	6MHz
T_s	receive temperature	300
L_t	transmit loss	1 dB
L_r	receive loss	1 dB

assumed that transmit and receive gains (G_T, G_R) include other potential gains. On the other hand, transmit and receive loss (L_T, L_R) also include other potential system loss.

The corresponding detection performances in respect of these three targets with different SCR are presented in Fig 4.11. For a given moving target, if it moves towards the radar observers, after a certain observation time, the detectable probability will be significantly enhanced. Conversely, if a target travels away from the radar, the probability of detection will be impaired.

The last figure shows the cumulative detection results for various MIMO radar systems. As is shown in Fig. 4.12, the MIMO radar systems are two by two, three by two, and three by three, respectively. It may be clearly observed that the detection performance may be significantly improved by spatial diverity. The target with 15 dBsm RCS is implemented in this example. The rest values of simulation parameters could be found in Table. 4.3.

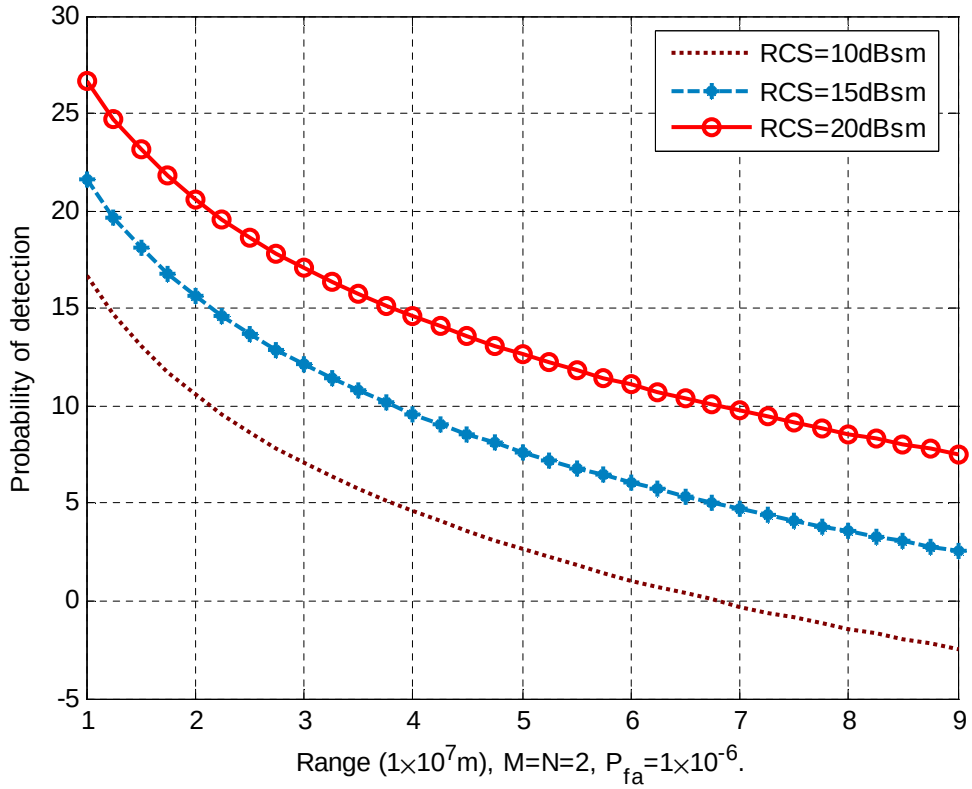

Figure 4.10: SNR calculation by range.

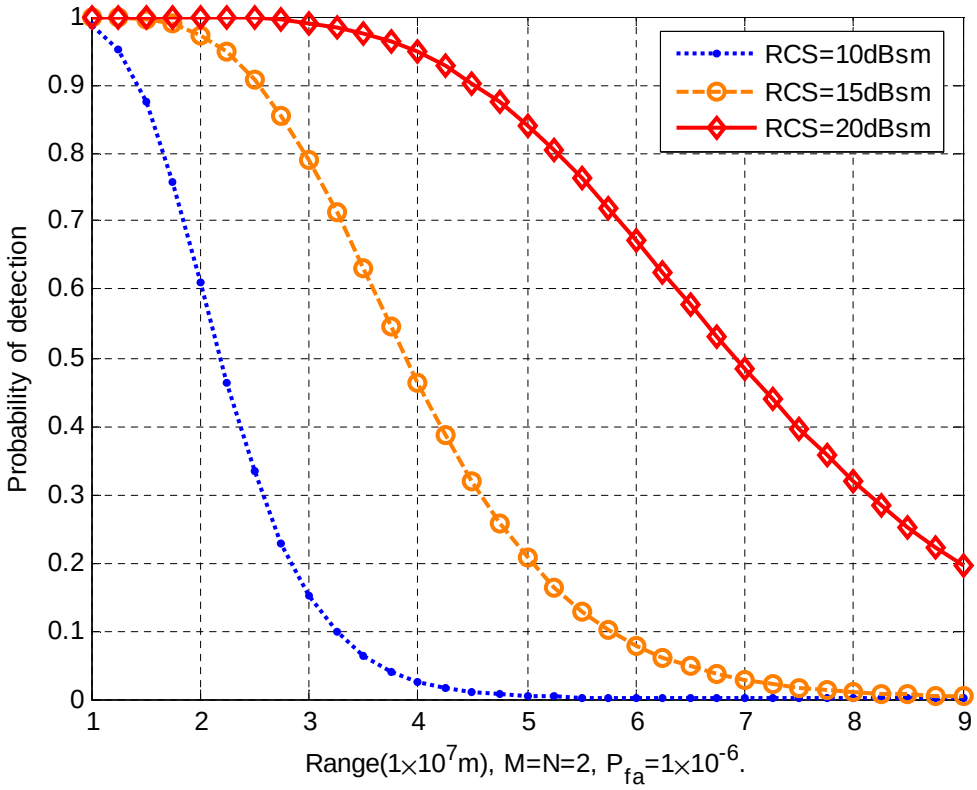

Figure 4.11: Detection performance versus range.

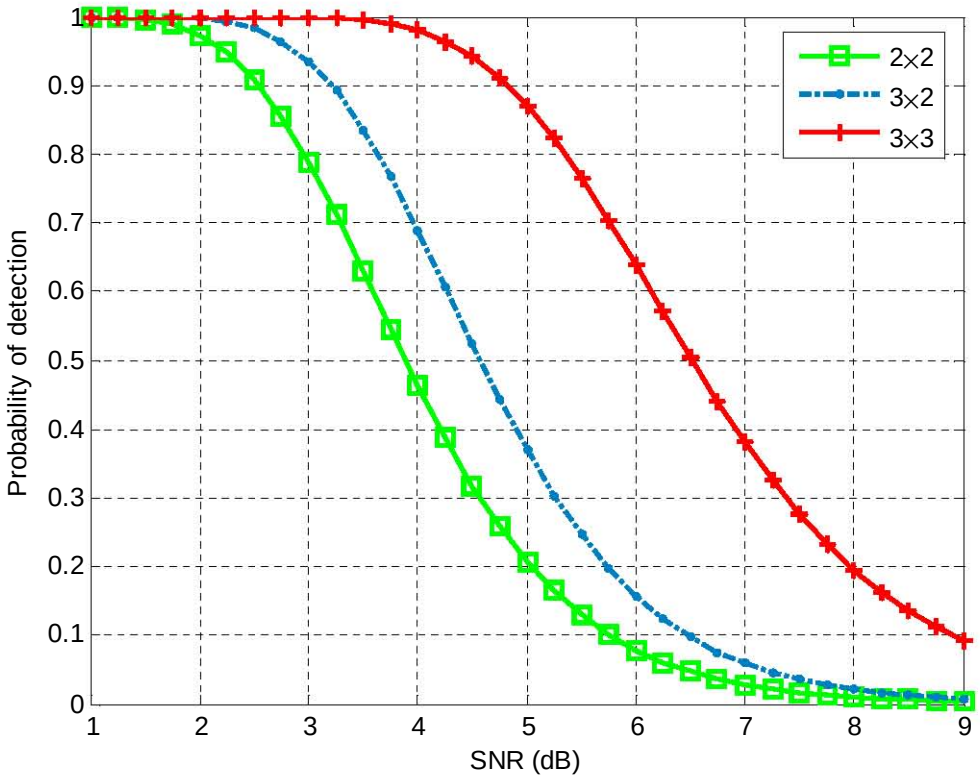

Figure 4.12: Cumulative detection with various numbers of antennas.

4.3 Summary

A study in respect of the detection of stationary targets by using MIMO radar systems was carried out in the previous chapter. Unlike the case of moving targets, the detection of stationary targets requires the receiver to know accurately the signal information. In practice, however, this may not be the case. Consequently, in this chapter, we examined the detection performance in respect of moving targets of MIMO, MISO, and phased array radar systems. In the case of moving targets, it is assumed that the phase is unknown, and this is affected by the initial phase and Doppler shift caused by the motion of targets. The analysis was verified by the simulation results. It may be observed that there is a good agreement between theoretical results and simulation results.

Based on the radar range equation, the cumulative probability of detection in respect of moving targets was calculated. This is influenced by the fact that it is more difficult to detect or track far objects than ones that are close to the observer. A long distance will decrease SNR. Consequently, this will impair the probability of detection. It should be noted that, given the theoretical study herein, the system model proposed in this dissertation is very simple. It is assumed that the distance between antennas compared with the travel distance of moving targets is too small to be neglected. In the future, a more realistic scheme would need to be explored.

Chapter 5

Conclusions

The MIMO technique can efficiently increase the capacity and reduce the fading of a channel in a wireless communication system. Recently, motivated by the development of MIMO techniques in the field of wireless communication, the concept of MIMO has been applied in the radar context to handle a similar issue, the variations in the returned signal power from different aspects of a target of interest. It is well know that those variations are responsible for impairing the detection and estimation performance of a radar system. A MIMO radar system can achieve better understanding or estimation of a target's RCS by observing it from various angles. Consequently, the detection and estimation of a radar system may be significantly improved by exploiting the angular or spatial diversity of targets. The basis of MIMO radar systems is widely separated antennas to assure angular or spatial diversity. This dissertation has been devoted to studying the detection performance of such a novel multiple-antenna radar system, which can be divided into two parts, viz. the detection of stationary targets and the detection of moving targets.

Chapter 2 introduces the background relating to the use of radar systems for detection of targets. The relevant theories and concepts in terms of Doppler frequency, matched filter and the ambiguity function have been summarised. The Doppler frequency relationship for a bistatic radar has been described, and the Doppler frequency calculation for a practical environment has been presented. The matched filter theory and the ambiguity function theory have been implemented to compute the probability of detection and to study the ambiguity property of FM waveform, respectively. Additionally, a critique is provided of the important literature relating to detection study and various MIMO radar mechanisms.

In Chapter 3, the detection performance of stationary targets for the MIMO radar systems has been examined. This chapter started with the detection performance of stationary targets in the white Gaussian noise. In order to gain a better understanding of this novel multiple-antenna radar system, a comparison study between MIMO radar systems and conventional phased array radar systems is presented to demonstrate their respective properties. In addition, the comparison, including a hybrid of MIMO and phased array radar systems, known as a MISO radar system, has also been presented. It has been found that in the high SNR region, the detection performance of a MIMO radar system is bet-

ter than that of a phased array radar system, while in the low SNR region, in contrast, the phased array radar system delivers better detection performance. Based on that, we can conclude that the MIMO radar system is better at detecting or tracking bigger targets, whereas the phased array radar system has advantages in detecting smaller targets. As expected, the detection performance of MISO radar systems lies between MIMO and phased array radar systems.

Afterwards, the robustness of MIMO radar systems to clutter has been studied. Compared with the relevant results of phased array radar systems, it has been shown that MIMO radar systems are able to mitigate the effects of clutter. It is evident from the results obtained in this study that MIMO radar systems are more sensitive to the changes of parameters than those of the phased array radar systems, which may be attributed to the degrees of freedom of the chi-square distribution random variables. It has been deduced that the degrees of freedom for the MIMO and phased array radar systems are $2MN$ and 2, where M and N are the number of transmit antennas and receive antennas, respectively.

A more practical distributed MIMO radar system has been proposed with bandwidth considerations. In this sub-optimal scheme, instead of all the decision messages, only part of the decision message has been sent to the fusion center to meet the low-bandwidth requirement. Three well-known distributed algorithms have been adapted to the MIMO radar context. They are the OR rule, AND rule, and MAJ rule, respectively. It is clearly observed that there is a performance loss compared with the optimal MIMO radar systems. However, considering bandwidth requirements, the sub-optimal scenarios are meaningful configurations in practice. Additionally, as the rule most commonly used in the literature and practice, the OR rule used in the sub-optimal system delivers a better detection performance than those of the other two sub-optimal scenarios.

Based on the FM waveform, a MIMO passive radar system has been proposed in Chapter 3. By exploiting non-cooperative illuminators of opportunity, a passive radar system attracts considerable attention due to its low hardware cost, covert operation, robustness against stealth, etc. By using Neyman-Pearson hypothesis, an optimal receiver for the MIMO passive radar has been developed. The closed-form equations for the probability of false alarm, the threshold, and the probability of detection have been derived. Lastly, the detection performance as a function of various parameters has correspondingly been presented.

Chapter 4 investigated the detection performance of moving targets for the MIMO radar systems. This chapter started with the Doppler frequency calculation for the MIMO radar systems. The detection study of moving targets was examined first by taking instantaneous Doppler frequency into account. Thereafter, the detection study was extended to a more complex system, including range considerations. The cumulative probability of moving target detection for the MIMO radar systems has been derived. The results showed that Doppler frequencies may cause a detection performance loss for a radar system.

Additionally, in order to assist both newcomers and current radar researchers who conduct detection studies of MIMO radar systems, the pertinent Matlab source codes used throughout the dissertation may be found in the appendix.

This served as a theoretical study and, consequently, many topics relevant to the MIMO radar systems are open in the future. Without attempting completeness, some are listed briefly here:

- A more realistic simulation should take the full radar equation into account, which means that different pairs of transmitters or receivers experience a different signal to noise or signal to clutter ratio.
- We should also mention that the modelling of clutter needs to be further explored. Many forms of clutter have symmetric (spiky) distributions, which would modify the results obtained here.
- The trade-offs between spatial diversity and coherent processing gain should be further explored in more detail, which means that a novel multiple-antenna radar configuration integrating MIMO and phased array radars should be examined further.
- As discussed in the section looking at MIMO passive radar, the trade-offs of expanding the minimum detectable reflected power in respect of the product of time-bandwidth and the number of antennas should be further explored.
- Moreover, the direct signal cancellation should be further developed for MIMO passive radar systems in order to improve their detection range and performance.
- Furthermore, the real data should be manipulated to test the performance of this novel multiple-antenna radar system.
- Lastly, more practical issues in relation to hardware should be addressed in the future.

Appendix A

Matlab Source Codes

All the Matlab source codes utilised in this research are listed here, which could be found in attached CD. All parameters are set according to the last simulation run.

Chapter 2:

1. Doppler.m demonstrates Doppler relationship for a bistatic radar, absolute value of Doppler frequency, and 3-D plot of Doppler frequency.

2. Detectionpdfs.m plots the PDFs relationship among the probability of detection, the probability of false alarm, the threshold, and the probability of mis-detection for non-fluctuated targets.

3. Matchedfilter.m is the Matlab code to compute and simulate the probability of detection and the probability of mis-detection for the matched filter receiver, which can be extended to multiple-samples straightforwardly.

4. Fmdemonstrate.m is the file to demonstrate FM signals.

5. AFofFM.m is the ambiguity function for FM signals.

Chapter 3:

1. MIMOPdperformance.m may compute and simulate the probability of detection and the probability of mis-detection subject to the probability of false alarm for MIMO, phased array, and MISO radar systems, which could provide various detection results in terms of different number of transmit antennas, different number of receive antennas, various values of SNR, etc.

2. ROCdifferentSNR.m may generate 3-D ROC plots for MIMO radar systems.

3. Robustnesstoclutter.m provides comparative results for MIMO and phased array radars with the effects of clutter, which may generate various results depending on different values of SNR and SCR.

4. DistribuatedMIMOradars.m embraces three classical distributed algorithms OR, AND, and MAJ, which can offer various detection results for distributed MIMO radar systems.

5. Varianceoffft.m tests variance assumption for the MIMO passive radar systems.

6. MIMOpassivedetection.m provides detection performance of the MIMO passive radar systems as a function of SNR, number of antennas, integral time, etc.

Chapter 4:

1. Dopplerformultipleantennas.m reveals Doppler frequency for multiple-antennas radar systems.

2. PfaMIMO.m represents the probability of false alarm and the threshold for MIMO, phased array and MISO radar systems.

3. Detectionofmovingtargets.m demonstrates the detection performance of moving targets for MIMO, phased, phased array and MISO radar systems, which can generate various detection results depending on various parameters such as number of antennas, SNR, Doppler frequency, etc.

4. SNRvsrange.m plots the impact of range to SNR for different targets and cumulative detection of MIMO radar based on range.

Bibliography

[1] http://www.ece.gatech.edu/research/labs/sarl/tutorials/ECE4606/14-MatchedFilter.pdf.

[2] http://en.wikipedia.org/wiki/Matched_filter.

[3] http://cnx.org/content/m10153/latest/.

[4] http://en.wikipedia.org/wiki/Discrete_Fourier_transform.

[5] M. Abramovitz and I. A. Stegun. *Handbook of Mathematical Functions*. Dover, 1972.

[6] T. Aittomaki and V. Koivunen. Exploiting correlation in target detection using mimo radar with angular diversity. In *In Proceeding of the 43rd Asilomar conference on signals, systems, and computers*, 2009.

[7] M. Akcakaya and A. Nehorai. Mimo radar detection and adaptive design in compound-gaussian clutter. In *IEEE International Radar Conference*, 2010.

[8] S. M. Alamouti. A simple transmit diversity technique for wireless communications. *IEEE Journal on Selected Areas in Communications*, 16:1451–1458, Oct 1998.

[9] S. Alhakeem and K. P. Varshney. A unified approach to the design of decentralized detection systems. *IEEE Trans on Aero and Elect Systems*, 31(1):9–20, 1995.

[10] I. Barany and V. Vu. Central limit theorems for gaussian polytopes. *The Annals of Probability*, 35:1593–1621, 2007.

[11] D. K. Barton. *Modern Radar System Analysis*. Artech House, Norwood, MA, 1988.

[12] D. Bliss, K. Forsythe, and G. Fawcett. MIMO Radar: Resolution, Performance and Waveforms. In *ASAP Workshop1*, 244 Wood St, Lexington, MA, June 2006. MIT LincoIn Lab.

[13] R. Blum, S. Kassam, and H. Poor. Distributed detection with multiple sensors: Part ii: advanced topics. *Proc. IEEE*, 85(1):64–79, 1997.

[14] R. F. C, C. Scott, W. Dennis, M. Jeffrey, and C. Kevin. MIMO radar theory and experimental results. In *Proc Thirty-Eighth Asilomar Conference on Signals, Systems and Computers*, 244 Wood St, Lexington, MA, Nov 2004. IEEE.

[15] C. Y. Chong, F. Pascal, and M. Lesturgie. MIMO Radar Detection under non-Gaussian clutter. In *Proc. IEEE International Radar Conference* , Bordeaux France, Oct 2009.

[16] E. B. Chun Yang, Mikel Miller and T. Nguyen. Comparative study of coherent, non-coherent, and semi-coherent integration schemes for gnss receivers. Technical report, Sigtem Technology, 2007.

[17] G. R. Curry. *Radar System Performance Modeling*. Artech House, Norwood, MA, 2001.

[18] F. Daum and J. Huang. Mimo radar: Snake oil or good idea? *IEEE Aerospace and Electronic Systems Magzine*, pages 8–12, May 2009.

[19] A. F. G. De Maio, A. Farina. New target fluctuation models and their experimental. In *IEEE International Radar Conference*, 2005.

[20] A. F. G. De Maio, A.; Farina. Target fluctuation models and their application to radar performance prediction. *IET Trans on Radar Sonar Navig*, 151:261–269, OCT, 2004.

[21] J. V. Difranco and W. L. Rubin. *Radar Detection*. Artech House, Norwood, MA, 1980.

[22] B. J. Donnet and I. D. Longstaff. Combining MIMO Radar with OFDM Communications. In *Proc. 3rd European Radar Conference*, Manchester, UK, Sep 2006.

[23] P. C. Dowdy. Rcs probability distribution function modeling of a fluctuating target. In *IEEE Radar Conference*, 1991.

[24] D. M. Drumheller. Detection of a chi-square fluctuating target in gaussian noise. Technical report, NAVAL Research Lab, 1994.

[25] C. Du, J. Thompson, B. Mulgrew, and Y. Petillot. Detection performance of MIMO radar with realistic target models. In *Proc. IEEE International Radar Conference*, Bordeaux France, Oct 2009.

[26] C. Du, J. Thompson, and Y. Petillot. Predicted detection performance of MIMO radar. *IEEE. Signal Process. Letter*, 15:83–86, 2008.

[27] P. P. E and T. L. L. False alarm analysis of the envelope detection go-cfar processor. *IEEE Transactions on Aerospace and Electronics Systems*, 30:848–864, 1994.

[28] E. Fishler, A. Haimovich, R. Blum, L. Cimini, D. Chizhik, and R. Valenzuela. MIMO radar: An idea whose time has come. In *Proc. IEEE Int. Conf. on Radar*, Philadelphia, PA, April 2004.

[29] E. Fishler, A. Haimovich, R. Blum, L. Cimini, D. Chizhik, and R. Valenzuela. Performance of MIMO radar systems: Advantages of angular diversity. In *Proc. 38th IEEE Asilomar Conf. Singals, Syst., Comput*, pages 305–309, Nov 2004.

[30] E. Fishler, A. Haimovich, R. Blum, L. Cimini, D. Chizhik, and R. Valenzuela. Spatial diversity in radars-models and detection performance. *IEEE trans. on Signal Processing*, 54(3), Mar 2006.

[31] A. S. Fletcher and F. C. Robey. performance bounds for adaptive coherence of spare array radar. In *11th Conf. Adaptive Sensors Array Processing*, Mar. 2003.

[32] K. W. Forsythe and D. W. Bliss. Waveform correlation and optimization issues for mimo radar. In *In the Proceeding of Asliomar Conference on Signals, Systems and Computers*, 2005.

[33] J. L. Haidong. Yan and G. Liao. Multitarget identification and localization using bistatic mimo radar systems. *EURASIP Journal on Advances in Signal Processing*, 2008.

[34] A. M. Haimovich, R. S. Blum, and L. J. Cimini. MIMO Radar with Widely Separated Antennas. *IEEE Signal Processing Magazine*, 25(1):116–129, 2008.

[35] A. M. Haimovich, E. Fishler, R. S. Blum, D. Chizhik, R. Valenzuela, and L. Cimini. Statistical MIMO Radar. In *Proc Adaptive Sensor Array Processing Workshop*, 244 Wood St, Lexington, MA, Dec 2004.

[36] P. W. Hall. Correlative range-doppler detectors and estimators in bistatic radar using commercial fm broadcasts. Master's thesis, University of Washington, 1995.

[37] J. M. Hansen. A new radar technique for remote sensing of atmospheric irregularities by passive observation of the scattering of commercial fm broadcasts. Master's thesis, University of washington, 1994.

[38] A. Hassanien and S. A. Vorobyov. Phased-mimo radar: A tradeoff between phased-array and mimo radars. *IEEE Transactions on Signal Processing*, 58:3137–3151, 2010.

[39] S. M. Hurley. Signal-to-noise ratio gains and synchronization requirements of a distributed radar network. Master's thesis, NAVAL Postgraduate School, Montery, California, 2006.

[40] M. Jeong, K. Bae, Y. Kim, J. Lee, and Y. Han. Target Detection Based on Rake Receiver for Multi-static Radar Systems. In *Proc. IEEE International Radar Conference*, Bordeaux France, Oct 2009.

[41] I. Jouny. Target identification in a mimo environment. In *IEEE international radar conference*, 2008.

[42] E. W. Kang. *Radar System Analysis, Design and Simulation*. Artech House, 2008m.

[43] S. M. Kay. *Fundamentals of Statistical Signal Processing , Vol. 2, Detection Theory*. Prentice Hall, 1998.

[44] S. M. Kay. *Fundamentals of Statistical Signal Processing: Detection Theory*. Prentice Hall, 1998.

[45] K. Kulpa and M. Malanowski. The concept of simple MIMO PCL radar. In *Proc. 5th European Radar Conference*, Amsterdam, Netherlands, Oct 2008.

[46] B. V. Kumar. Advanced concepts in distortion-invariant phased-only filter design. Technical report, Carnegie Mellon University, 1992.

[47] H. l and V. Trees. *Detection, estimation, and modulation theory*. John Wiley & Sons, Inc, 2001.

[48] F. E. H. A. B. R. C. D. C. L. V. R. Lehmann, N. H. Evaluation of transmit diversity in mimo-radar direction finding. *Signal Proc. IEEE Transactions on*, 55:2215–2225, May 2007.

[49] N. Lehmann. *Some Contributions on MIMO Radar*. PhD thesis, The New Jersey Institute of Technology, 2007.

[50] N. Lehmann, A. M. Haimovich, R. S. Blum, and L. Cimini. MIMO-radar application to moving target detection in homogenous clutter. In *Proc. 14th IEEE Workshop on Sensor Array and Multi-channel Processing*, Waltham MA, July 2006.

[51] N. Levanon and E. Mozeson. *Radar Signals*. Wiley, 2004.

[52] J. Li and P. Stoica. MIMO Radar with Collocated Antennas: Review of some recent work. *IEEE Signal Processing Magazine*, 24(5):106–114, Sept 2007.

[53] J. Li and P. Stoica. *MIMO Radar Signal Processing*. John Wiley & Sons, Inc, 2008.

[54] B. R. Mahafza. *Radar Systems Analysis and Design Using MATLAB*. Chapman and Hall/CRC, 2005.

[55] B. R. Mahafza and A. Z. Elsherbeni. *MATLAB Simulation for Radar Systems Design*. Chapman and Hall/CRC, 2004.

[56] J. I. Marcum. A Statistical Theory of Target Detection by Pulsed Radar. *IRE Trans*, 6(2):59–144, April 1960.

[57] D. North. Analysis of the Factors which Determine Signal/Noise Discrimination in Pulsed-Carrier Systems. Technical report, RCA Laboratories Rept, June 1943.

[58] J. Qu, J. Zhang, X. Wang, and C. Liu. Detection performance of MIMO radar for coherent pulses. In *Congress. Image and Signal Processing CISP*, pages 49–53, 2008.

[59] M. A. Richards. *Fundamentals of Radar Signal Processing*. McGraw-Hill, 2005.

[60] P. F. Sammartino, C. J. Baker, and H. D. Griffiths. MIMO radar performance in clutter environment. In *Proc. CIE Radar Conference*, Shanghai China, Oct 2006.

[61] P. F. Sammartino, C. J. Baker, and H. D. Griffiths. Target model effects on MIMO radar performance. In *Proc. IEEE International Conference on Acoustics, Speech and Signal Processing*, volume 5, pages 1129–1132, May 2006.

[62] A. Sheikhi and A. Zamani. Coherent detection for MIMO radars. In *Proc. IEEE International Radar Conference*, pages 302–307, April 2007.

[63] A. Sheikhi and A. Zamani. Temporal coherent adaptive target detection for multiple-input multiple-out radars in clutter. *IET Trans on Radar Sonar Navig*, 2:86–96, 2008.

[64] M. Skolnik. *Introduction to Radar Systems*. McGraw-Hill, 1221 Avenue of the Americas NY, 2001.

[65] S. Stein. Algorithms for ambiguity function processing. *IEEE trans. Acoust, Speech, and Signal Processing*, 29:588–599, 1981.

[66] P. Swerling. Probability of Detection for Fluctuating Targets. *IRE Trans*, 6(2):269–308, April 1960.

[67] J. Tang, N. Li, Y. Wu, and Y. Peng. On Detection Performance of MIMO Radar: A Relative Entropy-Based Study. *IEEE Signal Processing Letters*, 16(3):184–187, March 2009.

[68] J. Tang, Y. Wu, Y. Peng, and X. wang. On detection performance of MIMO radar for Rician target. *Springer trans on Computer Science*, 52(8):1456–1465, August 2009.

[69] S. Tao, T. Ran, W. Yue, and Z. Siyong. Study of detection performance of passive bistatic radars based on fm broadcast. *Journal of Systems Engineering and Electronics*, 18(1):22–26, 2007.

[70] J. H. Tarokh, V and A. R. Calderbank. Space-time block codes from orthogonal designs. *IEEE Transactions on Information Theory*, 45:1456–1467, 1999.

[71] V. Tarokh, A. Naguib, and A. R. Calderbank. Space-time codes for high data rate wireless communications: Performance analysis and code construction . *IEEE Trans. Inform. Theory*, 44:744–765, Mar 1998.

[72] E. Telatar. Capacity of multi-antenna Gaussian channels. Technical report, AT&T-Bell Laboratories, June 1995.

[73] A. T. Wei Wang and E. D. Target detection and identification using canonical correlation analysis and subspace partitioning. In *IEEE International Conference on Acoustics, Speech and Signal Processing*, 2008.

[74] N. J. Willis. *Bistatic Radar, 2nd Edition*. Technology Service Corporation, 1995.

[75] P. Woodward. *Probability and Information Theory with Applications to Radar*. McGraw-Hill, New York, 1953.

[76] X. H. Wu, A. A. Kishk, and A. W. Glisson. MIMO-OFDM radar for direction estimation. *IET Trans on Radar Sonar Navig*, 4(1):28–36, Feb 2010.

[77] S. Z. X. Song and P. Willett. Reducing the waveform cross correlation of mimo radar with space: time coding. *IEEE Transactions on Signal Processing*, 58:4213–4224, August 2010.

[78] Q. Yan and R. S. Blum. Distributed signal detection under the neyman-pearson criterion. *IEEE Trans on Inform Theroy*, 47(4), 2001.

[79] J. J. Zhang and A. P. suppappola. MIMO radar with frequency diversity. In *Proc. Int. Waveform Diversity Des (WDD) Conference*, pages 208–212, 2009.